

# SANDIA REPORT

SAND2004-5080

Unlimited Release

Printed October 2004

## Shroud Boundary Condition Characterization Experiments at the Radiant Heat Facility

James T. Nakos, Jill M. Suo-Anttila, and Walter Gill

Prepared by

Sandia National Laboratories

Albuquerque, New Mexico 87185 and Livermore, California 94550

Sandia is a multiprogram laboratory operated by Sandia Corporation, a Lockheed Martin Company, for the United States Department of Energy's National Nuclear Security Administration under Contract DE-AC04-94AL85000.

Approved for public release; further dissemination unlimited.



**Sandia National Laboratories**

Issued by Sandia National Laboratories, operated for the United States Department of Energy by Sandia Corporation.

**NOTICE:** This report was prepared as an account of work sponsored by an agency of the United States Government. Neither the United States Government, nor any agency thereof, nor any of their employees, nor any of their contractors, subcontractors, or their employees, make any warranty, express or implied, or assume any legal liability or responsibility for the accuracy, completeness, or usefulness of any information, apparatus, product, or process disclosed, or represent that its use would not infringe privately owned rights. Reference herein to any specific commercial product, process, or service by trade name, trademark, manufacturer, or otherwise, does not necessarily constitute or imply its endorsement, recommendation, or favoring by the United States Government, any agency thereof, or any of their contractors or subcontractors. The views and opinions expressed herein do not necessarily state or reflect those of the United States Government, any agency thereof, or any of their contractors.

Printed in the United States of America. This report has been reproduced directly from the best available copy.

Available to DOE and DOE contractors from  
U.S. Department of Energy  
Office of Scientific and Technical Information  
P.O. Box 62  
Oak Ridge, TN 37831

Telephone: (865)576-8401  
Facsimile: (865)576-5728  
E-Mail: [reports@adonis.osti.gov](mailto:reports@adonis.osti.gov)  
Online ordering: <http://www.osti.gov/bridge>

Available to the public from  
U.S. Department of Commerce  
National Technical Information Service  
5285 Port Royal Rd  
Springfield, VA 22161

Telephone: (800)553-6847  
Facsimile: (703)605-6900  
E-Mail: [orders@ntis.fedworld.gov](mailto:orders@ntis.fedworld.gov)  
Online order: <http://www.ntis.gov/help/ordermethods.asp?loc=7-4-0#online>



# Shroud Boundary Condition Characterization Experiments at the Radiant Heat Facility

James Nakos, Jill Suo-Anttila, and Walt Gill  
Fire Science and Technology Department 09132  
Sandia National Laboratories  
P.O. Box 5800  
Albuquerque, NM, 87185-1135

## Abstract

A series of experiments was performed to better characterize the boundary conditions from an inconel heat source (“shroud”) painted with Pyromark® black paint. Quantifying uncertainties in this type of experimental setup is crucial to providing information for comparisons with code predictions. The characterization of this boundary condition has applications in many scenarios related to fire simulation experiments performed at Sandia National Laboratories’ Radiant Heat Facility (RHF). Four phases of experiments were performed. Phase 1 results showed that a nominal 1000°C shroud temperature is repeatable to about 2°C. Repeatability of temperatures at individual points on the shroud show that temperatures do not vary more than 10°C from experiment to experiment. This variation results in a 6% difference in heat flux to a target 4 inches away. IR camera images showed the shroud was not at a uniform temperature, although the control temperature was constant to about  $\pm 2^\circ\text{C}$  during a test. These images showed that a circular shaped, flat shroud with its edges supported by an insulated plate has a temperature distribution with higher temperatures at the edges and lower temperatures in the center. Differences between the center and edge temperatures were up to 75°C. Phase 3 results showed that thermocouple (TC) bias errors are affected by coupling with the surrounding environment. The magnitude of TC error depends on the environment facing the TC. Phase 4 results were used to estimate correction factors for specific applications (40 and 63-mil diameter, ungrounded junction, mineral-insulated, metal-sheathed TCs facing a cold surface). Correction factors of about 3.0-4.5% are recommended for 40 mil diameter TCs and 5.5-7.0% for 63 mil diameter TCs. When mounted on the cold side of the shroud, TCs read lower than the “true” shroud temperature, and the TC reads high when on the hot side. An alternate method uses the average of a cold side and hot side TC of the same size to estimate the true shroud temperature. Phase 2 results compared IR camera measurements with TC measurements and measured values of Pyromark emissivity. Agreement was within measured uncertainties of the Pyromark paint emissivity and IR camera temperatures.

## **Acknowledgements**

The authors would like to acknowledge the excellent support of the technologists supporting all testing at Sandia's Radiant Heat Facility: Bennie Belone, Chuck Hanks, and D. Mike Ramirez. Their attention to detail and their performing many experiments as part of this study were crucial to the project's success. Support from Rod Mahoney from Sandia's Primary Standards Laboratory for emissivity measurements is also gratefully acknowledged. The analysis and modeling by Ron Dykhuizen (on short notice) to provide a better way to estimate the "true" shroud temperature is gratefully acknowledged. Finally, the thorough reviews by Bruce Bainbridge and Cecily Romero provided many thoughtful comments and were appreciated.

# **Contents**

Introduction .....	10
Experimental Approach and Uncertainty Analysis .....	11
Phase 1: .....	11
Phase 2: .....	11
Phase 3: .....	11
Phase 4: .....	11
Phase 1 Experiments .....	12
Phase 1 Experimental Observations.....	14
Test #1 (9:30 AM, partly cloudy, calm winds – 7/16/03).....	14
Test #2 (11:00 AM, partly cloudy, calm winds – 7/16/03).....	15
Test #3 (12:00 PM, partly cloudy, calm – 7/16/03).....	16
Test #4 (1:15 PM, partly cloudy, breezy – 7/16/03).....	17
Post-Phase 1 Photos .....	19
Quantification of Test-to-Test Variability .....	20
Recommendation for Thermocouple Use .....	22
Analysis of Experimental Variability .....	22
Phase 1 Summary and Conclusions .....	26
Phase 1 Conclusions .....	26
Phase 3 Experiments .....	28
Phase 3 Object / Shroud Coupling .....	28
Fin Analysis .....	28
Phase 3 Experimental Description .....	30
Phase 3 Experimental Results .....	31
Test #1 (9/25/03).....	31
“2-Color” Pyrometer Data, Test #1 .....	33
Test #2 (9/25/03).....	34
Test #3 (9/25/03).....	36
Test #4 (9/25/03).....	37
Phase 3 Summary and Conclusions .....	46
Results Relevant to MVTU-2 and Exclusion Region Barrier Experiments .....	46
Results From FCU Experiments .....	47
Overall Conclusions.....	47
Phase 4 Experiments .....	48
Phase 4 Results .....	48
Determining the “True” Shroud Temperature Using Two Methods .....	55
“True” Shroud Temperature by the Extrapolation Method .....	55
Interpretation of Intrinsic TC Data .....	55
Shroud Temperature Results versus Junction Displacement .....	56
Extrapolation Using “Cold” Side Data .....	60
“True” Shroud Temperature by the Average Temperature Method .....	65
Recommendation for Estimating “True” shroud Temperature .....	66
Phase 4 Summary and Conclusions .....	66
Phase 2 Experiments.....	68

Phase 2 Experiments: Instrument Response, Discretization, and Temperature Distribution .....	68
Shroud Photographs for Experiments 1-3 .....	70
Analysis of Phase 2 Experimental Results .....	72
Pyromark Emissivity .....	74
Analysis of the IR images .....	76
Comparison of TC and IR Camera Image Data .....	78
Typical Overall Uncertainty Estimate .....	83
Phase 2 Summary and Conclusions .....	84
<b>Summary and Conclusions .....</b>	<b>85</b>
Summary .....	85
Phase 1: .....	85
Phase 2: .....	85
Phase 3: .....	85
Phase 4: .....	85
Phase 1 Results .....	85
Phase 2 Results .....	86
Phase 3 Results .....	87
Results relevant to MVTU-2 and Exclusion Region Barrier Experiments .....	87
Results From FCU Experiments .....	87
Overall Conclusions for Phase 3 .....	87
Phase 4 Results .....	88
Conclusions and Recommendations .....	89
Lessons Learned .....	89
References .....	89
Appendix A: Fin Analysis .....	91
Appendix B: Average Shroud Temperature Analysis .....	95
Appendix C: Pyromark Emissivity .....	104

## List of Figures

Figure 1 Schematic of Shroud Instrumentation for Phase 1 Experiments .....	13
Figure 2 Section View of Layout for Shroud Characterization Experiments .....	13
Figure 3 Before Test 1 Showing Level, Black Shroud .....	14
Figure 4 Underside of Shroud Before Test 1, Seen Through Base Plate.....	14
Figure 5 Top of Shroud Prior to Test 2.....	15
Figure 6 Underside of Shroud Prior to Test 2.....	15
Figure 7 Top of Shroud Before Test 3 .....	16
Figure 8 Underside of Shroud Before Test 3 .....	16
Figure 9 Top of Shroud Before Test 4.....	17
Figure 10 Underside of Shroud Before Test 4.....	17
Figure 11 Top of Shroud Before Test 5 .....	18
Figure 12 Underside of Shroud Before Test 5.....	18
Figure 13 Top of Shroud at End of Phase 1 .....	19
Figure 14 Underside of Shroud at End of Phase 1 .....	19
Figure 15 Comparison of Shroud Control Thermocouple (A) Temperature for all 5 Phase 1 Tests .....	21
Figure 16 Comparison of Shroud Backup Thermocouple (B) Phase 1 Tests.....	21
Figure 17 Upper Plot Mean Computed from Lab View, Lower Plot Fortran Computed Mean .....	24
Figure 18 Upper Plot: Standard Deviation (in C) Computed from Lab View, Lower Plot: Fortran Computed Standard Deviation .....	25
Figure 19 Predicted Response of TC vs. TC Diameter For Target at 300 or 700K.....	29
Figure 20 Phase 3 Shroud Thermocouple Locations .....	31
Figure 21 Phase 3, Test #1 Results .....	32
Figure 22 Phase 3, Test #1 Results, 40 and 63-mil TCs .....	34
Figure 23 Phase 3, Test #2 Results .....	36
Figure 24 Phase 3, Test #3 Results, Shroud and Calorimeter Data .....	37
Figure 25 Phase 3, Test #3 Results, Shroud Data .....	38
Figure 26 Phase 3, Test #4, Shroud and Calorimeter Temperature Results .....	38
Figure 27 Phase 3, Test #4, Shroud Temperature Results (note lamp failure at ~12 minutes).....	39
Figure 28 FCU Shroud TC Locations .....	40
Figure 29 Typical Pair of TCs (63-mil Ungrounded Junction and Intrinsic) .....	40
Figure 30 Front Face Photograph of FCU .....	41
Figure 31 Side View of FCU Test Setup – FCU Not in Place.....	42
Figure 32 Shroud Temperature Control TCs .....	43
Figure 33 Temperature Differences, FCU Not in Place .....	43
Figure 34 Shroud Control Temperatures, “Stair Step” Test .....	44
Figure 35 Temperature Differences, FCU in Place .....	45
Figure 36 Typical FCU Front Face Temperatures (Separate DAS Terminated after 68 minutes).....	46
Figure 37 Shroud TCs used in Phase 4 Experiments .....	49
Figure 38 Shroud TC Locations, Phase 4 Experiments .....	50
Figure 39 Typical Data Set, TCs Facing Lamps, Test #1 .....	53

Figure 40 Typical Data Set, TCs Facing Lamps, Test #4.....	53
Figure 41 Indicated Shroud Temperature versus Junction Displacement, Tests 1 & 2, TCs A1-A4 .....	56
Figure 42 Indicated Shroud Temperature versus Junction Displacement, Tests 1 & 2, TCs B1-B4.....	57
Figure 43 Indicated Shroud Temperature versus Junction Displacement, Tests 3 & 4, TCs A1-A4 .....	57
Figure 44 Indicated Shroud Temperature versus Junction Displacement, Tests 5 & 6, TCs A1-A4 .....	58
Figure 45 Indicated Shroud Temperature versus Junction Displacement, Tests 7 & 8, TCs A1-A4 .....	58
Figure 46 Shroud TC Layout for MVTU-2 Experiments .....	59
Figure 47 Typical Steady Shroud Temperatures for MVTU-2 Experiments .....	60
Figure 48 Estimated Error Between a 40 Mil Ungrounded Junction Sheathed TC and the “True” Shroud Temperature .....	64
Figure 49 Estimated Error Between a 63 Mil Ungrounded Junction Sheathed TC and the “True” Shroud Temperature .....	65
Figure 50 Schematic of Phase 2 Shroud Instrumentation.....	69
Figure 51 Photograph of Shroud Looking into Mirror from IR Camera Location.....	70
Figure 52 Photographs before Test 1 (top and bottom) .....	70
Figure 53 Photographs before Test 2 .....	71
Figure 54 Photographs before Test 3 .....	71
Figure 55 Photographs before Phase 3 Test 1.....	71
Figure 56 Typical Shroud Temperatures During a Phase 2 Experiment .....	72
Figure 57 Phase 2 and 3 TC Results .....	74
Figure 58 Emissivity Measurements for Inconel Plate .....	75
Figure 59 Emissivity Measurements for Phase 1 Inconel Disk .....	76
Figure 60 Setup for Mirror Emissivity Experiment.....	77
Figure 61 Calculation of the Mirror Correction Factor .....	78
Figure 62 IR Image of Shroud with $e=0.78$ .....	80
Figure 63 IR Image of Shroud with $e=0.82$ .....	81
Figure 64 Shroud Temperature Distribution from IR image with $e=0.76$ .....	82
Figure 65 Flux Comparisons (TC average of 1043°C, IR average of 1025°C, IR distribution from Figure 63).....	83
Figure 66 Ratio of Flux from the IR Average Temperature to the IR Distribution.....	83

## **List of Tables**

Table 1 Summary of Phase 3 Test Results.....	35
Table 2 Phase 4 Experimental Matrix.....	51
Table 3 Summary of Phase 4 Experimental Data (All Data in °C) .....	54
Table 4 Estimation of True Shroud Temperature .....	62
Table 5 Estimated Error, % Between 40 Mil TC and “True” Shroud Temperature (Figure 48 ) .....	63
Table 6 Estimated Error, % (of Absolute) Between 63 Mil TC and “True” Shroud Temperature (Figure 49 ) .....	63
Table 7 Estimated Errors for 40 and 63 mil Diameter TCs, % of Absolute Temperature	65
Table 8 Summary of TC temperatures (average of Tests 1-3).....	78
Table 9 Summary of IR Image Temperatures (from Test 3) .....	80

## **Introduction**

Accurate characterization of experimental boundary conditions is crucial if experimental results are to be compared to computational model calculations. Currently, experiments in Sandia National Laboratories' Radiant Heat Facility are underway for phenomenon discovery (W76-1 Firing Set Exclusion Region Barrier, W76-1 ERB), model validation (Model Validation Test Unit-2, MVTU-2), and in the future for system qualification. The boundary condition (typically the temperature) of the radiating surface (the "shroud") must be characterized more rigorously than was required in past performance acceptance testing. Therefore, a series of experiments was performed in four (4) phases to better understand the shroud temperature, temperature distribution, and experimental uncertainties. Knowledge of these variables is important because the shroud technique is often used to generate high temperature (e.g., 1000°C) simulated hydrocarbon fuel fire environments to study the thermal response of high-consequence systems and for comparison with computational simulations. The next section describes the approach used to characterize the shroud temperature distribution and quantify the experimental uncertainty. Remaining sections describe the results and conclusions.

## **Experimental Approach and Uncertainty Analysis**

The shroud temperature distribution and thermocouple (TC) uncertainty were determined in a series of experiments consisting of four phases. The objectives of each phase are listed below.

### **Phase 1:**

1. Assess the repeatability of the experiments; and
2. Determine the shroud temperature profile based on IR measurements.

### **Phase 2:**

1. Provide information to allow assessment of the “true” shroud temperature;
2. Provide more data on the shroud temperature distribution; and
3. Provide information on discretization errors.

### **Phase 3:**

1. Assess the magnitude of the TC error based on coupling between the shroud and target/test unit; and
2. Test the hypothesis that fin theory can partially explain the TC error as a function of sheath diameter and environment temperature.

### **Phase 4:**

1. Obtain experimental data on the response of thermocouples (TCs) of various sheath diameters and intrinsically mounted TCs;
2. Develop methodologies to estimate the “true” shroud temperature;
3. Provide correction factors for various sized TCs (20, 40, and 63-mil diameter ungrounded junction, inconel sheathed) to estimate the true shroud temperature; and
4. Further test the hypothesis that fin theory is an appropriate way to explain the temperature variation with sheath diameter.

Because of the results generated, the order in which the results are discussed is not sequential. Phase 1 results will be first, followed by Phase 3, Phase 4, and finally Phase 2. In this way the results of each phase can be used to build on the results of the preceding sections.

## **Phase 1 Experiments**

The purpose of Phase 1 was to assess the repeatability of the experiments and determine the shroud temperature profile based on IR measurements. The shroud was instrumented with two 40-mil diameter, ungrounded junction TCs on the cold side of the shroud (facing away from the lamps) as shown in Figure 1. One TC was for control and the other served as backup. Additional TCs were not installed to minimize the effect on IR camera readings. Forty-mil TCs were selected to use throughout the experimentation as control TCs, giving a consistent basis for the shroud temperature measurements.

Five tests were conducted as part of this phase and the results were compared point-to-point using the TC data and IR images to assess repeatability of the experiments. The results of this phase generated information on test-to-test repeatability and shroud temperature profiles.

Phase 1 experiments were conducted to (see Reference [1]):

1. Assess the repeatability of the radiant heat experiments; and
2. Estimate the shroud temperature distribution and repeatability based on IR camera measurements.

Five nominally identical experiments using a setup similar to Figure 2 were conducted with the following characteristics.

- Shroud control temperature of 1000°C for 20 minutes
- 4.75” diameter, 1/8” thick inconel shroud, oriented horizontally
- Two 40-mil ungrounded junction thermocouples (TCs), 0.50 inch off center mounted on cold side of shroud
- Pyromark® 2500 black paint sprayed on, dried, and cured in oven according to manufacturer’s directions
- Shroud carefully centered and leveled
- No shutter used during heat-up (shutter shown in Figure 2 was not used)
- Water-cooled base plate, painted black, with 4.25 inch diameter hole in center to support shroud
- No target object present
- IR camera used with emissivity = 1.0 capturing 1 frame every 2 seconds
- TC leads routed towards main Radiant Heat (RH) building 6536 (Figure 1)
- Control TC was A (as shown in Figure 1)
- TCs were resistance checked prior to experiments
- DAS (data acquisition system) calibrated post-test

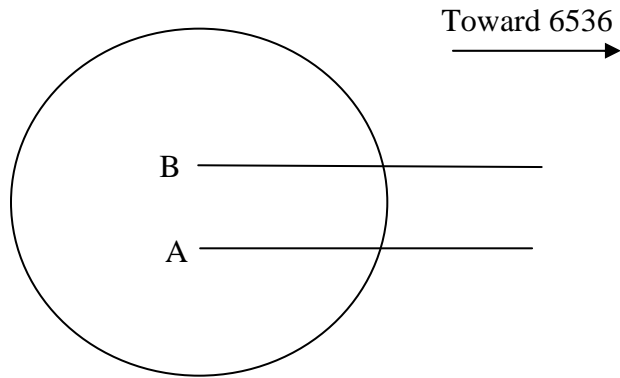


**Figure 1 Schematic of Shroud Instrumentation for Phase 1 Experiments**

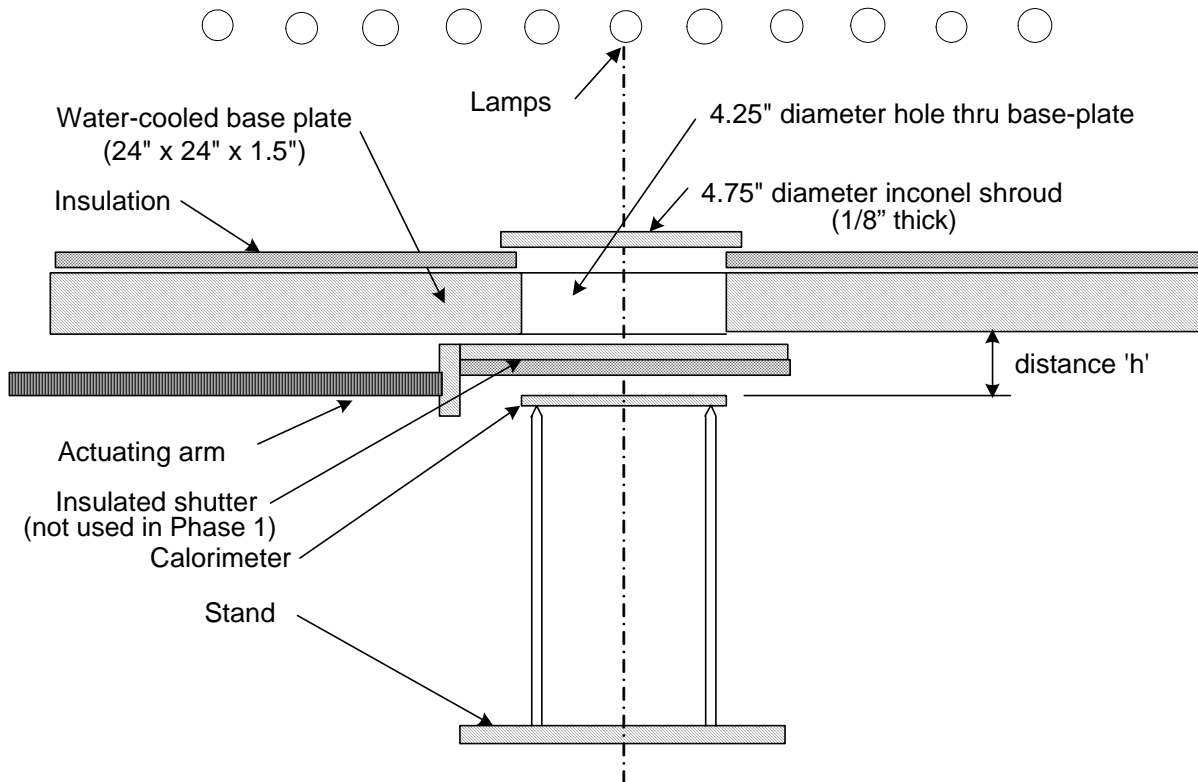


**Figure 2 Section View of Layout for Shroud Characterization Experiments**

## Phase 1 Experimental Observations

**Test #1** (9:30 AM, partly cloudy, calm winds – 7/16/03)

Photographs show that paint is very black and has an even coating prior to test (see Figure 3 and Figure 4). Smoke was visible for the first few minutes of the test, likely from the binder in the insulating felt underneath the shroud, and some from the paint binder.

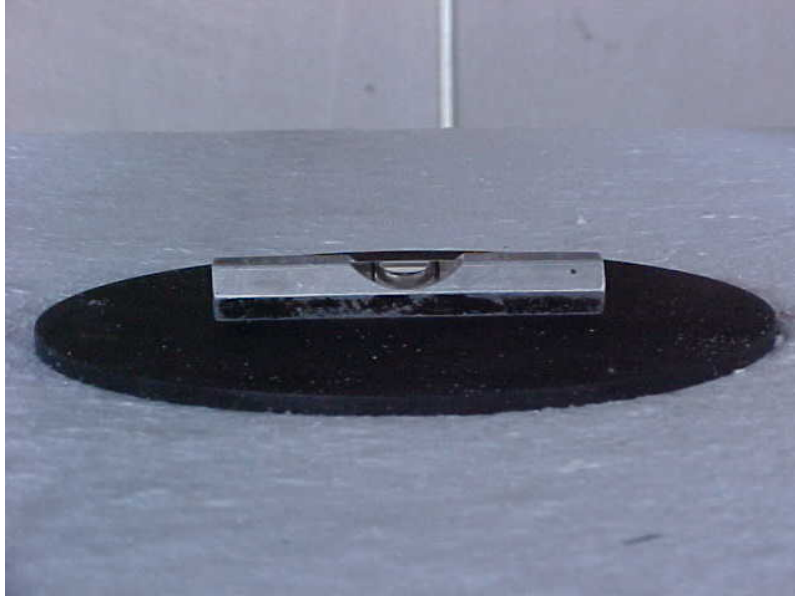


**Figure 3 Before Test 1 Showing Level, Black Shroud**

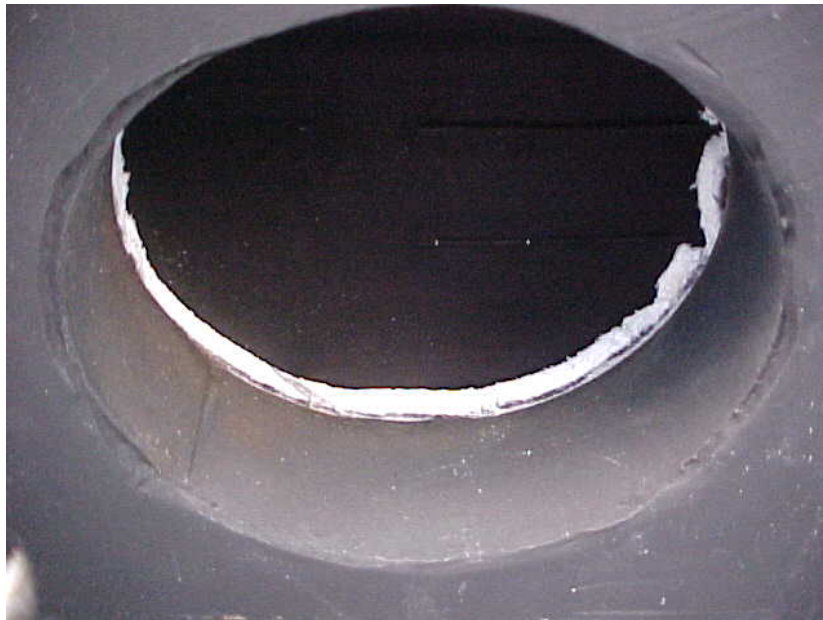


**Figure 4 Underside of Shroud Before Test 1, Seen Through Base Plate**

**Test #2** (11:00 AM, partly cloudy, calm winds – 7/16/03)

After Test 1 and before Test 2, paint is noticeably grayer than it was before as shown in Figure 5 and Figure 6. No smoke rises from fixture during test.



**Figure 5 Top of Shroud Prior to Test 2**



**Figure 6 Underside of Shroud Prior to Test 2**

**Test #3** (12:00 PM, partly cloudy, calm – 7/16/03)

No smoke observed, and the shroud surface looks the same as it did before Test 2.



**Figure 7 Top of Shroud Before Test 3**



**Figure 8 Underside of Shroud Before Test 3**

**Test #4** (1:15 PM, partly cloudy, breezy – 7/16/03)  
No change in shroud surface observed.



**Figure 9 Top of Shroud Before Test 4**

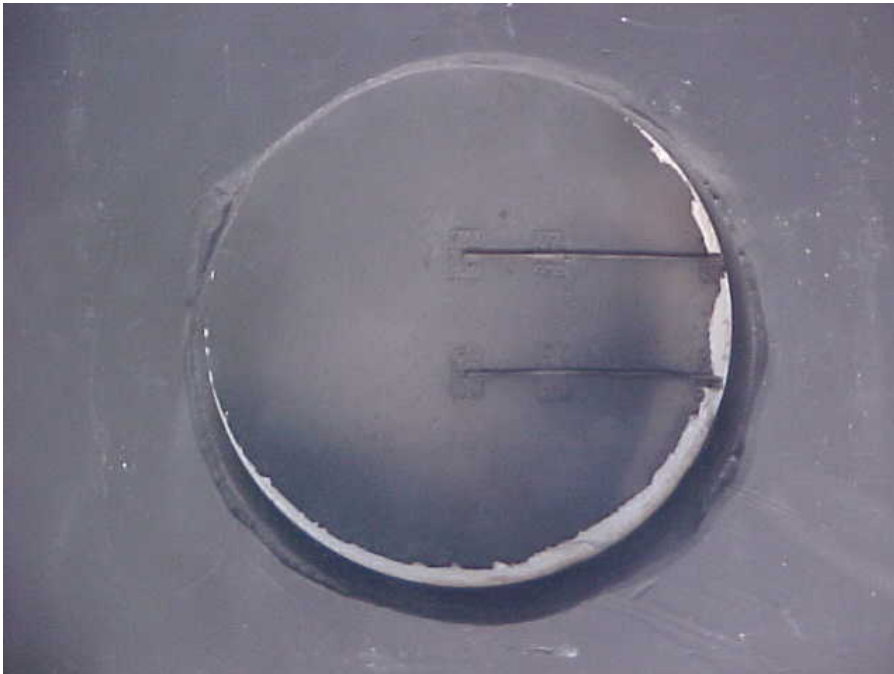


**Figure 10 Underside of Shroud Before Test 4**

**Test #5** (2:30 PM, partly cloudy, breezy – 7/16/03)  
Again, shroud appears to be unchanged.



**Figure 11 Top of Shroud Before Test 5**



**Figure 12 Underside of Shroud Before Test 5**

## Post-Phase 1 Photos

- Post-test all TC resistances checked and only a single TC changed by  $1\Omega$  ( $< 1\%$ )
- Shroud surface color (and potentially the emissivity) changed most during first heating but is believed to remain mostly constant for subsequent heating cycles, except when the paint begins to peel off, which did not occur in these experiments.



**Figure 13 Top of Shroud at End of Phase 1**

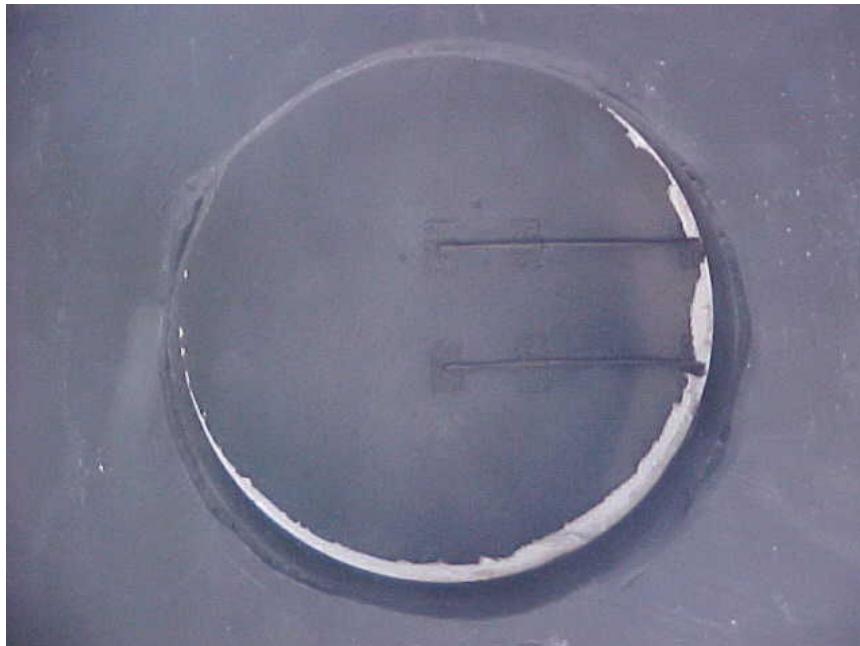


**Figure 14 Underside of Shroud at End of Phase 1**

## Quantification of Test-to-Test Variability

As described previously, the purpose of this phase was to assess the repeatability of the experiments, and determine the shroud temperature distribution based on thermocouple measurements and IR images. The shroud was instrumented with two 40-mil diameter, ungrounded junction (Type K) TCs each located 0.50 inch from the center of the shroud. One was used for control and the other served as backup.

Five tests were conducted, and the results are presented below. The resulting temperature distributions for each experiment will be compared point-to-point using the IR images to assess the repeatability of the experiments.

First, the repeatability of the two shroud thermocouples was investigated. The plots below show the recorded temperatures for the control thermocouple (A) and the backup thermocouple (B). The first plot (Figure 15) demonstrates that the control system consistently achieves the desired set point of approximately 1000°C in all experiments. Note that the start of heating relative to the start of the data acquisition was different for the five experiments displayed in the plot. The range in recorded temperatures was  $998.8 \pm 1.4^\circ\text{C}$  (over a 400 second period, 95% confidence interval) for all five experiments. The range in temperatures recorded by the control thermocouple is within the control system limitations. Additional constraints could be placed on the system to reduce the deviation from the set point (2°C observed) but that would result in a larger initial overshoot and potential damage to the shroud. In addition, tighter control system tolerances typically require extensive tuning which is time consuming and costly.

The variation in the backup TC (Figure 16) is slightly larger (about 7°C) since it is not under direct control. Differences between the control and backup TCs are due to a number of possible sources: gradients in the shroud temperature, differences in the individual TC accuracies, TC bead locations within the sheath, slight differences in TC mounting, or slight shifts on the calibration after heating. A combination of these factors is likely, but not definitively, the cause of the observed differences.

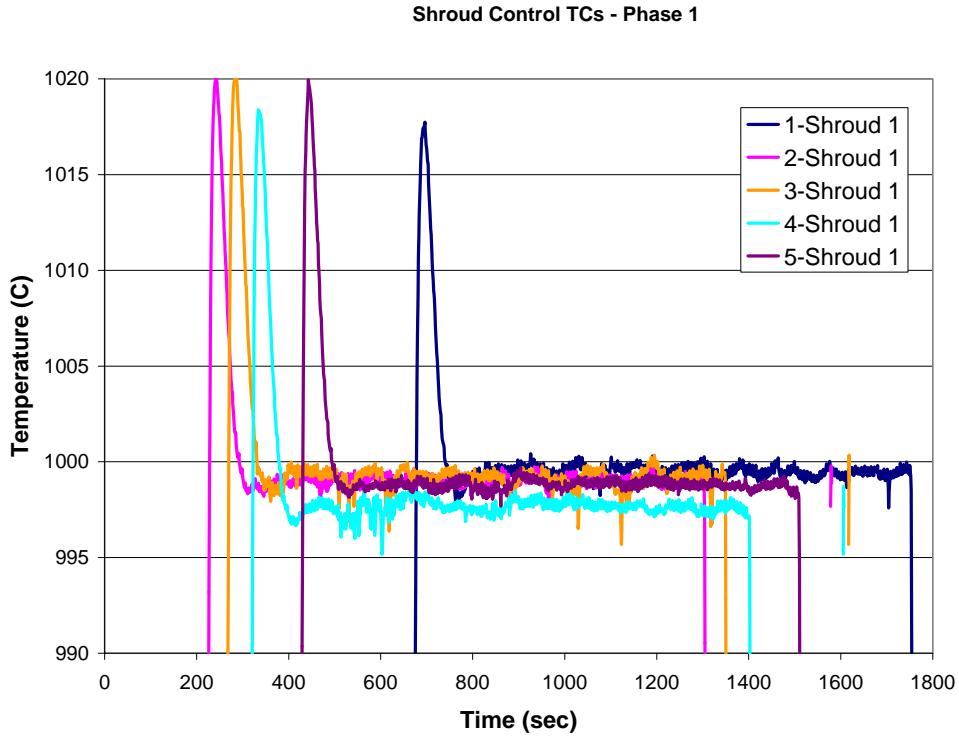


**Figure 15 Comparison of Shroud Control Thermocouple (A) Temperature for all 5 Phase 1 Tests**

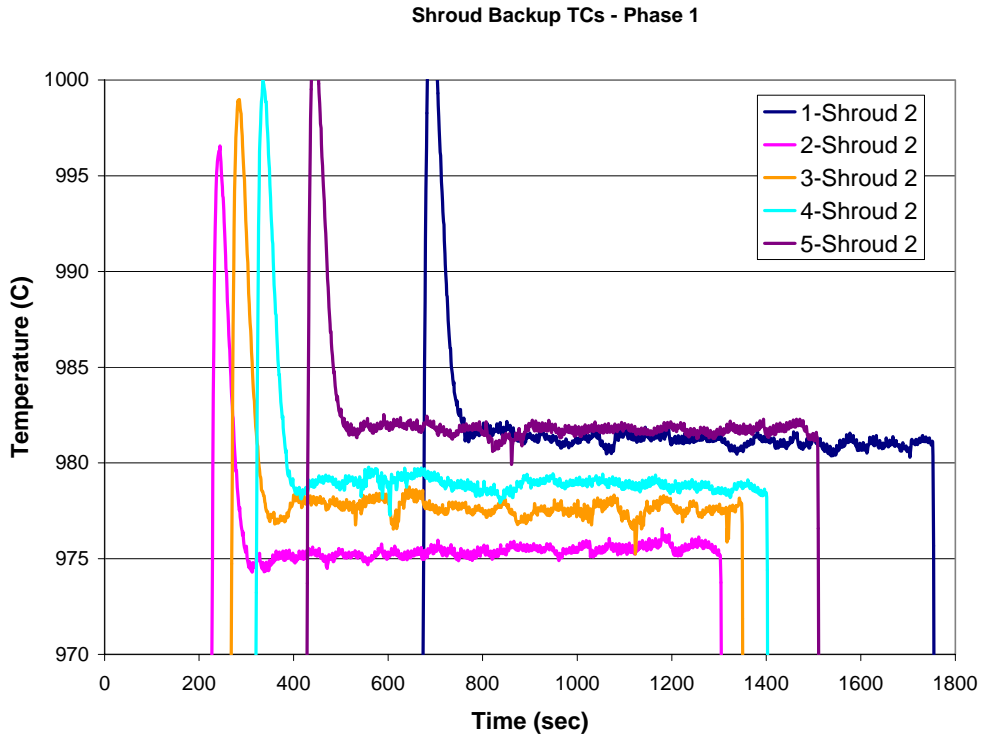


**Figure 16 Comparison of Shroud Backup Thermocouple (B) Phase 1 Tests**

## Recommendation for Thermocouple Use

As part of this effort, a recommendation is made below for future experiments conducted for model validation purposes. All instrumentation used in validation experiments will be carefully controlled according to the method outlined below (subject to project schedule and resources). Type K thermocouples are required to have error in temperature measurements less than  $\pm 2.2^{\circ}\text{C}$  or  $\pm 0.75\%$  of the reading in  $^{\circ}\text{C}$  (per ANSI standards). Thermocouples periodically calibrated at the primary standards laboratory have satisfied this requirement, and representative thermocouples will continue to be sent to the primary standards laboratory several times per year to ensure their quality.

The data acquisition system (DAS) will be calibrated by disconnecting the thermocouple and replacing it with a Fluke or Ectron calibrator. The calibrator will be used to calibrate each instrument channel at temperatures that span the expected experimental temperature range.

Thermocouples will be ordered from a reputable manufacturer and carefully monitored throughout their use. Initially, each thermocouple will be assigned a serial number and put through a series of tests. Personnel will check the resistance and temperature outputs using the following procedure. The thermocouple pedigree will be included in the experimental data files sent to experimentalists and analysts following the completion of the validation experiment.

1. Connect meter (Fluke model 1520 meg-ohmmeter or a Fluke model 89IV multimeter) to both thermocouple leads (red and yellow). Set the meg-ohmmeter to ohms, or the multimeter to ohms auto scale. Measure and record resistance.
2. Connect one meter lead to the sheath and the other lead to the red thermocouple wire. Set meg-ohmmeter to 250 volt range, or multimeter to auto scale. Measure and record resistance. Connect one meter lead to the yellow wire and repeat the measurement.
3. Place the thermocouple in an ice bath and record the temperature.
4. Place the thermocouple in a boiling water bath and record the temperature.
5. Repeat 1-4 as installed and after the experiment (where possible) to ensure that the thermocouple has not sustained any damage.

If Type K thermocouples are not sufficient for a particular experiment, Type N thermocouples or tight tolerance thermocouples may be substituted. Type N thermocouples can operate in the same temperature range as Type K but are less susceptible to issues associated with thermal cycling. Tight tolerance TCs have half the error stated above and are more expensive.

## Analysis of Experimental Variability

A detailed point-to-point comparison of the shroud temperature distribution from test to test was performed by different methods using IR camera images. A Lab View program and a Fortran code computed the average and standard deviation of the temperature point-by-point using an image from each of the five experiments. A single image

represented each experiment because analysis of all images, taken one second apart after the shroud stabilized, showed that the temperature distribution was essentially constant. The measurement points were extracted from the IR images (at 10 min after the start of heating) using the FLIR IR “Researcher” software. The files containing the resulting data points from each of five experiments were used in the variability analysis as presented in the Tecplot images that follow. Results from the Lab View analysis and the Fortran analysis provide additional confidence in the accuracy of the data manipulation and calculations. Equations used were (note  $n=5$ ):

$$T_{avg} = \frac{1}{n}(T_1 + T_2 + \dots + T_n) \quad stdev = \sqrt{\frac{\sum_{i=1}^n (T_i - T_{avg})^2}{n-1}}$$

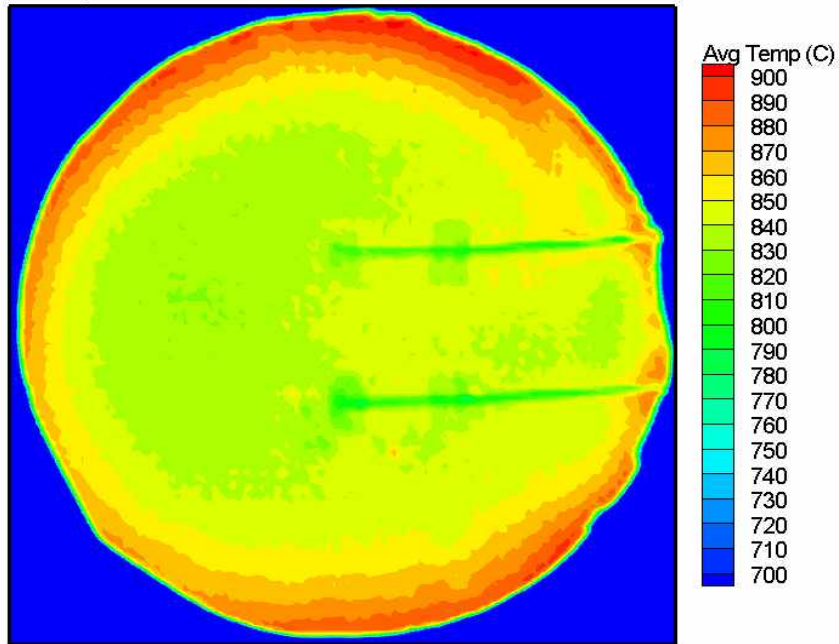
The average temperature distribution was calculated using each pixel temperature value from the five IR images using both Lab View and Fortran; two independent evaluations provide confidence in the accuracy of the analysis. Figure 17 shows the average shroud temperature results, Lab View results above, Fortran below. The results are very similar and minor variations are likely due to rounding differences in the calculations.

Distribution of the shroud temperatures shows that the hottest location is at the perimeter and the coolest is near the center. The shroud is hotter near the edges where it is supported by the insulation. In addition, the temperature distribution appears to be correlated with images of the shroud surface shown earlier, indicating that the gradients may be due in part to differences in surface emissivity as evident by gray regions on the shroud.

Outlines of the two TC sheaths are easily seen. This image clearly shows that the TC sheath is cooler than the surrounding shroud, which implies the TC reading will lower than the true shroud temperature. The thermocouple leads are coolest since they are offset from the shroud by the TC diameter. The nichrome straps holding the thermocouple wires in place are also cooler. Figure 18 displays the spatially varying standard deviation corresponding to the average temperatures for the five Phase 1 experiments. Again, the top image was obtained using Lab View while the bottom image was obtained using a Fortran code. As expected, regions of high temperature gradients also have the highest variability. Variabilities in these regions would be very sensitive to the IR camera placement. A minor shift in the node locations (due to camera placement) could magnify the variability. In general, away from the high gradient regions, a test-to-test comparison shows that the standard deviation for points on the shroud is less than 10°C.

The impact of the variability in shroud temperature on heat flux to a target (the same size as the shroud and surrounding area shown in the IR images) from IR images was evaluated. The average temperatures from the (lower) image in Figure 17 were combined with the standard deviation values from Figure 18 (lower image) and a temperature  $\pm 2$  was used to estimate a heat flux profile to a target about 4 inches away from the shroud.

**Average Shroud Temperature Distribution**  
Computed using 5 Phase 1 Experiments and LabView  
e= 1.0, TC control = 1000 C



**Average Shroud Temperature Distribution**  
Computed using 5 Phase 1 Experiments (15min) and Fortran  
e= 1.0, TC control = 1000 C

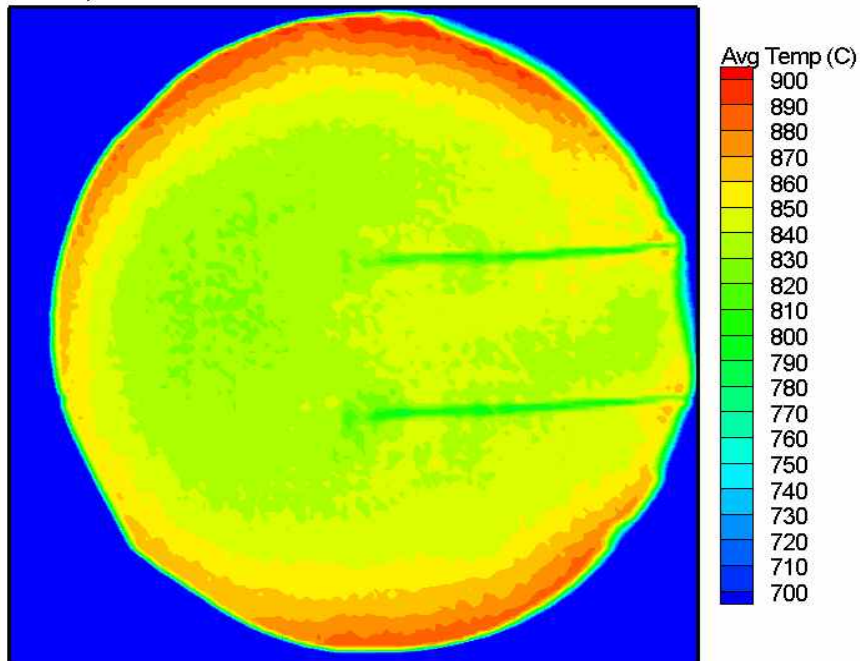
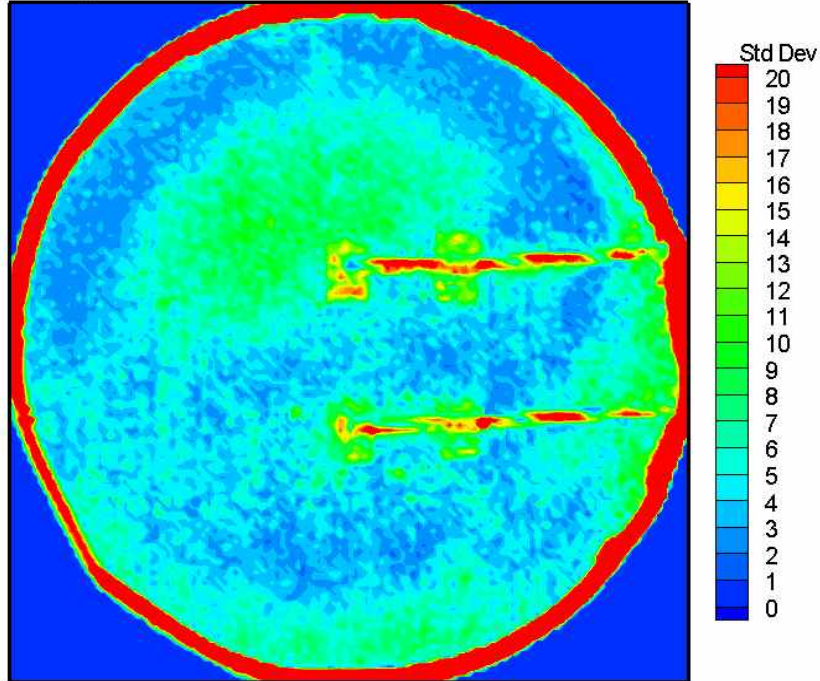


**Figure 17 Upper Plot Mean Computed from Lab View, Lower Plot Fortran Computed Mean**

Average Shroud Standard Deviation  
Computed using 5 Phase 1 Experiments and LabView  
e= 1.0, TC control = 1000 C



Average Shroud Standard Deviation  
Computed using 5 Phase 1 Experiments (15min) and Fortran  
e= 1.0, TC control = 1000 C

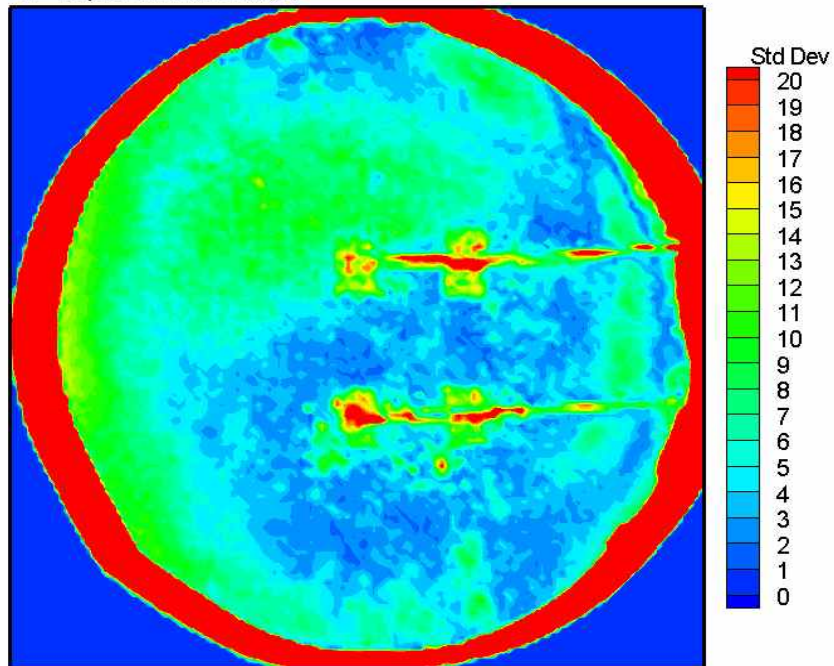


Figure 18 Upper Plot: Standard Deviation (in C) Computed from Lab View,  
Lower Plot: Fortran Computed Standard Deviation

Flux at each location was estimated and the results showed that for the highest temperature (average +2 ) the heat flux was about 6% higher than if one used just an average shroud temperature profile. Similarly, using the lowest temperature (average – 2 ), the flux was about 6% lower than if the average shroud temperature profile were used. Analysts should consider this flux difference when deciding whether or not to use a single shroud temperature for modeling purposes.

## Phase 1 Summary and Conclusions

- Five experiments were performed with a nominally 1000°C shroud.
- Paint and insulation smoked on first experiments, but not thereafter.
- Paint seemed to be stable after initial bake-out.
- Emissivity may have changed after/during the first experiment.
- TC control repeatable to about 2°C (Figure 15).
- TC control constant to within about  $\pm 2^\circ\text{C}$  during a test (Figure 15).
- Back-up TC repeatable to about 7°C (Figure 16).
- IR images were averaged over 5 tests using two methods; results from two methods were consistent (Figure 17).
- Point to point comparison of data from 5 experiments indicates that the results were repeatable within a standard deviation of about 10°C (Figure 18) away from the regions of high gradients.
- Average shroud temperature profile showed higher temperatures at shroud edges and lower temperatures near center. An assessment of the shroud temperature uniformity revealed a maximum distribution over the shroud surface (not including TC leads) of about 75°C (825-900°C).
- Variability in shroud temperature shown in Figure 18 has an effect on heat flux to a target 4 inches from the shroud of about  $\pm 6\%$ .
- Analysts should consider this flux difference when deciding whether or not to use a single shroud temperature for modeling purposes.

## Phase 1 Conclusions

This phase of experiments has shown the shroud temperature (1000°C) is controlled to within about  $\pm 2^\circ\text{C}$  during an individual experiment (usually within about  $\pm 1^\circ\text{C}$ ), as demonstrated in the TC traces in Figure 15. In addition, the TC control temperature was repeatable to within 2°C from experiment to experiment.

The ability to reproduce the same nominal boundary condition (temperature) from test to test was also evaluated. According to IR camera images, the majority of the shroud temperatures are repeatable within a standard deviation of about 10°C. Regions of higher standard deviations are present in areas with increased gradients, such as the edge of the shroud and the TC wires. A slight shifting of the points in the domain (due to camera location) could magnify the standard deviation. Overall, it has been shown that the

shroud control temperature is repeatable to about 2°C and shroud temperature profiles are repeatable to a standard deviation of about 10°C.

The impact on heat flux due to the repeatability of shroud temperature from IR camera images (Figures 17 and 18) from the 5 tests was estimated. The heat flux to an imaginary target about 4” away from the shroud was used to estimate the change. For the highest temperature profile used (+2 , where is from Figure 18) the difference in heat flux was about +6%. Similarly, for the lower temperature the flux was reduced by about 6%.

Note that the emissivity used to create the images was assumed to be 1.0, which is larger than expected for inconel covered with Pyromark 2500 paint. Due partly to this treatment of the emissivity, ~140°C difference exists between IR and thermocouple temperatures. Measurements were performed to determine better estimates of the emissivity of this paint and the results of these experiments are shown in a later section and in Appendix C.

## **Phase 3 Experiments**

Four Phase 3 experiments were performed to assess the magnitude of the TC error based on coupling between the shroud and target/test unit [1]. Details of the setup include:

- Insulated shutter used to provide a difference between a cold environment (no shutter) and a higher temperature target (insulated shutter in place).
- Model Validation Test Unit 2 (MVTU-2) calorimeter painted with Pyromark 2500 used to simulate a target with increasing temperature during the experiment.
- No IR camera data recorded.
- New IR pyrometer used to estimate shroud temperature in a spot in the center of the shroud.
- Data from previous experiments on “Furnace Characterization Unit” (FCU) used to compare TC errors with no target (i.e., a cold environment), and a large steel target (FCU) whose temperature increased with time.

## **Phase 3 Object / Shroud Coupling**

Placing an object near the shroud has the potential to impact the temperature of the shroud and TCs due to thermal coupling. The impact of this phenomenon for experiments typical of the W76-1 ERB and MVTU-2 was assessed (using a water-cooled base plate) using a shroud instrumented with six (6) ungrounded junction sheathed TCs (see Figure 20). A “2-color” IR pyrometer was used to compare temperatures with TC data. A calorimeter was placed approximately 4 inches below the shroud.

## **Fin Analysis**

An analysis was performed to determine if fin theory could predict trends in thermocouple response depending on the sheath diameter and the presence or absence of a target. Figure 19 shows the results of an analysis (using fin theory) where the sheathed TC is approximated by a square fin with side dimension the same as the sheath diameter. A square fin is used for ease of analysis. The analysis is shown in Appendix A. Radiation is allowed off the end and sides of the fin; convection is neglected. Details of basic fin analysis are shown in a number of heat transfer textbooks, e.g., [2]. It was assumed the constant temperature (1300 K) shroud radiates to a constant temperature “target” at either 300 or 1000 K. Figure 19 shows the computed response of the fin as a function of the distance from the shroud for a 63 mil diameter TC. Plots for 40 and 20 mil sheath diameters are virtually the same, so only one plot is shown. The maximum fin distance is the outer surface of the TC sheath, and the half-way distance where the bead is located. The model predicts a lower temperature at the bead compared with the shroud surface, and higher errors with the colder (300 K) target. As an example, if one had a 40 mil diameter TC, the bead would be located at the 20 mil location. At the 20 mil location and assuming a cold target, the bead temperature would be about 1260 K, or about a 40 K

difference between the shroud temperature and the bead temperature. As will be seen, these features agree at least qualitatively with experimental data.

Results shown in Figure 19 were adjusted to agree with experimental data by varying the apparent thermal conductivity of the fin. For a “cold” target (300K), the difference between a 40 and 63-mil TC is about 1211-1181= 40K, so ‘k’ was adjusted until the results agreed with the experimental data. Three key results are:

1. The fin temperature decreases with distance from the shroud, or in the real case the TC sheath diameter;
2. The relationship with distance from shroud (or sheath diameter) is almost linear;
- and
3. The error decreases with a hot target or test object.

All these results are consistent with experimental data.

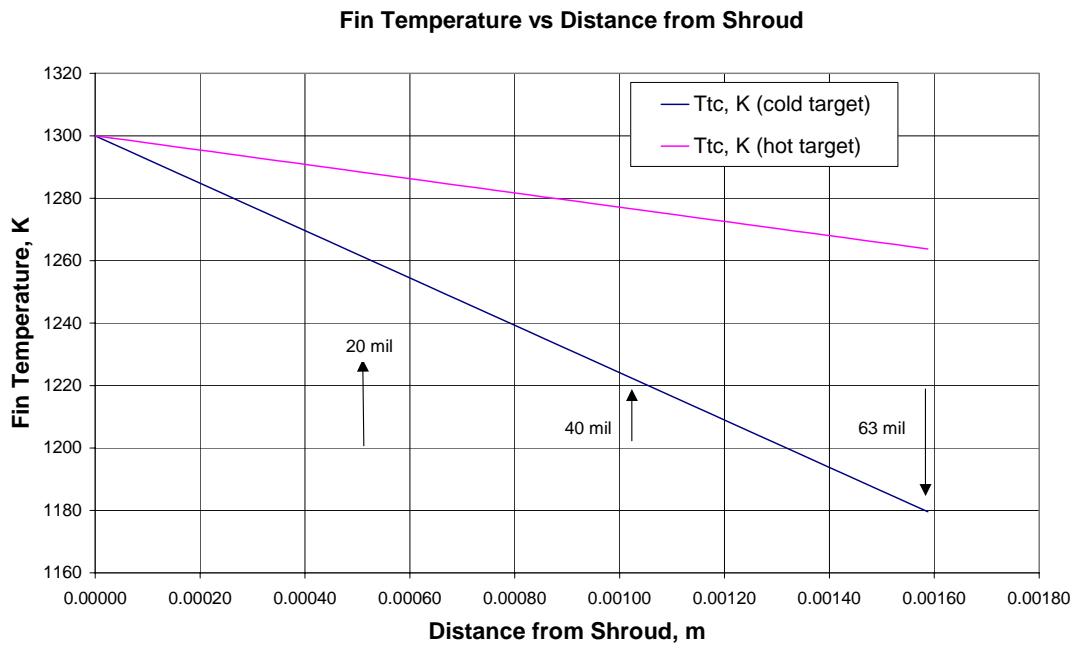


**Figure 19 Predicted Response of TC vs. TC Diameter For Target at 300 or 700K**

Implicit in the fin analysis is that the fin temperature at the junction of the shroud (x=0) is the same as the shroud temperature. This assumes that any contact resistance between the shroud and TC creates a negligible temperature difference. The heat transfer across the TC/shroud interface, assuming a contact resistance, can be estimated using the following relation:

$$\Delta T_{cr} = q * R_{cr}$$

where  $\Delta T_{cr}$  is the temperature drop due to contact resistance,  $q$  is the nominal heat flux across the TC/shroud interface, and  $R_{cr}$  is the contact resistance. As discussed in Appendix B the nominal heat flux at a 1000°C shroud temperature is about 100,000 W/m<sup>2</sup>. Contact resistances relevant for this application vary from about 10<sup>-4</sup> to 10<sup>-5</sup> m<sup>2</sup>-K/W.<sup>1</sup> Using an average value of 2E-05 one obtains a value of 2 K for  $\Delta T_{cr}$ , assumed negligible for our purposes.

### Phase 3 Experimental Description

Four experiments were performed to determine the effect of coupling due to the presence of a test target. A new shroud was fabricated for Phase 3 experiments, shown in Figure 20. It had six TCs – two 20-mil diameter, two 40-mil, and two 63-mil (all ungrounded junctions, inconel sheathed, Type K) located on the cold side of the shroud – in two groupings, each grouping containing a 20, 40, and 63-mil TC. It was assumed that within each grouping the shroud temperature is uniform. The 40-mil TC A2 was used as the control TC; the nominal shroud temperature was about 1100°C.

In the first two experiments the shroud temperature was raised with the shutter in place to a nominal 1100°C and held there for about six minutes. In this case a hotter target (insulated stainless steel shutter, hotter than the MVTU-2 calorimeter) was in place. Then the shutter was removed, exposing the shroud to a cold environment. TCs were again allowed to stabilize for another six minutes.

In the second test, the opposite occurred, i.e., the shutter was not in place until the shroud stabilized for about seven minutes, then the shutter was closed and the temperature was allowed to stabilize again.

In the third and fourth tests the same shroud was used with one of the MVTU-2 calorimeters to simulate a more realistic case, one with a test “target” that increased in temperature. The calorimeter was about 2 inches down from the bottom of the base plate (approximately 3.5 inches from the shroud). To assess the magnitude of the coupling effect, data was obtained using the same control TC with no target (no shutter, no calorimeter), with a reflective target (shutter in place), and with a target between those limiting cases (no shutter but with a calorimeter). These results would apply to setups similar to the ERB and MVTU-2 experiments (with water-cooled plates). Later, additional data from a test series performed in 1999 will be presented to show the effect of a large, hot target that radiates back to the shroud.

---

<sup>1</sup> MS Thesis draft, Victor Figueroa, April 2004.

## Shroud Temperature Characterization Experiments - Phase 3 Setup

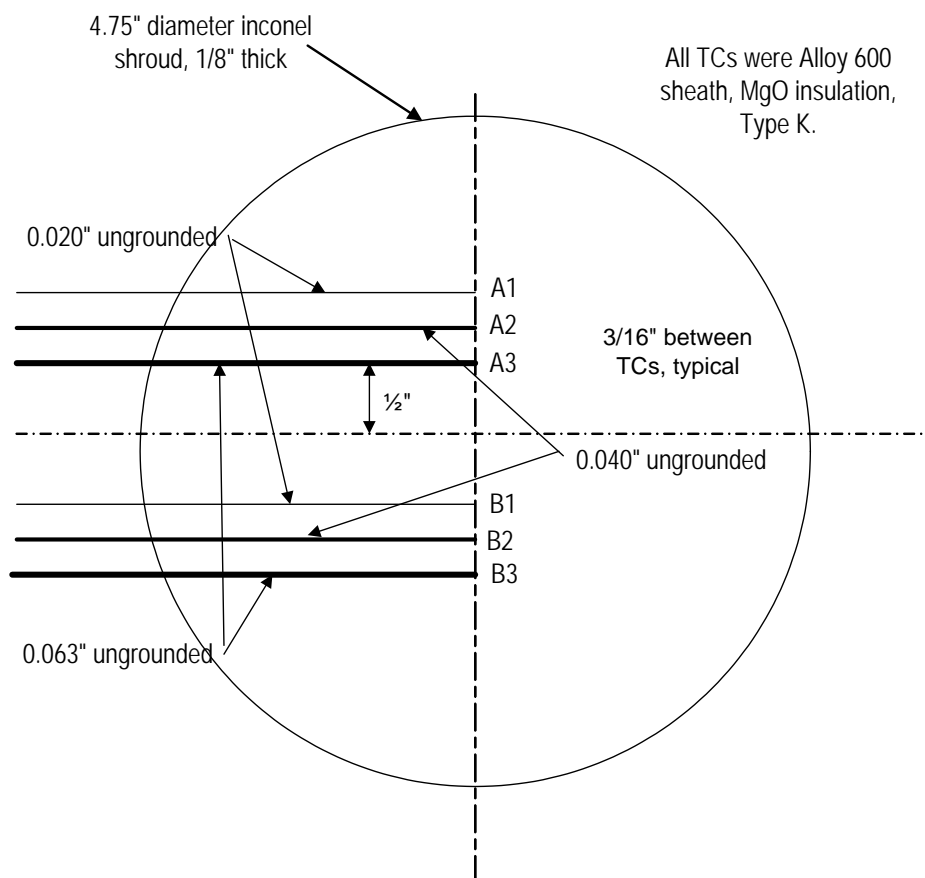


Figure 20 Phase 3 Shroud Thermocouple Locations

## Phase 3 Experimental Results

### Test #1 (9/25/03)

As stated above, in Test #1 the insulated stainless steel shutter was closed, (i.e., in place below the base plate), almost touching the bottom of the base plate. The insulation faced the bottom of the shroud. No calorimeter was used. Note that the overall experimental setup was similar to the schematic shown in Figure 2. Results can be seen in Figure 21 and Figure 22 where the shroud temperatures are plotted versus time.

### Phase 3 Shroud Temp. Characterization, Coupling Check, Test #1

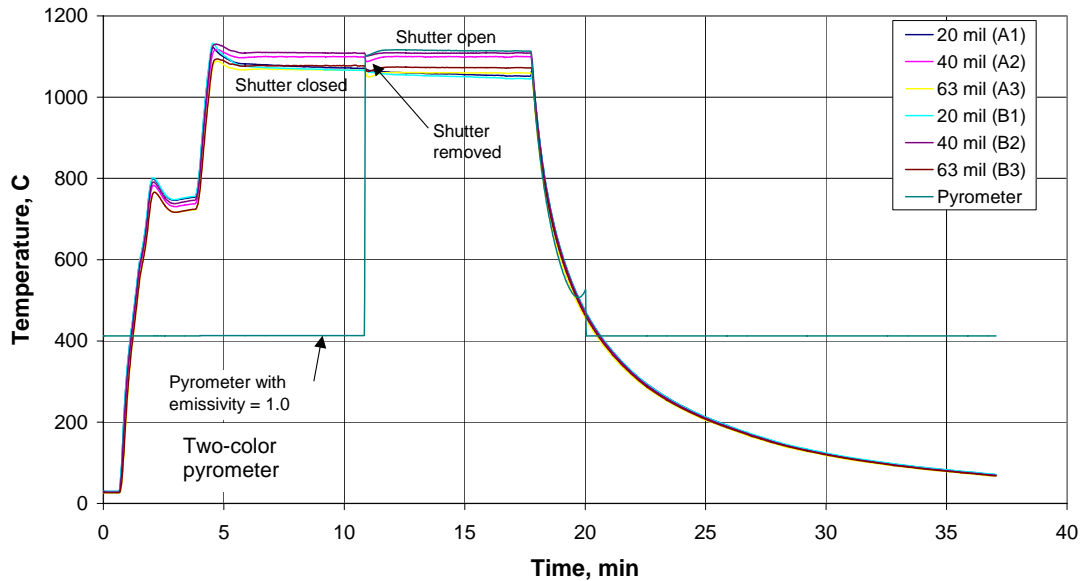


**Figure 21 Phase 3, Test #1 Results**

Careful analysis of the data from Figure 21 shows that 40 and 63-mil TCs are steady and almost constant for the duration of the test, except when the shutter was opened. In contrast, the 20-mil TCs showed a consistent drop in temperature and were below the 40 and 63-mil TCs. Since the behavior of the 20-mil TCs was unexpected, both 20-mil TCs were checked thoroughly. No obvious problem could be identified. However, though no problems were found, the behavior is not realistic (decreasing shroud temperature, below the 40 and 63-mil TCs) so the data were assumed faulty and not used. It is speculated that the problem was due to shunting (virtual junctions form away from the tip), which could cause a lower temperature.

Figure 22 shows a plot of the 40 and 63-mil TC readings with a reduced scale (1000-1200°C). Inspection of the data from TCs A2 (40-mil) and A3 (63-mil) showed that the difference between the two increased slightly from the point when the shutter was closed early in the experiment to when it was open later in the experiment. This behavior is consistent with the predictions shown using a fin model.

Similar results can be seen in Figure 22 when viewing TCs B2 (40-mil) and B3 (63-mil). Table 1 shows average values estimated from the data, and the times used for averaging. For Test #1, the average difference between A2 and A3 was about 32.3°C during the time when the shutter was in place, and about 39.6°C when the shutter was removed, for an increase of 7.3°C. As expected, the difference was larger in the second case with a cold target. Similar results are seen for TCs B2 and B3; the difference is 31.5°C when the shutter was in place and 35.8°C when the shutter was removed, for an increase of 4.3°C.

Assuming all other factors do not change during the test, one can assume that the presence of the shutter caused the change in the temperatures. Therefore, these results imply a small coupling effect (less than 10°C) between the shroud and the shutter for this setup.

### **“2-Color” Pyrometer Data, Test #1**

Figure 22 shows data from a “2-color” optical pyrometer in addition to the TC data. The pyrometer uses two closely spaced wavelengths (“2-colors”) to estimate the temperature of a radiating surface. It assumes a Planck-like distribution with wavelength so one can estimate the surface temperature without needing to know the emissivity. Requirements are that the surface is diffuse and the emissivity is the same at the two closely spaced wavelengths. The pyrometer focuses on a spot of about 4 cm (1.6 inch) so provides an average over that (rather large) spot size.

The manufacturer’s literature estimated the total uncertainty to be  $\pm 6-7^{\circ}\text{C}$ . Figure 22 shows that the pyrometer could not “see” the shroud when the shutter was in place. When the shutter was opened at about 11 minutes, the pyrometer registered a temperature slightly greater than the 40-mil TCs. Using the same time span to average the pyrometer data (14-16 min) as the TC data, the mean pyrometer temperature was about 1114.5°C. This compares with 1099.4 for 40-mil TC A2, and 1108.5°C for 40-mil TC B2. The pyrometer reads about 1% higher than TC A2 but only about 0.4% higher than TC B2. Based on Phase 4 experimental data discussed below, the temperature measured by the 2-color pyrometer should be slightly higher. Indications suggest that a correction may be required when using this device, but that data are not yet available so the pyrometer will not be modified.<sup>4</sup>

---

<sup>2</sup> Personal conversation between Walt Gill and Jim Nakos, December 2003.

**Phase 3 Shroud Temp. Characterization, Coupling Check, Test #1**

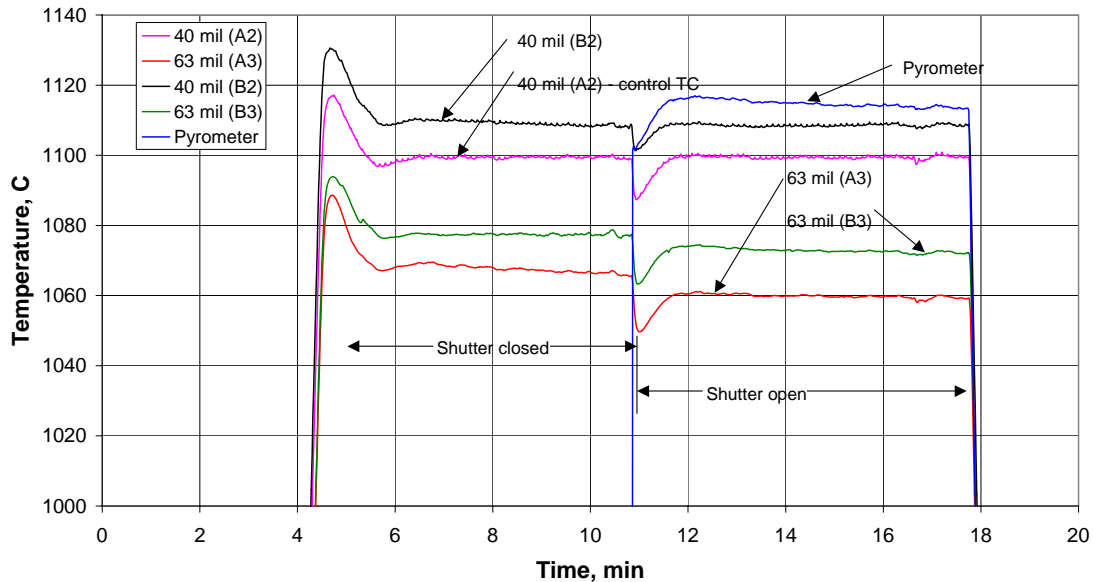


**Figure 22 Phase 3; Test #1 Results, 40 and 63-mil TCs**

**Test #2 (9/25/03)**

In Test #2, the shutter was not initially in place, and was moved into place after the shroud temperature stabilized at about seven minutes. As shown in Figure 23, in this test the difference between A2 and A3 decreased when the shutter was closed, as expected, but the difference between B2 and B3 actually increased, which was unexpected. This occurrence could have been due to TC B3 steadily decreasing in temperature after the shutter closed (see Figure 23) from about 12-20 minutes.

The results of this test are not conclusive if one includes data from TC B3, but is consistent with data from Test #1 in that a slight coupling effect exists if only data from A2 and A3 are used.

The 2-color pyrometer reads slightly higher than both TCs A2 and B2, as expected. The mean 2-color pyrometer data from Test #2 between 8 and 10 minutes is about 1122.8°C, as compared to 1098.5°C for TC A2 and 1109.3°C for TC B2. In this case the pyrometer reads about 1.8% higher than A2 but only 1.0% higher than B2.

**Table 1 Summary of Phase 3 Test Results**

Test #	Thermocouple	Averages, °C		Comments
		Shutter closed, 8-10 min	Shutter open, 14-16 min	
1	All			
1	40-mil, A2	1099.4	1099.4	Control TC so temperature did not change
1	40-mil, B2	1108.9	1108.5	Very slight change
1	63-mil, A3	1067.2	1059.8	Temperature decreased when shutter opened.
1	63-mil, B3	1077.5	1072.7	Temperature decreased when shutter opened.
1	A2-A3	32.3	39.6	Difference increased 7.3°C when shutter opened.
1	B2-B3	31.5	35.8	Difference increased 4.3°C when shutter opened.
2	All	Shutter open, 8-10 min	Shutter closed, 18-20 min	
2	40-mil, A2	1098.5	1098.6	Control TC so temperature did not change
2	40-mil, B2	1109.3	1111.0	Slight change
2	63-mil, A3	1062.3	1066.2	Temperature increased when shutter closed.
2	63-mil, B3	1072.6	1071.6	Temperature decreased when shutter closed.
2	A2-A3	36.2	32.4	Difference decreased by 3.8°C
2	B2-B3	36.7	39.4	Difference increased by 2.7°C
3	All	5-7 min	18-20 min	No shutter
3	40-mil, A2	1099.6	1099.6	Control TC so temperature did not change
3	40-mil, B2	1104.7	1103.0	Slight change
3	63-mil, A3	1069.8	1069.6	Almost no change between early and late times.
3	63-mil, B3	1074.1	1071.6	Temperature decreased between early and late times.
3	A2-A3	29.8	29.9	Negligible change
3	B2-B3	30.6	31.4	Negligible change
4	All	5-7 min	14-16 min	No shutter
4	40-mil, A2	1098.9	1099.2	Control TC so temperature did not change
4	40-mil, B2	1096.8	1089.7	Dropped about 7°C
4	63-mil, A3	1073.3	1072.3	Slight change
4	63-mil, B3	1071.8	1064.4	Dropped about 7°C
4	A2-A3	25.6	26.9	Small increase
4	B2-B3	25.0	25.3	Negligible change

**Phase 3 Shroud Temp. Characterization, Coupling Check, Test #2**

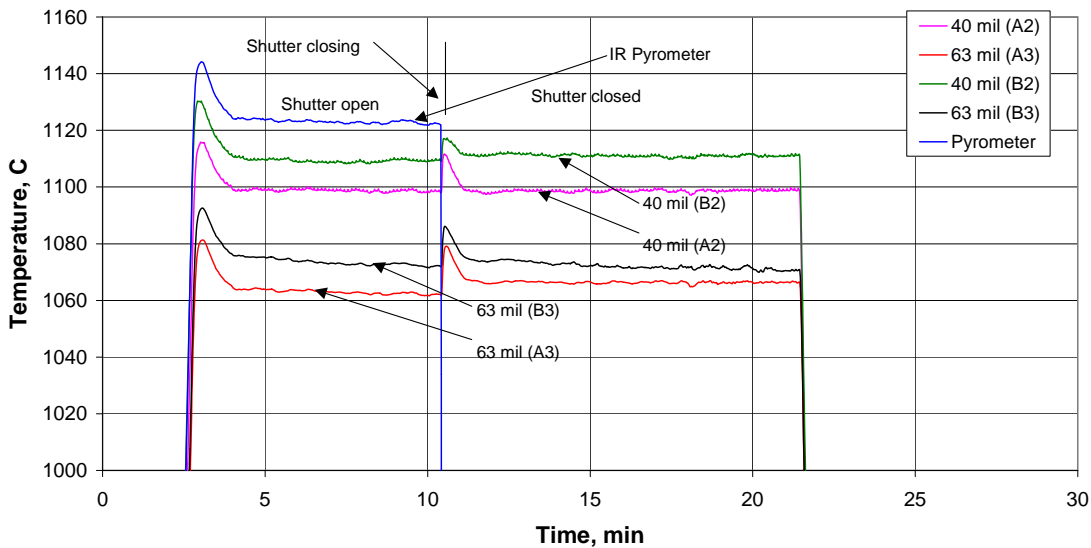


**Figure 23 Phase 3, Test #2 Results**

**Test #3 (9/25/03)**

This test was conducted without a shutter, and with the MVTU-2 calorimeter (painted with Pyromark 2500°F black) installed 2 inches below the base plate. The calorimeter temperature rose from ambient to about 500°C. This scenario most accurately represents a typical radiant heat experiment (i.e. W76 ERB and MVTU-2) where the test article is located several inches below the shroud. A second experiment (Test #4) was performed using the same parameters and settings to obtain redundant data.

Data are shown in Figure 24 and Figure 25 . Figure 24 shows that the calorimeter temperature stabilizes to about 500°C in about 20 minutes. The shroud temperature is almost constant for that time period.

Figure 25 shows shroud temperatures on a reduced scale. The temperature recorded by A2 is constant because it was the control TC, B2 and B3 dropped slightly during the test, while A3 was almost constant. It is thought that the decrease in temperature with time was due to slight changes in the paint, slight changes in the thermocouple attachment, or a decrease in the lamp power due to heat feedback from the test setup as the test progressed.

Table 1 shows differences between the 40 and 63-mil TCs for early times (five - seven minutes) when the calorimeter was relatively cool (300°C) and late times (18-20 min) when the calorimeter had reached 500°C. The change in the difference between the 40

and 63-mil TCs from early to late times is negligible, indicating virtually no coupling between the shroud and the MVTU-2 calorimeter.

**Test #4 (9/25/03)**

This last coupling test was intended to be a duplicate of Test #3. Results are shown in Figure 26 and Figure 27. As with Test #3, TCs B2 and B3 both decreased slightly during the test.

Averages were taken at 5-7 and 14-16 minutes, and the results are shown in Table 1. Similar to results from Test #3, there is very little change between the differences for the early and late times. This implies negligible coupling when using a calorimeter similar to the one used for the MVTU-2 tests.

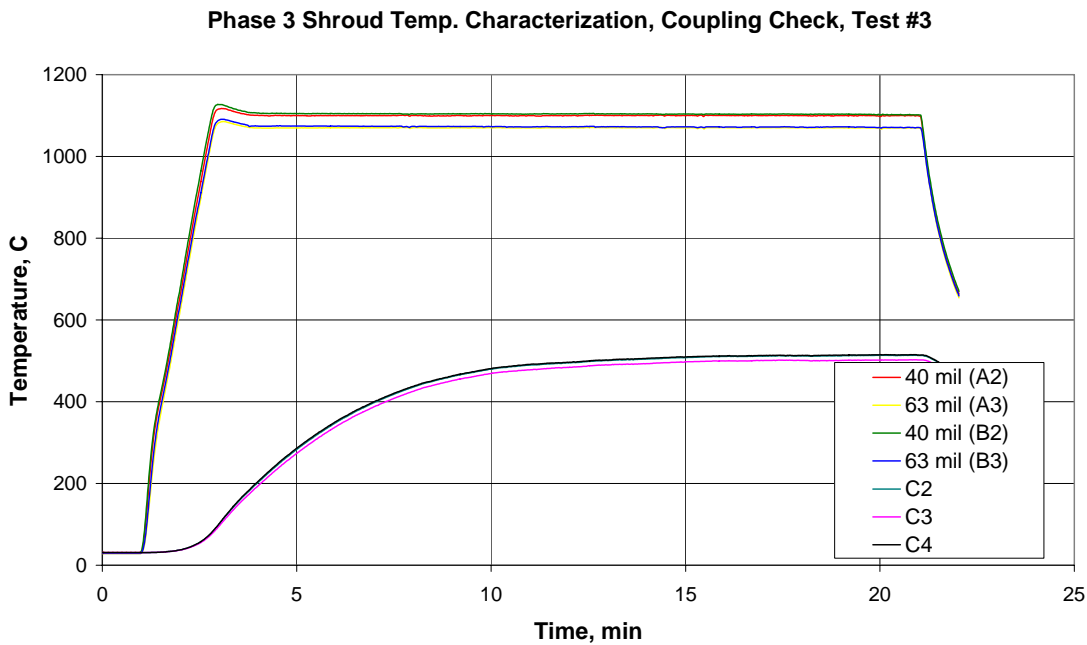


**Figure 24 Phase 3, Test #3 Results, Shroud and Calorimeter Data**

**Phase 3 Shroud Temperature Characterization, Test #3**

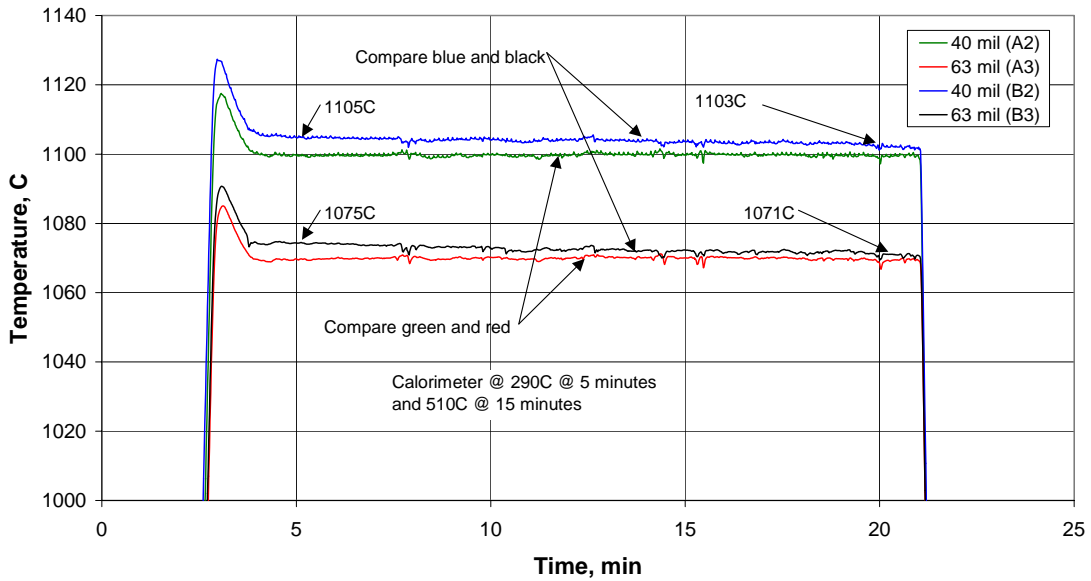


**Figure 25 Phase 3, Test #3 Results, Shroud Data**

**Phase 3 Shroud Temp. Characterization, Coupling Check, Test #4**

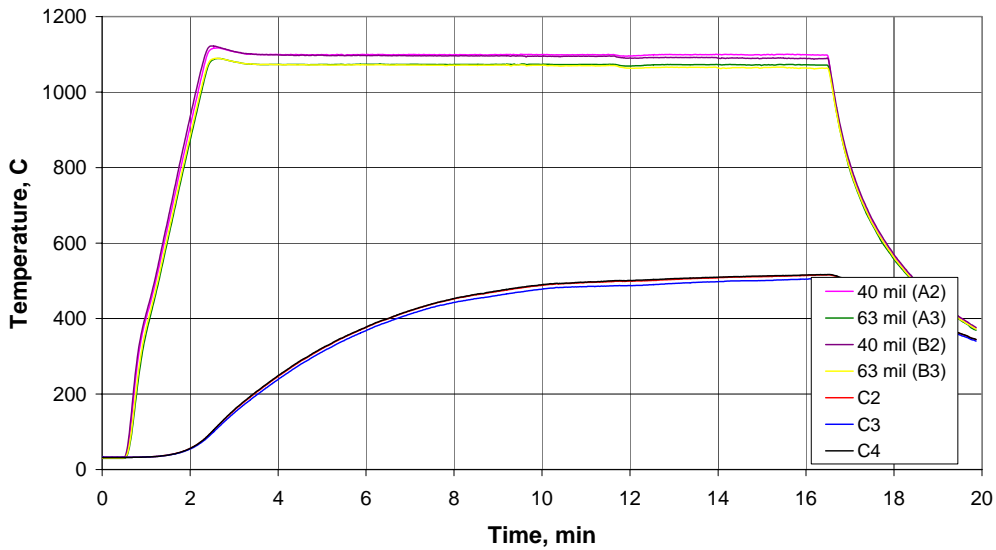


**Figure 26 Phase 3, Test #4, Shroud and Calorimeter Temperature Results**

### Phase 3 Shroud Temp. Characterization, Coupling Check, Test #4

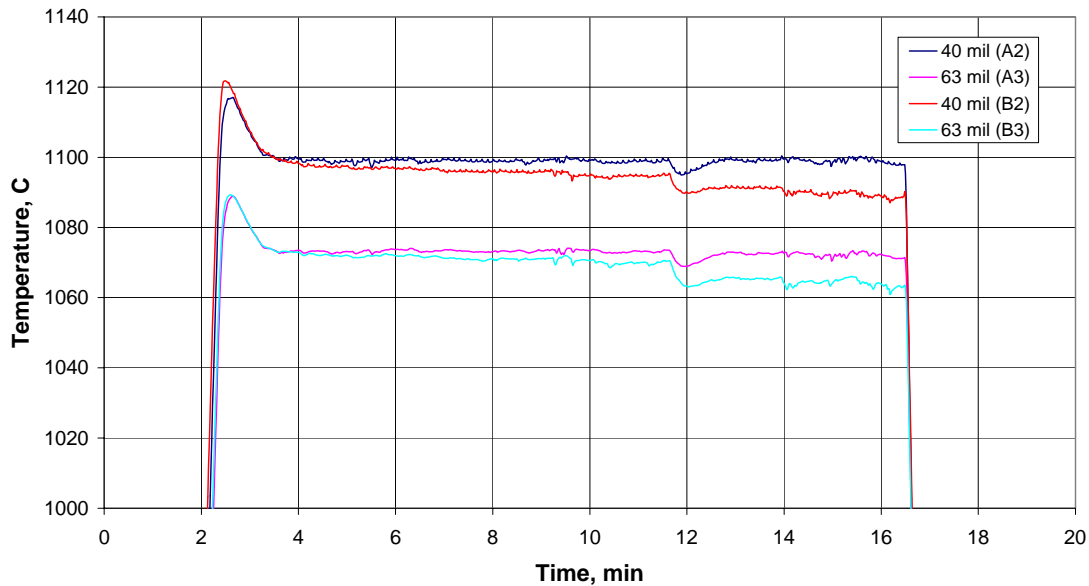


Figure 27 Phase 3, Test #4, Shroud Temperature Results (note lamp failure at ~12 minutes)

### Furnace Characterization Unit Tests

In 1999, a series of experiments was performed to study the response of a “Furnace Characterization Unit” (FCU). The FCU was built to characterize furnaces used for fire testing (check for furnace uniformity from test lab to test lab). Results of that study were documented in [3].

As part of that effort, 20 pairs of TCs were installed on the 1m x 1m flat shroud. At each location was a pair of TCs: one 63-mil ungrounded junction inconel sheathed TC and one intrinsically-mounted TC made from a 63-mil TC with the sheath stripped away. Assuming that the TCs are attached to a surface at a uniform temperature and the intrinsic TC is closer to the true temperature; differences between intrinsic and 63-mil TCs provide an estimate of the bias error of the 63-mil TC.

Figure 28 shows a sketch of the TC locations, Figure 29 is a photograph detailing how each pair of TCs was mounted, and Figure 30 is a photograph of the FCU.

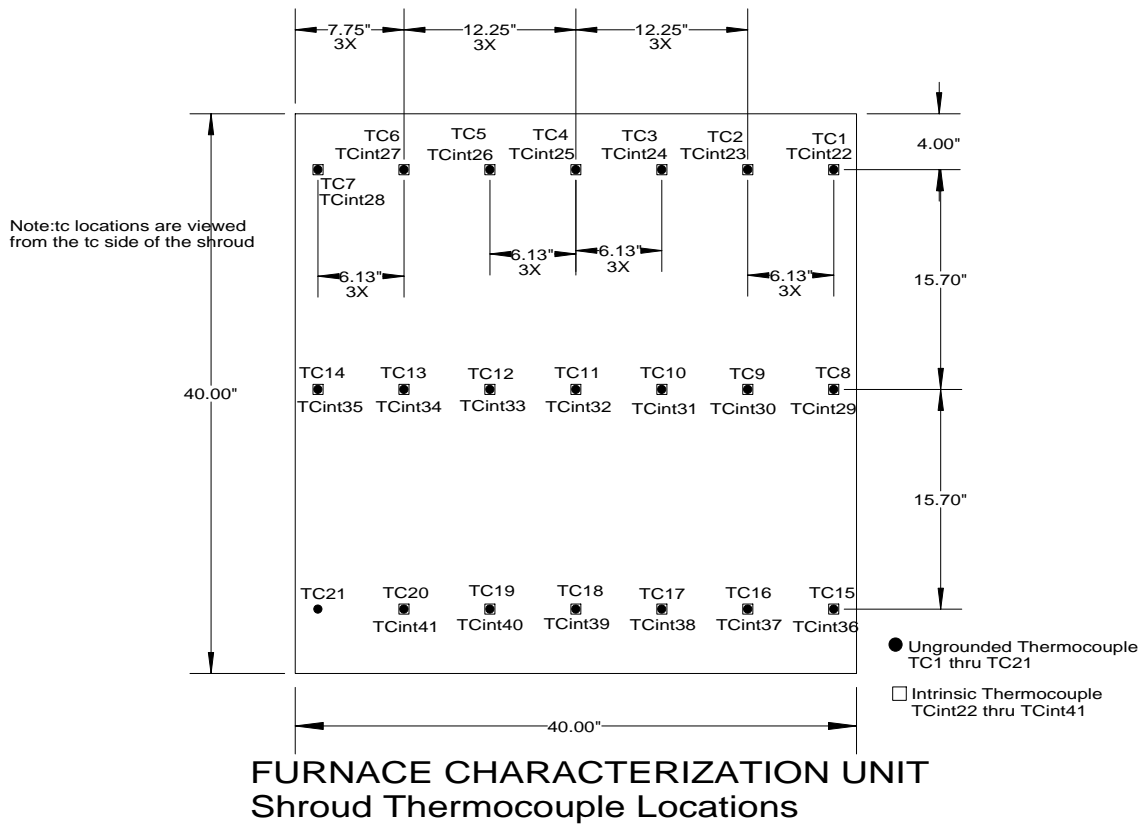


**Figure 28 FCU Shroud TC Locations**

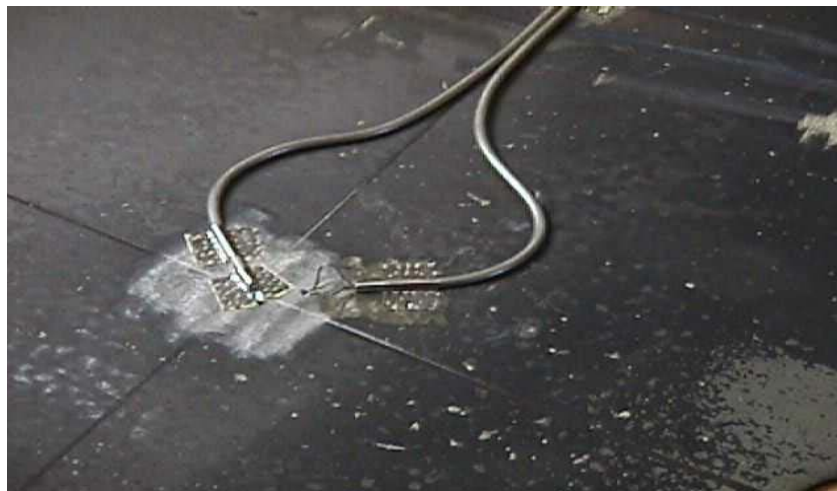


**Figure 29 Typical Pair of TCs (63-mil Ungrounded Junction and Intrinsic)**

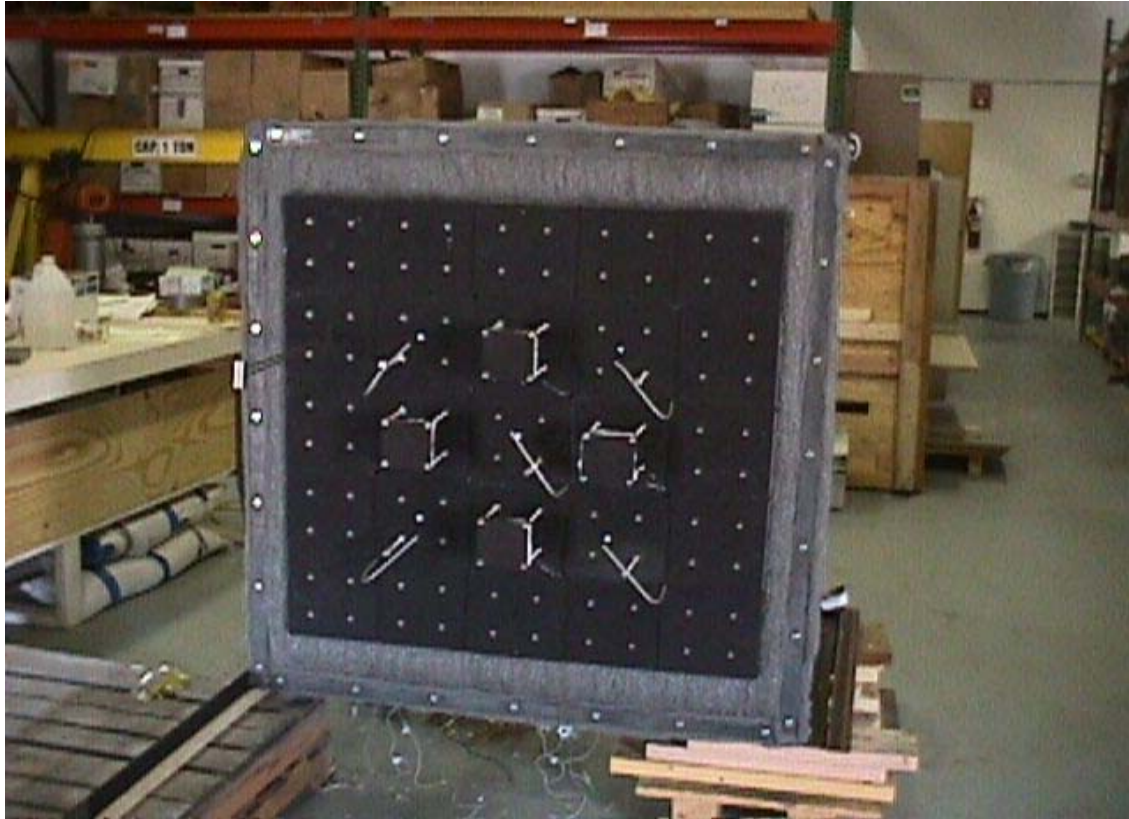


**Figure 30 Front Face Photograph of FCU**

Data from several tests will be presented to show the temperature differences between pairs of TCs (intrinsic-sheathed) when the FCU is in place, and when it is not. The FCU was a large (1m x 1m frontal area) steel structure, painted black. The front face temperature of the FCU rose in response to the shroud temperature. Additional instrumentation was present on the FCU front face, but that information is not presented here.

Two “check” tests were performed to be sure the setup worked properly, and to obtain IR camera data of the shroud with no FCU present. In all tests, the cold side of the shroud was surrounded by a rectangular mild steel enclosure (painted black) as shown in Figure 31. The only differences between the tests were the presence of the FCU and the shroud temperature profiles. After the two check tests, the FCU was installed and several tests were performed with differing shroud temperature profiles.



Figure 31 Side View of FCU Test Setup – FCU Not in Place

### Check Test Results (“Stair-Step” Shroud Profile)

Figure 32 shows the nominal shroud temperature profile for the second check test (control TCs). A failure occurred in the middle of the test due to control system problems; the problems were fixed and the test resumed. The shroud temperature was ramped from ambient to 1000°C in 100°C increments with a 5 minute hold at each temperature. Figure 33 shows results of the agreement between three pairs of TCs (each trace is the sheathed value subtracted from the intrinsic value) located in the middle of the shroud, away from the edges. In all cases, the intrinsic TC reads higher than the sheathed TC, resulting in positive values. In Figure 33 one would expect that TC31/TC10 and TC33/TC12 pairs should read the same, because they in symmetric locations on the shroud. For most of the test this is the case, but the TC33/TC12 pair show a larger error than does the TC31/TC10 pair. The reason is not known but could be due to changes in the intrinsic TC (not reliable for long periods at high temperatures) or gradients in the shroud temperature.

Results that can be compared with Phase 3 results (presented earlier) appear toward the end of the test, when the shroud temperature was at 900 or 1000°C. At 900°C the intrinsic value ranged from about 40-55°C (once the initial transient was over) higher than the sheathed value and at 1000°C the intrinsic TCs were 45-65°C higher than the sheathed thermocouples. As discussed later, the FCU shroud data and Phase 4 results are of the same magnitude. In these check tests the FCU is not in place, so the shroud is radiating to a “cold” environment.

**FCU Shroud Check Test 2, 10/20/99, Control TCs**

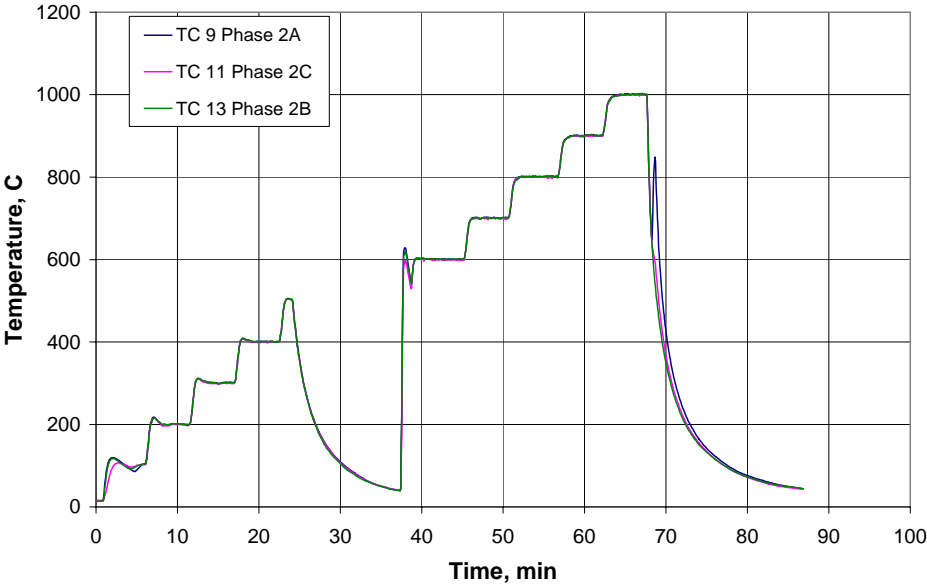


**Figure 32 Shroud Temperature Control TCs**

**Shroud Temperatures - Differences Between Intrinsic and Ungrounded Junction (63 mil), Calibration Test, 10\_20\_99, FCU Not in Place**

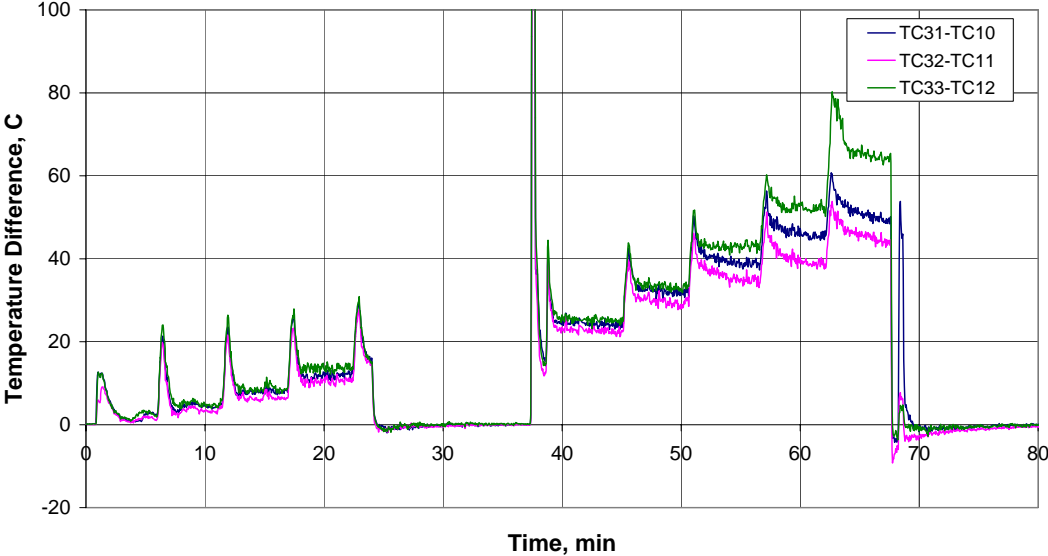


**Figure 33 Temperature Differences, FCU Not in Place**

## FCU Results (“Stair-Step” Shroud Profile)

Figure 34 and Figure 35 show results from an experiment when the FCU is in place. All other parts of the setup were unchanged. Figure 34 shows the nominal shroud temperature profile from the control TCs. Aside from the temporary failure (Figure 31), this profile is the same as for the check test except that the maximum temperature was only 900°C. Figure 35 shows temperature differences from the same three (plus one additional pair of) TCs as those in Figure 33. At 900°C, the differences range from 14-20°C just before the power was turned off. This difference is significantly lower than the 40-55°C differences seen in Figure 33. It is clear that a large difference exists between intrinsically mounted TCs and sheathed TCs depending on the properties of the enclosure (i.e., the “target” or test unit) facing the TC. The TC error is larger when radiating to a cold environment.

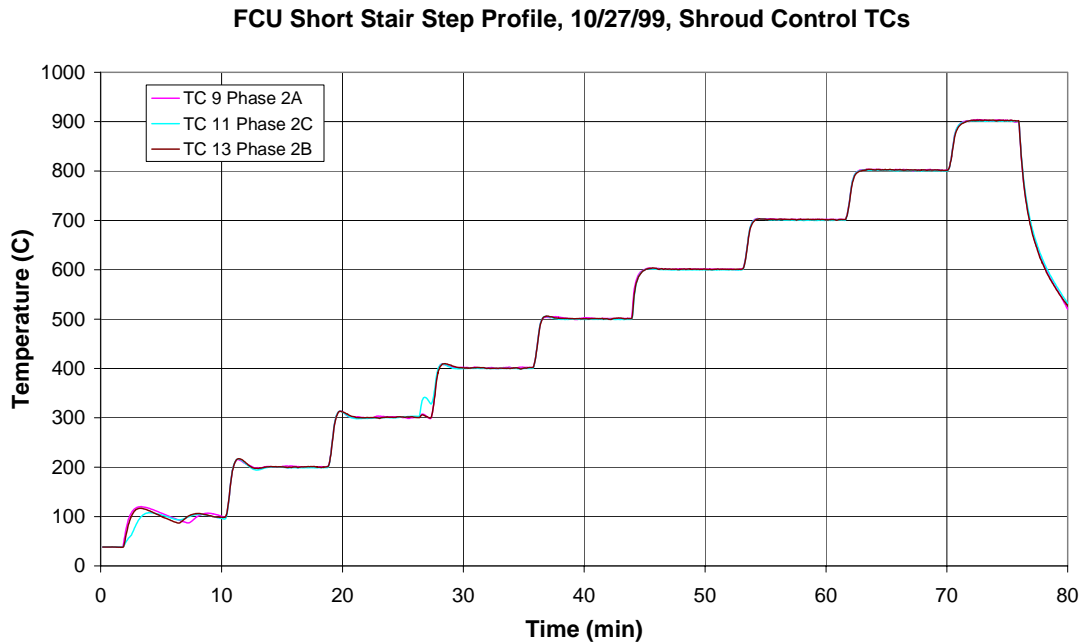


**Figure 34 Shroud Control Temperatures, “Stair Step” Test**

The total heat transfer from the TC to the environment is dependent on the total resistance to heat flow and the energy being radiated back to the TC from the environment. The total resistance has two components, 1) the “surface radiative resistance” ( $(1-\epsilon_i)/\epsilon_i A_i$ ) due to a finite surface emissivity (not equal to 1.0) and 2) “space or geometrical” resistance ( $(1/A_i F_{ij})$ ) due to the view factor and surface area [2]. Depending on surface areas and emissivities one will be larger than the other, but the resistance does not change with the target temperature. However, the presence of the FCU, initially cold then warming up (Figure 36), markedly decreases the difference between the intrinsic and sheathed TCs due to radiation from the FCU back to the TC. This statement is equivalent to saying the TC bias error is less with a large, high temperature target in place.

Repeat experiments, one without the FCU in place and another with the FCU in place showed similar results: the difference between the intrinsic and ungrounded sheathed TC was much higher when the FCU was not in place.

Therefore, importantly (and unfortunately), the TC bias error will be significantly dependent on the TC enclosure/environment. As a result, estimates of shroud temperature error should be assessed on a case-by-case basis if precise shroud boundary condition measurements are required. The magnitude of the coupling between a shroud and an object is dependent on the object's size, temperature, and distance from the shroud. This magnitude should be assessed prior to performing validation experiments using the particular test fixture relevant to that experiment.

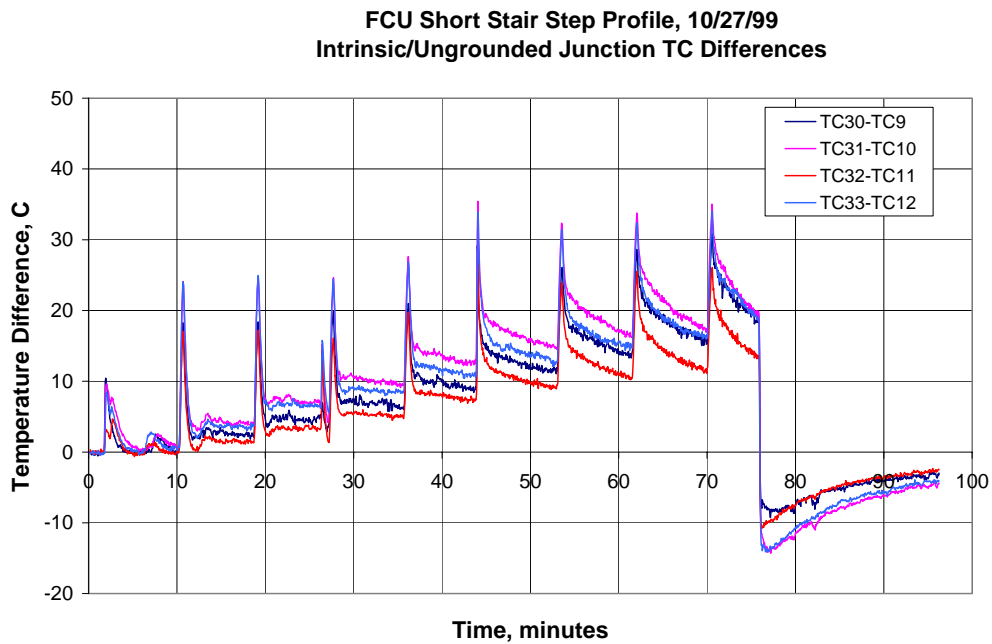


**Figure 35 Temperature Differences, FCU in Place**

Typical FCU Temperatures, Stair Step Test

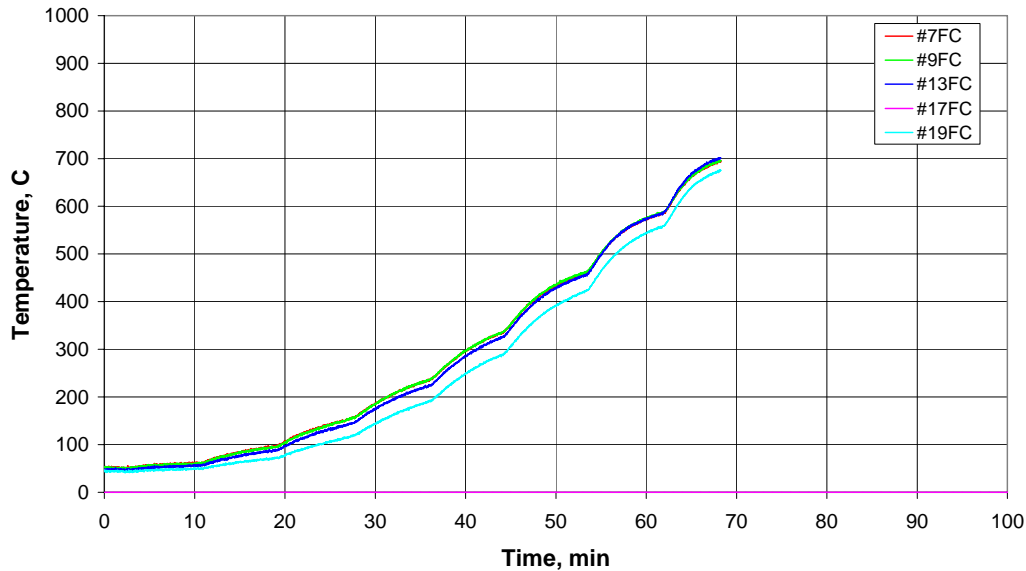


Figure 36 Typical FCU Front Face Temperatures (Separate DAS Terminated after 68 minutes)

## Phase 3 Summary and Conclusions

### Results Relevant to MVTU-2 and Exclusion Region Barrier Experiments

- 4 experiments were performed to obtain information on the coupling effect of test target presence and shroud TC response.
- 2 experiments were performed, one with and one without a shutter.
- 2 experiments were performed with a calorimeter in place to simulate a test target similar to ones used in the Campaign 6 MVTU-2 and W76-1 ERB projects, with an increasing temperature.
- A 2-color IR pyrometer was used to measure the shroud temperature in a 1.6” diameter spot. For Test #1 the pyrometer read about 0.4-1.1% higher than the 40-mil TCs, and 1.0-1.8% higher in Test #2. As will be seen in Phase 4 results, the corrections estimated from TC data are larger than these values (Figure 48: 3.6-4.2%). The discrepancies could be due to the relatively large spot size used by the pyrometer (1.6 inches” diameter), or because a correction is needed for the pyrometer.
- Fin theory was used to estimate the effect of both TC sheath size and test target presence.
- Fin theory predicted that the difference between different sized TCs would be greater with no target present, and less with a high temperature (1000K) target present.

- Fin theory predicted an increasing error with sheath diameter with an almost linear trend, consistent with experimental results.
- Fin theory predicted a larger error with a cold target, consistent with experimental results.
- Experimental results showed negligible differences between 40 and 63-mil diameter TCs between a cool target (300K) and a hot target (773K), but did show differences consistent with fin theory when an insulated target (shutter in place) was compared to one at 300K.
- For targets typical of the W76-1 ERB and MVTU-2 tests, coupling considerations on shroud temperatures are negligible. For larger, higher temperature targets, coupling does need to be investigated.
- 20-mil TCs provided unreliable readings when used at typical (1000°C) shroud temperatures.

## Results From FCU Experiments

- Results from testing with no FCU in place (shroud radiating to a cold environment) showed that intrinsic TCs read 45-65°C higher than sheathed TC at a nominal 1000°C. This result is about a 3.5-5.1% difference (absolute temperature). (Note that to obtain a correction factor the intrinsic TC has to be corrected as well – see Phase 4 results.)
- Results from testing with the FCU in place (shroud radiating to and being irradiated by a large steel structure) showed the smallest differences (14-20°C) at a nominal 900°C shroud temperature. This result reflects about a 1.2-1.7% difference.

## Overall Conclusions

- For MVTU-2 and ERB experiments, the effect of test object/target coupling is negligible on TC bias error, but the bias error itself is not negligible.
- For other setups (e.g., a large object whose temperature increases with time) the TC bias error can be much less, but coupling can be important.
- The magnitude of coupling should be assessed for each experimental setup using a mock fixture if schedule and resources permit. Generalizations about when coupling is important are difficult to formulate since the coupling magnitude depends on the size and temperature of the target.

## **Phase 4 Experiments**

The purpose of Phase 4 experiments was:

1. To obtain experimental data on the response of thermocouples (TCs) of various sheath diameters and intrinsically mounted TCs;
2. To develop a methodology that allows estimates of the “true” shroud temperature;
3. To provide correction factors for various sized TCs (40 and 63-mil diameter ungrounded junction, inconel sheathed) used to measure shroud temperature to estimate the true shroud temperature; and
4. To further test the hypothesis that fin theory is an appropriate way to explain the temperature variation with sheath diameter.

Intrinsic TCs are fabricated by stripping away a portion of the metal sheath of MIMS TCs. In this case the 0.063 inch diameter sheathed TCs were stripped to expose the individual chromel and alumel wires. In applications where the shroud can be welded to metal (e.g., inconel and stainless steel), each wire is individually spot welded to the shroud surface, so the shroud surface completes the electrical circuit. In this way the shroud is an “intrinsic” part of the measurement system. This technique is believed to be the most accurate surface temperature method using TCs. (These are also called “exposed junction” TCs.)

Eight thermocouples were mounted on one side of a 1/8 inch thick, 4.75 inch diameter shroud, in two groupings of four TCs each. Each set had an intrinsic TC, a 0.020 inch diameter, ungrounded junction TC, a 0.040 inch diameter ungrounded junction TC, and a 0.063 inch diameter ungrounded junction TC. Each set of four TCs was mounted in close proximity so that temperature gradients in the shroud would have the least effect on measurements. It was assumed that each group of four TCs measured the same temperature. Figure 37 shows a photograph of the shroud side containing the eight TCs.

In Figure 37 it is difficult to see the individual chromel and alumel wires coming out of the sheath of the intrinsic TCs, so locations are noted. Figure 38 shows a schematic view in the same orientation as shown in Figure 37.

In addition to the eight TCs mounted on one side of the shroud, there were two 40-mil diameter, grounded junction TCs on the other side. These were installed to provide control TCs during those tests when the eight TCs were on the hot side of the shroud (facing the lamps), and to provide lamp-side data when the eight TCs were facing away from the lamps (cold side). Grounded junction TCs were used only because ungrounded junction TCs were not available. See Figure 38 for locations of these two TCs.

## **Phase 4 Results**

Eight experiments were performed as part of the Phase 4 effort. Table 2 shows the test matrix. The first two experiments were conducted with the eight TCs facing the lamps (hot side). The last six experiments had the two 40-mil TCs facing the lamps. The shroud temperature was controlled by the TCs on the side facing away from the lamps

(cold side), to avoid exposing the control TCs to the harsh environment caused by the very high temperature lamps. Therefore, the control TC was always on the cold side of the shroud. Each TC was sampled once per second.

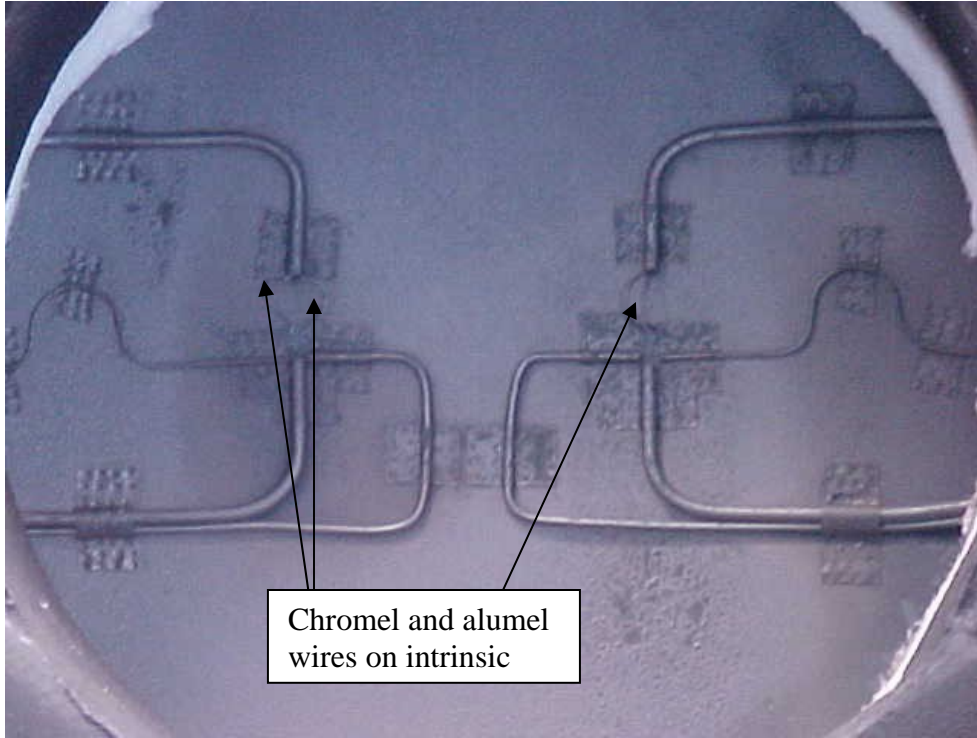


**Figure 37 Shroud TCs used in Phase 4 Experiments**

# Shroud Temperature Characterization Experiments - Phase 4 Setup

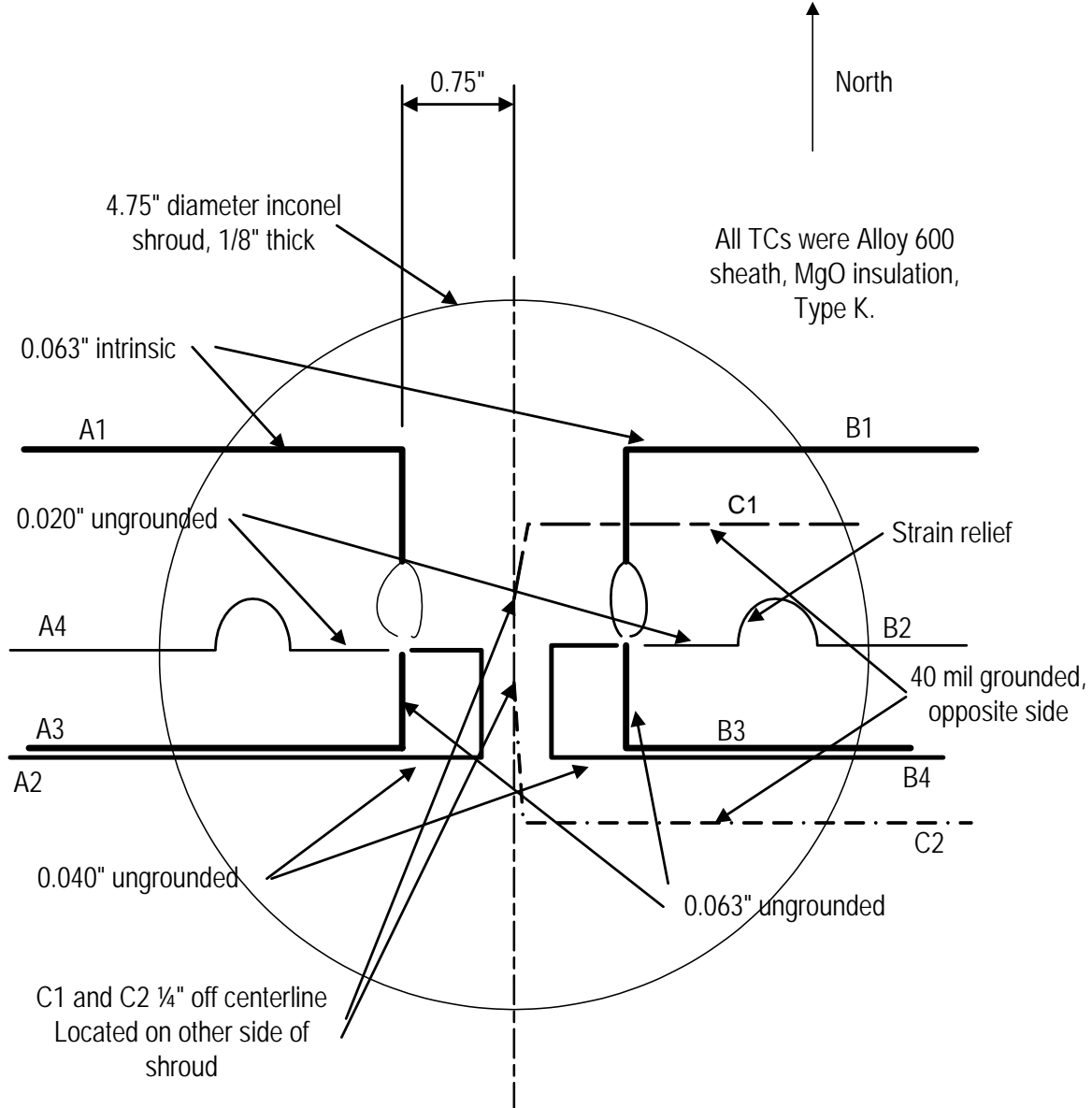


**Figure 38 Shroud TC Locations, Phase 4 Experiments**

**Table 2 Phase 4 Experimental Matrix**

Test #	Orientation	Nominal Shroud Temperature, C	Control TC	Comments
1	8 TCs on hot side	1000	C1	One lamp failed, calm winds, dry, hot, 17 lamps.
2	8 TCs on hot side	1000	C1	One lamp failed, calm winds, dry, hot, 17 lamps.
3	8 TCs on cold side	1000	A4	All lamps good, slight breeze (< 5 mph), dry, hot, 17 lamps.
4	8 TCs on cold side	1000	A4	All lamps good, slight breeze, dry, hot, 17 lamps.
5	8 TCs on cold side	900	A2	All lamps good, minimal breeze, cloudy, warm, 17 lamps.
6	8 TCs on cold side	900	A2	One lamp failed, calm winds, cloudy, warm, 17 lamps.
7	8 TCs on cold side	1100	A2	All lamps good, slight breeze, dry, hot, 17 lamps.
8	8 TCs on cold side	1100	A2	All lamps good, slight breeze, dry, hot, 21 lamps. More lamps to decrease load on each lamp.

Tests 1 & 2 were nominally identical, to obtain redundant data, as were Tests 3 & 4, 5 & 6, and 7 & 8. Tests 1, 2, 3 & 4, were controlled at a nominal shroud temperature of 1000°C. Tests 5 & 6 were at 900°C and Tests 7 & 8 at 1100°C.

In each experiment, the shroud temperature was raised from ambient (about 30°C) to the nominal value in approximately two minutes. The temperature was held until the shroud temperatures stabilized and then maintained for a few extra minutes (five minutes typically) to obtain steady data. No shutter was used and the shroud was free to radiate to a cold environment. This scenario would bound the maximum expected error (i.e., the error would be less with a hot target close to the cold side of the shroud).

Figure 39 and Figure 40 show data typical of all the tests. Figure 39 shows data from Test #1 where the eight TCs faced the lamps. The data shows that the intrinsic TC reads the lowest, followed by the 0.020 inch diameter TC, then the 0.040 TC, and then the 0.063 TC. The 0.063 inch diameter TC reads the highest, or in other words has the

largest error (bias). Notice the slight temperature dip at about 400 sec. A lamp failed at that time so the shroud temperature was temporarily reduced by a few degrees. The control system automatically compensated and added more power to the remaining lamps and returned the temperature to the set-point.

Data from the cold side of the shroud, facing away from the lamps, shows the two 40-mil diameter TCs (C1 and C2) reading lower than the ones on the lamp side, as was expected. Note that C1 and C2 read different values, which could be partially attributed to non-uniform shroud temperature since the thermocouples were located ½” apart. TC C1 reads about 1000°C at 300-400 sec, while TC C2 reads about 1013°C. This variation is within the uncertainty bounds of the TCs and data acquisition system and is consistent with the data on the shroud temperature distribution collected during Phase 1 experiments.

An uncertainty analysis for these experiments was performed and found the TC uncertainty without compensating for the bias due to the finite TC diameter (which we are trying to determine via this study) to be about 0.6% of the reading in Kelvin. The largest part of that uncertainty is due to the standard TC accuracy of 0.75% of the reading (in °C). Other components are almost negligible. See Reference [4] for details of the uncertainty analysis. For a nominal temperature of 1000°C, the uncertainty bounds for each TC is about ±8°C, so a 13°C difference between the two TCs is within the maximum difference of 16°C.

Figure 40 shows data from Test #4, where the two 40-mil TCs faced the lamps and the eight TCs faced away from the lamps. In this case, the 40-mil TCs facing the lamps read highest. On the other side, the intrinsic TCs read highest, followed by the 20-mil TCs, the 40-mil TCs, and finally the 63-mil TCs. Again, the 63-mil TCs had the largest error.

Results shown in Figure 39 and Figure 40 indicate that the larger diameter TCs have the largest error. Steady state data from all eight experiments were reduced by averaging 100 data points (100 sec) during a time period when the temperature was constant. Average values and standard deviations (variations about the mean) were estimated for all ten TCs. Average data for all TCs and all eight tests are shown in Table 3. Only a single average standard deviation is shown for each TC because they were small and almost the same for all cases. This result implies stable TC readings.

**Shroud Temperature Characterization, Phase 4, Test #1,  
TCs Facing Lamps, 7/31/03**

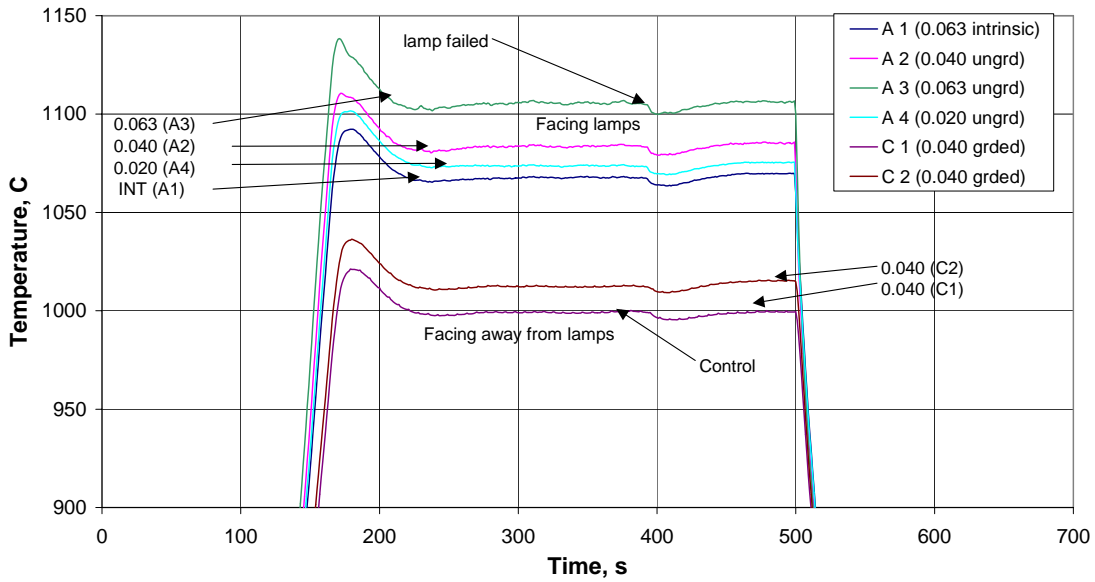


**Figure 39 Typical Data Set, TCs Facing Lamps, Test #1**

**Shroud Temperature Characterization, Test #4,  
TCs Facing Away from Lamps**

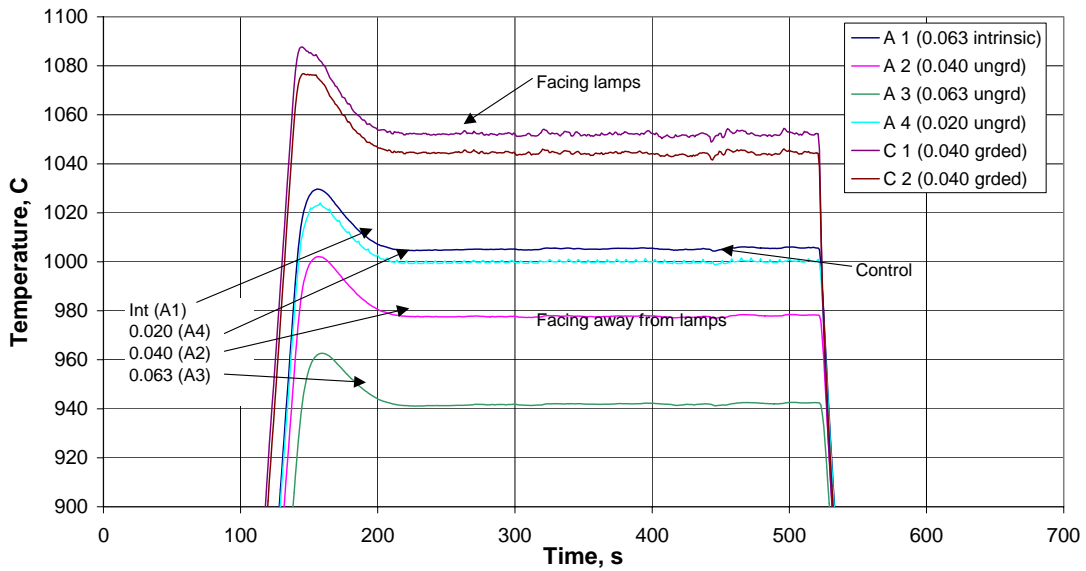


**Figure 40 Typical Data Set, TCs Facing Lamps, Test #4**

**Table 3 Summary of Phase 4 Experimental Data (All Data in °C)**

Test #	Averaging times, sec	A1 avg	A2 avg	A3 avg	A4 avg	B1 avg	B2 avg	B3 avg	B4 avg	C1 avg	C2 avg
1	290-390	1067.7	1083.7	1105.7	1073.7	1073.4	1077.0	1092.0	1092.4	999.3	1012.3
2	300-400	1069.0	1088.4	1108.0	1074.8	1079.4	1085.1	1100.6	1100.1	998.9	1010.3
3	350-450	1004.9	979.0	941.5	999.9	1000.0	992.0	944.6	964.3	1053.8	1045.2
4	290-390	1005.3	977.7	941.8	1000.0	999.8	992.0	943.4	964.1	1052.2	1044.4
5	290-390	921.9	899.1	865.8	915.9	917.3	907.2	867.3	885.5	961.9	952.1
6	290-390	922.2	899.0	866.5	916.0	917.5	907.0	867.3	885.4	962.4	952.0
7	1000-1100	1132.3	1099.1	1053.8	1123.2	1125.0	1111.4	1055.2	1080.7	1186.2	1175.1
8	1000-1100	1132.4	1098.2	1052.6	1124.1	1125.3	1113.8	1053.0	1081.8	1189.2	1179.7
All	Avg std dev	0.3	0.3	0.3	0.3	0.4	0.4	0.4	0.4	0.5	0.4

A1 = intrinsic TC made from 0.063 inch diameter sheathed TC

A2 = 0.040 inch diameter sheathed TC

A3 = 0.063 inch diameter sheathed TC

A4 = 0.020 inch diameter sheathed TC

B1 = intrinsic TC made from 0.063 inch diameter sheathed TC

B2 = 0.020 inch diameter sheathed TC

B3 = 0.063 inch diameter sheathed TC

B4 = 0.040 inch diameter sheathed TC

## **Determining the “True” Shroud Temperature Using Two Methods**

One of the results of this study is the evaluation of two different methodologies by which to find the “true” shroud temperature: 1) the extrapolation method; and 2) the averaging method. In the first method, a correction factor allows the shroud temperature data gathered via 40 or 63-mil TCs to be adjusted to an estimated “true” temperature that can be used by thermal analysts to represent the shroud boundary condition. A second method is proposed which relates the temperature of two thermocouples on opposite sides of the shroud to the “true” shroud temperature, but no experimental data are available to compare with the model since thermocouples placed on opposite sides of the shroud in earlier experiments were not at the exact same location. As additional experimental data become available, the two models will be further evaluated.

The results of an ongoing project to model the response of sheathed TCs may be able to answer this question. A detailed CALORE model is being developed to assess the errors of 63-mil ungrounded junction, sheathed TCs mounted on a flat shroud.<sup>5</sup> However, results of those simulations are not available at this time.

### **“True” Shroud Temperature by the Extrapolation Method**

The true shroud temperature will be estimated by plotting the average shroud temperatures from the 20, 40, and 63-mil diameter TCs along with the intrinsic TCs, and then extrapolating to “zero” TC diameter. The intrinsic TCs allow the closest measure of surface temperature (without the use of non-contact devices like an IR camera). Details of the method are shown in the sections that follow.

### **Interpretation of Intrinsic TC Data**

A large body of published data (References [5] - [8]) on the response of intrinsic TCs on solid surfaces exists. Keltner and Beck [5] model a stylized intrinsic TC as a right circular cylinder welded perpendicular to the shroud surface. Though our geometry is different (the cylinder is welded parallel to the surface) the behavior shown in [5] is consistent with data from the experiments described here for TCs with “displaced junctions,” i.e., where the location of the junction is above the surface being measured.

Data from the 20, 40, and 63-mil TCs can be plotted versus the displaced distance of the junction assuming the junction is located half the sheath diameter from the surface, in the midpoint of the TC. Locating the displaced distance for the intrinsic TCs is less obvious.

Because the surface being measured is part of the electrical circuit for an intrinsic TC, one might say there is zero displacement. However, using the same analogy as that used for the MIMS TCs, half of the wire diameter should be used as the junction location. For intrinsic TCs made from 63-mil diameter sheaths, the individual chromel and alumel wire diameters are about 0.012 inches. Because the wires are flattened to perhaps two thirds of the original diameter (about 0.008 inches) at the weld location, an “average” diameter

---

<sup>5</sup> Draft Masters Thesis by Victor Figueroa, September 2004.

then might be about 0.010". Therefore, the effective displacement will be about half of 0.010 inches, or about 0.005 inches. This estimate will be used for intrinsic TCs.

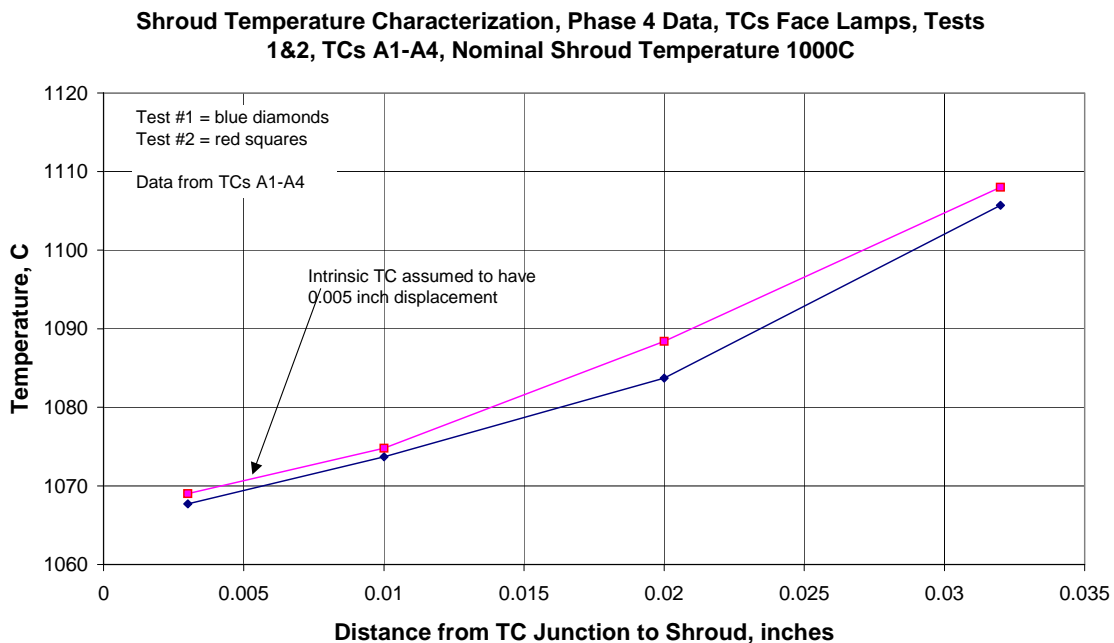
### Shroud Temperature Results versus Junction Displacement

Figure 41 and Figure 42 plot the average temperature (100 samples) versus displacement from the surface for the two sets of four TCs (hot side, facing lamps). Figure 41 shows results from Test #1, TCs A1-A4, and Figure 42 shows data from Test #1, TCs B1-B4. As can be seen in Figure 41, larger diameter TCs have higher temperatures, smaller diameter TCs lower temperatures. Similar data can be seen in Figure 42 except the 63-mil TC is almost the same as the 40-mil TC. This result is not consistent with the trends in the other TCs (the 63-mil should be higher); therefore, the TC is assumed to be an outlier and the data were not used in the analysis.

Figures 43 shows data from Tests 3 & 4, Figure 44 shows data from Tests 5 & 6, and Figure 45 shows data from Tests 7 & 8. Trends similar to what was observed for Tests 1 & 2 are seen in these plots where the eight TCs face away from the lamps. However, the curves are now concave downward.

Figures 43 through 45 clearly indicate a temperature decrease with an increase in sheath diameter when the thermocouples are on the cold side. This trend is the opposite of what occurred in Tests 1 & 2 when the eight TCs faced the lamps, but expected. Overall, the largest diameter TC has the largest error.

To obtain an estimate of the "true" shroud temperature, the measured values were extrapolated from Figures 41 through 45 (below) to zero displacement. One may choose to fit a curve through those figures to obtain such an estimate, however that may not be the best method.



**Figure 41 Indicated Shroud Temperature versus Junction Displacement, Tests 1 & 2, TCs A1-A4**

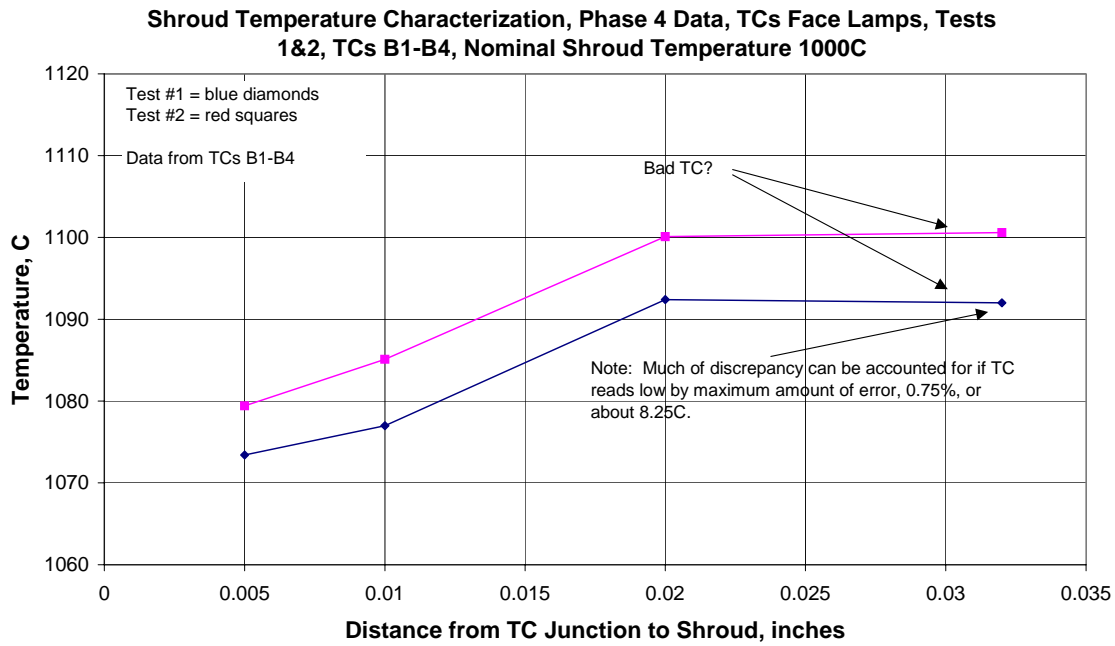


**Figure 42 Indicated Shroud Temperature versus Junction Displacement, Tests 1 & 2, TCs B1-B4**

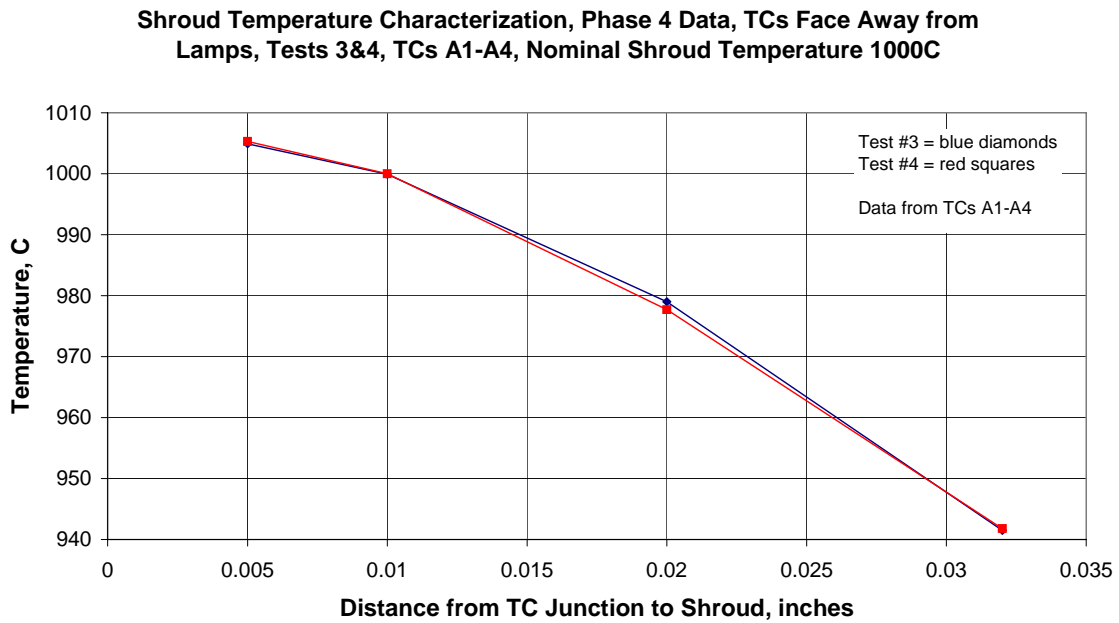


**Figure 43 Indicated Shroud Temperature versus Junction Displacement, Tests 3 & 4, TCs A1-A4**

**Shroud Temperature Characterization, Phase 4 Data, TCs Face Away from Lamps, Tests 5 & 6, TCs A1-A4, Nominal Shroud Temp. 900C**



**Figure 44 Indicated Shroud Temperature versus Junction Displacement, Tests 5 & 6, TCs A1-A4**

**Shroud Temperature Characterization, Phase 4 Data, TCs Face Away from Lamps, Tests 7 & 8, TCs A1-A4, Nominal Shroud Temp. 1100C**



**Figure 45 Indicated Shroud Temperature versus Junction Displacement, Tests 7 & 8, TCs A1-A4**

In another similar series of experiments performed for the MVTU-2 project, three sets of three TCs (20, 40, and 63-mil ungrounded junction) were mounted in a fashion similar to the eight experiments described above. Four (4) experiments were performed on the same setup, two at 900°C and two at 1000°C. A sketch of the shroud TC layout is shown in Figure 46 and results are shown in Figure 47.

## MVTU-2 Shroud TC Check - Different Diameters

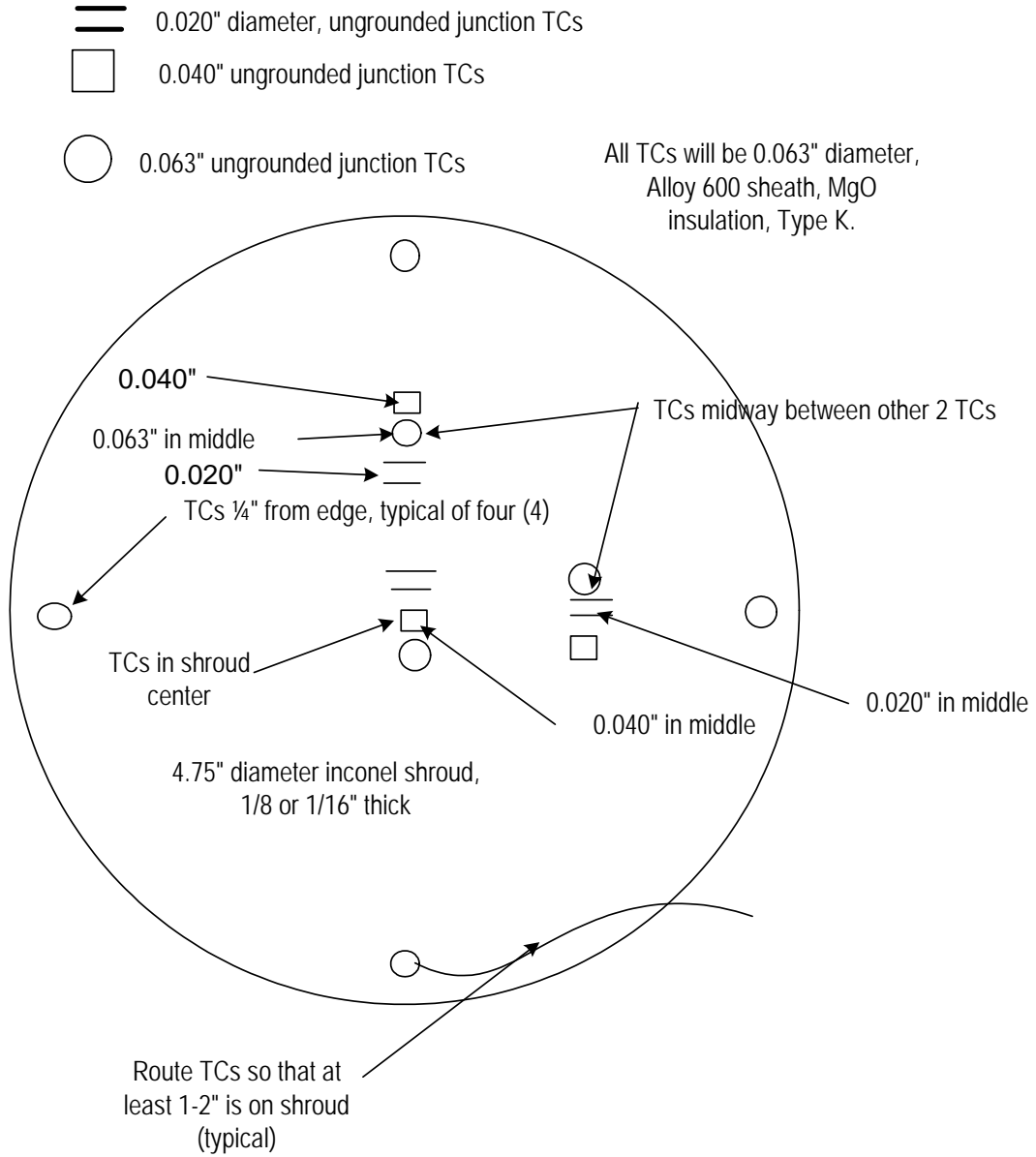


**Figure 46 Shroud TC Layout for MVTU-2 Experiments**

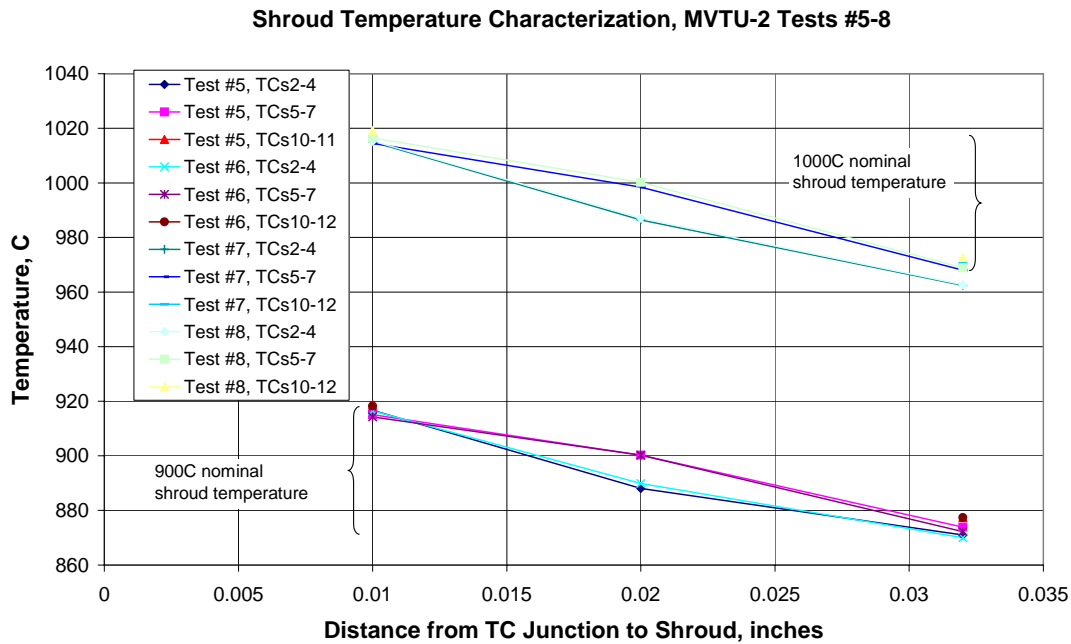


**Figure 47 Typical Steady Shroud Temperatures for MVTU-2 Experiments**

Figure 47 shows the shape of the curve to be concave up in some cases and concave down in others. These differing results are partially due to the uncertainties in typical TC measurements. For example, if one modified a single 20-mil TC reading to the maximum value possible due to uncertainty levels, the curve could change from concave down to concave up, or to almost linear. This result implies no clear experimental justification for assuming the extrapolation to the true shroud temperature should be concave up, down, or linear. Therefore, a more theoretical basis is needed to help define how to extrapolate the data.

As described in Appendix A, the response of a TC approximated by a square fin has the same characteristics as the experimental data. Results from Appendix A indicate an almost linear temperature variation with distance from the shroud. This feature is in contrast to the data in Figures 43 through 45 which show a slight concave downward shape, but is consistent with the trends in Figure 47. The fin theory model is idealized and may not be truly representative of actual TC behavior. The linear shape will be used to best estimate the extrapolation to zero diameter.

### Extrapolation Using “Cold” Side Data

In the extrapolation method, it will be assumed that the true shroud temperature can be determined by linearly extrapolating the data from the intrinsic, 20, 40, and 63-mil TCs to zero displacement. It is expected that a linear extrapolation is an adequate estimate of the relevant physics. Average values of each of the cold side TCs were used in a linear

regression fit to the data, and results that estimate the “true” shroud temperature (zero diameter) are shown in Table 4.

The true shroud temperature can also be estimated via the 40-mil diameter, grounded junction<sup>3</sup> TCs on the hot side of the shroud. First, the 40-mil grounded junction TCs are corrected by an amount estimated from data in Tests 1 & 2 (Figure 41 and Figure 42). Then an approximate temperature gradient through the shroud thickness is estimated, and the 40-mil TC readings are adjusted to estimate a true shroud temperature on the cold side.

Those results are seen in the last two columns of Table 4. In most cases, the adjusted temperatures from hot side TCs C1 and C2 are close to the extrapolated, “true” temperatures (columns two and three) using cold side data. These results lend more credibility to the extrapolated values. Table 5 shows the error between the “true” shroud temperature and the cold side 40-mil TCs at three nominal shroud temperatures. A plot of percent error versus nominal shroud temperature is shown in Figure 48 (TCs on cold side). Figure 48 indicates that the estimated error for a 40-mil TC rises slightly with nominal shroud temperature, and is 3.26-3.86% of the temperature in K.

---

3 Note: the response of grounded and ungrounded junction TCs were compared with intrinsic TCs on the same shroud in another set of shroud temperature characterization experiments performed under the MVTU-2 project. Results showed that out of 12 sets of data (where all TCs faced away from the lamps), the grounded junction TC read higher than the ungrounded junction TC in four cases by about 1%, the reverse was true in four cases by about 2%, and the two read virtually the same in four cases. Differences are due to slight variations in TC calibration and junction location within the sheath. It will therefore be assumed that there is negligible difference between the response of grounded and ungrounded junction TCs.

**Table 4 Estimation of True Shroud Temperature**

Test #	“True” Shroud Temp Extrapolated from TCs A1-A4 (°C)	“True” Shroud Temp Extrapolated from TCs B1-B3 (°C)	TC C1, Adjusted to zero displacement (°C)	TC C2, Adjusted to zero displacement (°C)	Approx Shroud Temp Gradient (°C)	Approx “True” Shroud Temp from Adjusted C1 & Temp Gradient (°C)	Approx “True” Shroud Temp from Adjusted C2 & Temp Gradient (°C)
1	1059.5 <sup>4</sup>	1065.7	1050.2	1063.7	17.2	NA	NA
2	1062.9	1071.9	1049.8	1061.6	17.4	NA	NA
3	1021.3	1013.9	1024.6	1016.2	14.7	1009.9	1001.5
4	1021.3	1013.8	1023.0	1015.4	14.7	1008.3	1000.7
5	935.6	928.2	934.7	925.1	11.2	923.5	913.9
6	935.6	928.3	935.2	925.0	11.2	924.0	913.8
7	1150.9	1140.4	1154.1	1143.2	21.7	1132.4	1121.5
8	1151.8	1141.3	1157.0	1147.7	21.5	1135.5	1126.2

<sup>4</sup> Note that for Tests 1 & 2 TCs A1-A4 and B1-B3 were on the hot side. To estimate the “true” shroud temperature on the cold side one has to correct for the estimated temperature gradient through the shroud.

**Table 5 Estimated Error, % Between 40 Mil TC and “True” Shroud Temperature (Figure 48 )**

Test #	Nominal Shroud Temp., °C	“True” Shroud Temp from TCs A1-A4 (°C)	40 Mil TC reading, °C, A2	40 Mil TC Error, % from A2 & True temp. (absolute)	“True” Shroud Temp from TCs B1-B3 (°C)	40 Mil TC reading, °C, B4	40 Mil TC Error, % from B4 & True temp. (absolute)
1	1000	1059.5	NA	NA	1065.7	NA	NA
2	1000	1062.9	NA	NA	1071.9	NA	NA
3	1000	1021.3	979.0	3.26	1013.9	964.3	3.85
4	1000	1021.3	977.7	3.37	1013.8	964.1	3.86
5	900	935.6	899.1	3.02	928.2	885.5	3.55
6	900	935.6	899.0	3.03	928.3	885.4	3.57
7	1100	1150.9	1099.1	3.64	1140.4	1080.7	4.22
8	1100	1151.8	1098.2	3.76	1141.3	1081.8	4.21

**Table 6 Estimated Error, % (of Absolute) Between 63 Mil TC and “True” Shroud Temperature (Figure 49 )**

Test #	Nominal Shroud Temp., (°C)	“True” Shroud Temp from TCs A1-A4 (°C)	63 Mil TC reading, °C, A3	63 Mil TC Error, % from A3 & True temp. (absolute)	“True” Shroud Temp from TCs B1-B3 (°C)	63 Mil TC reading, °C, B3	63 Mil TC Error, % from B3 & True temp. (absolute)
1	1000	1059.5	NA	NA	1065.7	NA	NA
2	1000	1062.9	NA	NA	1071.9	NA	NA
3	1000	1021.3	941.5	6.16	1013.9	944.6	6.06
4	1000	1021.3	941.8	6.14	1013.8	943.4	6.06
5	900	935.6	865.8	5.77	928.2	867.3	5.67
6	900	935.6	866.5	5.72	928.3	867.3	5.71
7	1100	1150.9	1053.8	6.82	1140.4	1055.2	6.72
8	1100	1151.8	1052.6	6.96	1141.3	1053.0	6.66

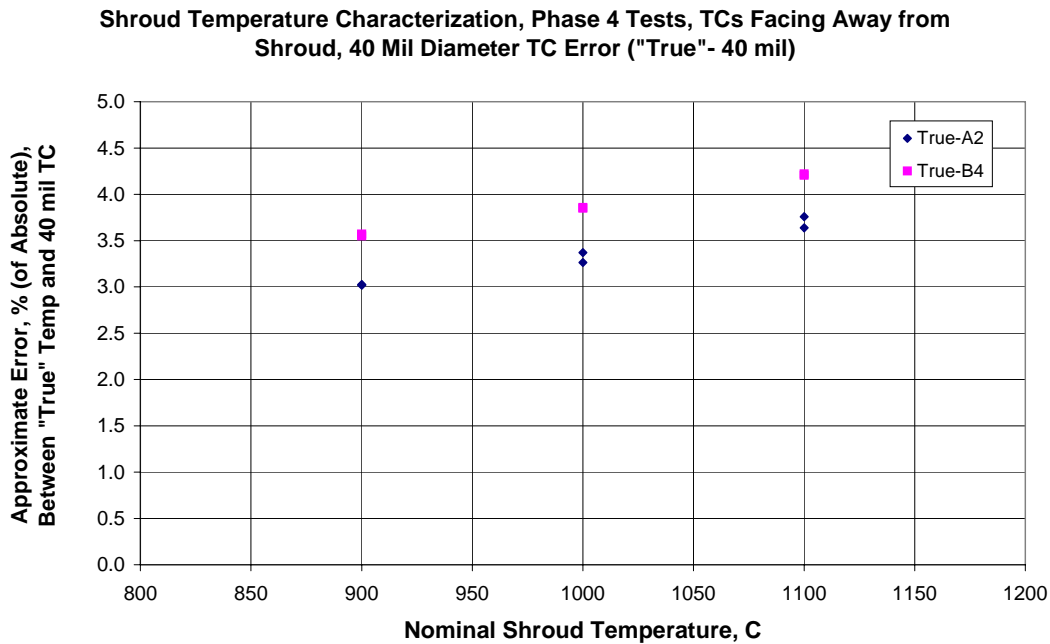


**Figure 48 Estimated Error Between a 40 Mil Ungrounded Junction Sheathed TC and the “True” Shroud Temperature**

As can be seen in Table 4, the “true” shroud temperature extrapolated from TCs A1-A4, B1-B3, C1, and C2 are approximately equal for Tests 3-8. The maximum/minimum differences between pairs (A1-A4, B1-B3, C1-C2) of estimated true shroud temperatures are 19.8°C/4.0°C for Test #3, 20.6/5.5°C for Test #4, and 21.7/4.7°C, 21.8/4.3°C, 29.4/8.0°C, and 25.6/5.8°C for Tests #5-8. This result compares with the  $\pm 0.6\%$  (of absolute temperature) DAS uncertainty which is about a 15°C spread for Tests 3 & 4, a 14°C variation for Tests 5 & 6, and a 17°C variation for Tests 7 and 8. The  $\pm 0.6\%$  uncertainty results in an overlap in the uncertainties of the “true” shroud temperature estimated from TCs on opposite sides of the shroud. Uncertainty in estimating the temperature gradient across the shroud is another reason for the discrepancies.

Therefore, it is assumed that for 40-mil diameter ungrounded junction TCs mounted on the shroud facing away from the lamps, the correction factors shown in Figure 48 should be used to increase the effective shroud temperature. This is the case when no target is present. Assuming the target present is similar to that used in the Phase 3 studies (target was MVTU-2 calorimeter), the error in Figure 48 does not need to be adjusted further.<sup>5</sup>

A similar analysis was performed for 63-mil TCs, often used for shroud temperature measurements in the past due to their robustness. Table 6 and Figure 49 show the results. At a

<sup>5</sup> Both Figure 48 and Figure 49 plot error as a function of nominal shroud temperature, which is the only measurement one has during a test. The error values in Table 5 and 6 were calculated using the “true” shroud temperatures rather than the “nominal” shroud temperature. Therefore, when using Figures 48 and 49 there will be a slight error incurred because one has to multiply the % error by the nominal shroud temperature (which is known) rather than the true shroud temperature (unknown).

nominal shroud temperature of 1000°C, the approximate error is about 6.1%. Note that the trend in the correction factor for different size thermocouples is not necessarily linear (see fin theory section in Appendix A).

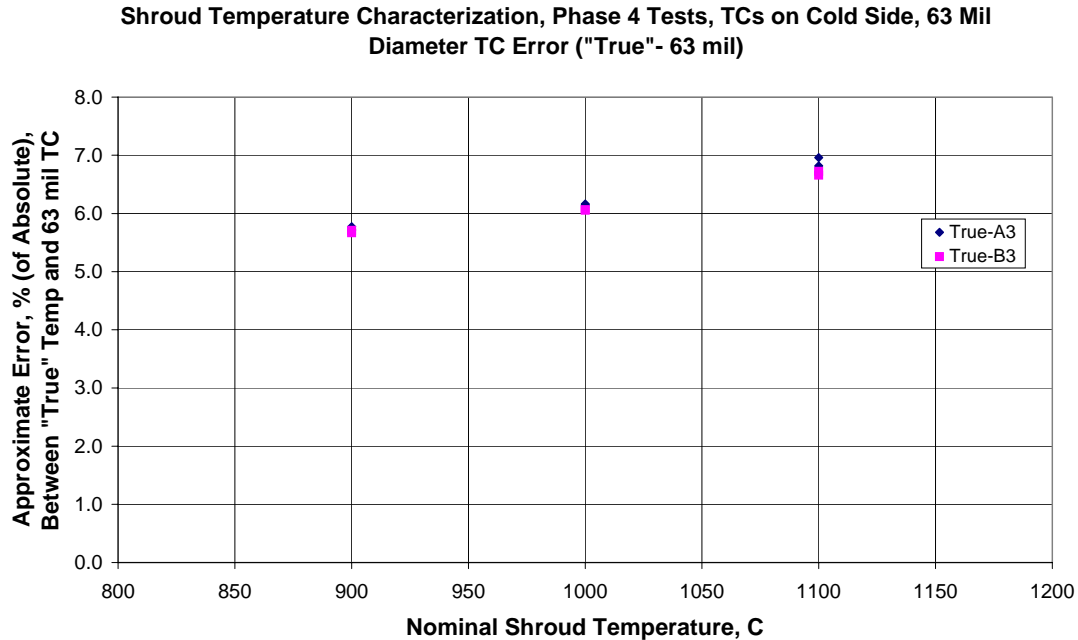


**Figure 49 Estimated Error Between a 63 Mil Ungrounded Junction Sheathed TC and the “True” Shroud Temperature**

Table 7 is provided to facilitate use of Figures 48 and 49. It provides approximate values of the error, as a function of nominal shroud temperature, for 40 and 63 mil diameter TCs.

**Table 7 Estimated Errors for 40 and 63 mil Diameter TCs, % of Absolute Temperature**

Nominal Shroud Temperature, C	40 mil Sheath Diameter, % of absolute temperature (average of 4 values in Table 6) <sup>4</sup>	63 mil Sheath Diameter, % of absolute temperature (average of 4 values in Table 6)
900	3.3	5.7
1000	3.6	6.1
1100	4.0	6.8

### “True” Shroud Temperature by the Average Temperature Method

Dykhuisen and Gill [9] have analyzed the shroud temperature and proposed an alternative method for estimating the true shroud temperature. Their analysis is reproduced in Appendix B. The analysis assumes 1-dimensional conduction through the shroud, and radiative heat loss from

<sup>4</sup> See footnote 5.

the back (cold) side to the ambient. The “true” hot and cold side shroud temperatures were assumed to be equal to the TC measurements indicated by hot and cold side TCs plus a correction due to the bias error. The correction factor was assumed to be linearly proportional to the TC sheath diameter, heat flux and a “free parameter” ( ), and inversely proportional to the shroud temperature raised to an unknown power ‘n’. The free parameter and power ‘n’ were adjusted to agree with experimental data. Results of the analysis suggest a simple method to estimate the true shroud temperature. Two TCs of the same size are used, one mounted on the hot side facing the lamps, the other on the cold side facing the test object. Averaging the two temperatures to obtain a representative value for the “true” cold side temperature is proposed, and is suitable for the accuracy of the TC data normally acquired.

While weighting the average toward the cold (nearest the test fixture) side is an option, it is difficult to assess the impact an object might have on the shroud. Therefore, a simple average is likely the best approach. This conclusion can be further investigated during initial experiments. The averaging method is believed to be favorable because it is simple and easy to use, and can be done for each experiment. Therefore, the correction factors in Figure 48 and Figure 49 are provided as information on potential uncertainties. It should be noted that these correction factors may not apply to test setups significantly different from the MVTU-2 and W76-1 ERB experiments.

### **Recommendation for Estimating “True” shroud Temperature**

The authors of this report recommend using both methods. Obtaining two “identical” TCs is often difficult, and the TCs facing the lamps are in a very severe environment and sometimes fail or give anomalous readings. Therefore, for each shroud temperature measurement used for model validation purposes, three TCs should be installed. The first two are as proposed in the averaging method (2 TCs of nominally equal size and type, on opposite sides of the shroud at the same location) and the third, positioned on the cold side, should be a different diameter than the other two so the extrapolation method can be used. In this manner two independent methods can provide the most confidence possible. Therefore, if either method fails, the redundancy will ensure that the experimental data are not lost. Differences in the two methods (inevitable) should be resolved using engineering judgment. If initial experiments indicate that one method is preferable, all future tests will use that method with the alternative method simply as a backup. Experience (V&V milestone activities) will indicate which method is best.

### **Phase 4 Summary and Conclusions**

- Eight (8) experiments were performed.
- Shroud was instrumented with two, 40-mil TCs on one side and eight TCs on the other. Eight TCs consisted of two groups of four (4) TCs: a 20-mil diameter; a 40-mil diameter; a 63-mil diameter; and an intrinsic TC made from removing the sheath of a 63-mil TC.
- On hot side of shroud, larger diameter TCs read higher and had the largest errors.
- On cold side, larger diameter TCs read lowest and had the largest errors.
- On hot side, intrinsic TCs read lowest; on cold side intrinsic TCs read highest.
- Behavior of TCs with respect to sheath diameter is consistent with fin theory.
- Correction factors are estimated for 40 and 63-mil TCs at three relevant nominal shroud temperatures (900, 1000, and 1100°C) as shown in Figure 48 and Figure 49. These correction factors are relevant for MVTU-2 and ERB experiments.

- At a 1000°C nominal shroud temperature, the 40-mil TC reads low by about 3.6% and the 63-mil TC reads low by about 6.1% (Temperature in K).
- If analysts use a single shroud temperature from a 40 or 63-mil TC, they should increase the effective radiation temperature by the bias correction factors in Figure 48 and Figure 49, or Table 7.
- Two TCs of the same size and location, but on opposite sides of the shroud, can be averaged to estimate the “true” shroud temperature. This is the averaging method.
- It is recommended that both the “extrapolation” and “averaging” methods be used to provide an estimate of the true shroud temperature suitable for use in modeling activities, until and if one proves to be demonstrated to be favorable.
- Upcoming validation experiments will provide us with information on the potential suitability of the methods.

## **Phase 2 Experiments**

The goal in Phase 2 was to provide information on shroud temperature distribution, TC errors, and discretization errors.

A shroud was instrumented with intrinsic TCs in addition to two 40-mil ungrounded junction TCs, and the approximate locations of the intrinsic TCs are shown in Figure 50. The responses of the different instruments (IR camera, 40-mil, intrinsic TCs) were assessed and it was discovered that the IR image provided the most complete representation of the temperature distribution; an average temperature distribution was easily calculated. Uncertainty in the temperature generated from an IR image can be attributed to the instrument uncertainty ( $\pm 2\%$ ) and uncertainty in emissivity.

Thermocouple measurements and IR images were compared to check for agreement. The discretization error was assessed. This error results when a limited number of TCs are used to represent the shroud temperature.

### **Phase 2 Experiments: Instrument Response, Discretization, and Temperature Distribution**

Three (3) Phase 2 experiments were conducted as follows:

- 1000°C for 22 minutes;
- 4.75" diameter, 1/8" thick inconel shroud;
- Two 40-mil ungrounded junction TCs, 0.50" off center;
- Seven intrinsic TCs as shown in Figure 50 and Figure 51 (wires 1/32" to 1/16" apart);
- Pyromark 2500, sprayed on, dried, and cured in oven;
- Shroud carefully centered and leveled;
- No shutter used during heat-up;
- Shroud was not perfectly level due to the large number of large thermocouple wires attached;
- IR camera used with  $\varepsilon = 1.0$  (corrected later) capturing one frame every two seconds; and
- TC resistance checked prior to experiments.

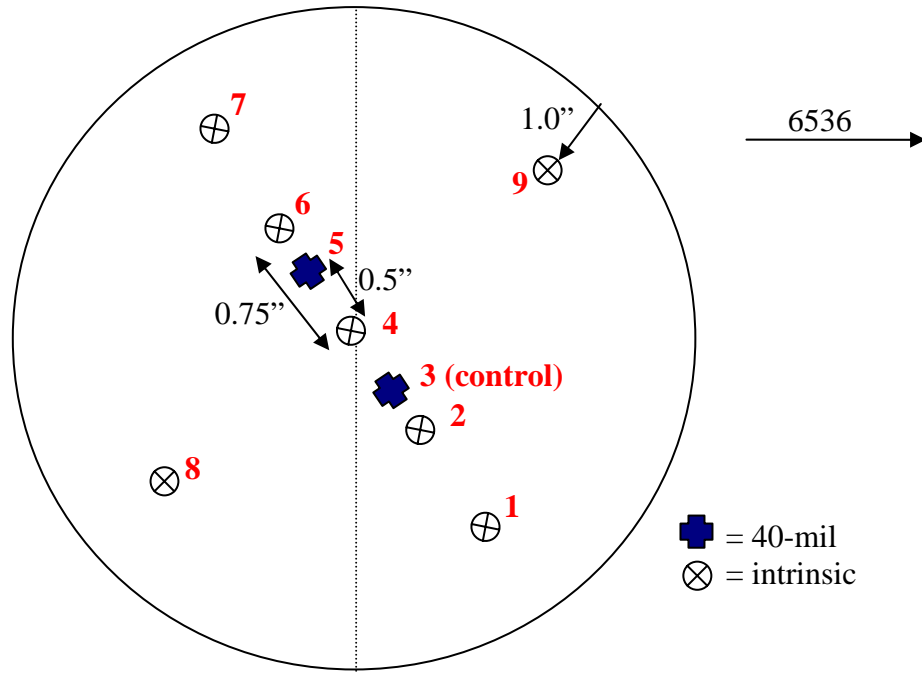
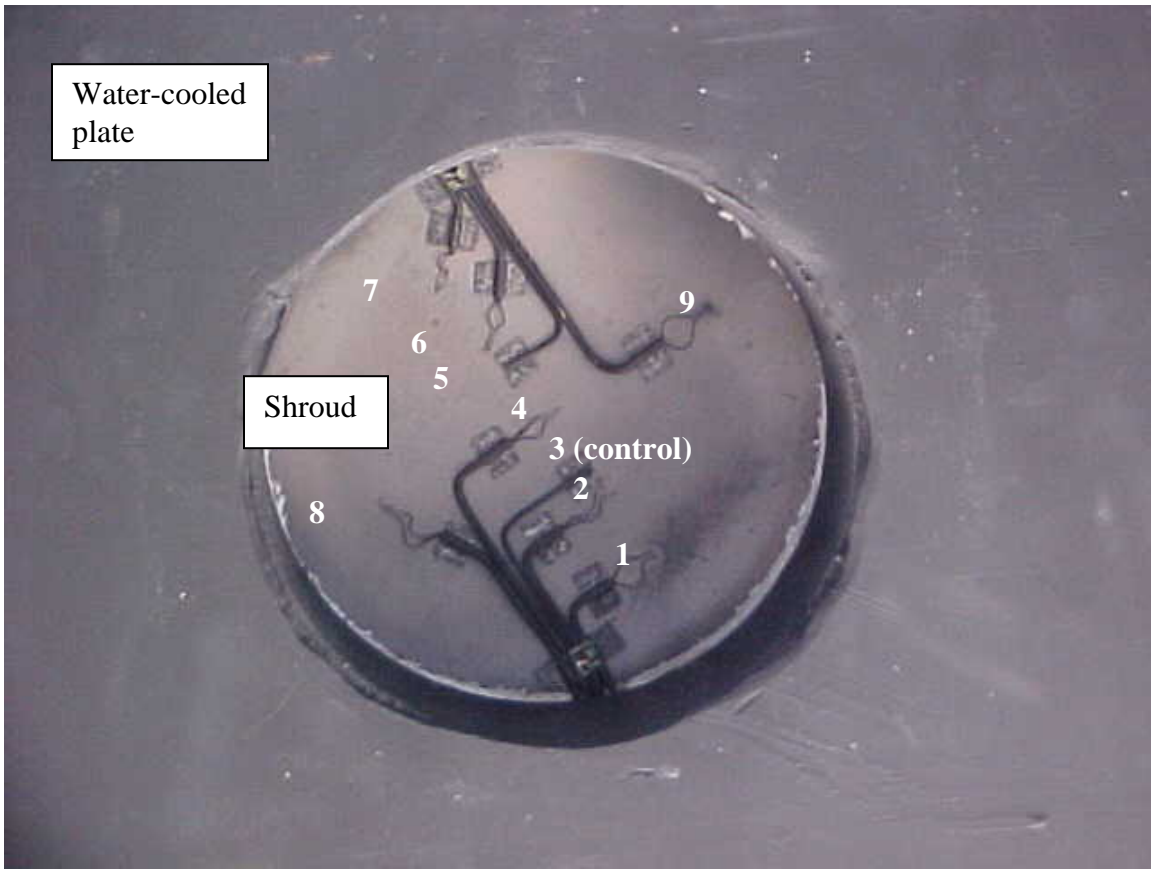


Figure 50 Schematic of Phase 2 Shroud Instrumentation



**Figure 51 Photograph of Shroud Looking into Mirror from IR Camera Location**

**Shroud Photographs for Experiments 1-3**

The following photographs show the condition of the shroud before each experiment. The color (black to gray) of the surface changed during the first experiment, but was fixed from that point forward.



**Figure 52 Photographs before Test 1 (top and bottom)**



**Figure 53 Photographs before Test 2**



**Figure 54 Photographs before Test 3**



**Figure 55 Photographs before Phase 3 Test 1**

## Analysis of Phase 2 Experimental Results

A plot of TC data from a typical Phase 2 experiment is shown in Figure 56. The highest temperatures were recorded shortly after the lamps were turned on due to typical control system overshoot. Once the control TC (#3, yellow, 40-mil ungrounded junction) reached the set point, it and most of the other thermocouples remained fairly stable. Intrinsic TCs are very fragile and frequently fail; therefore, their readings must be carefully analyzed. The readings from intrinsic TCs 6 and 7 are anomalous and it is believed that they failed shortly after the experiments began or during pre-test handling.

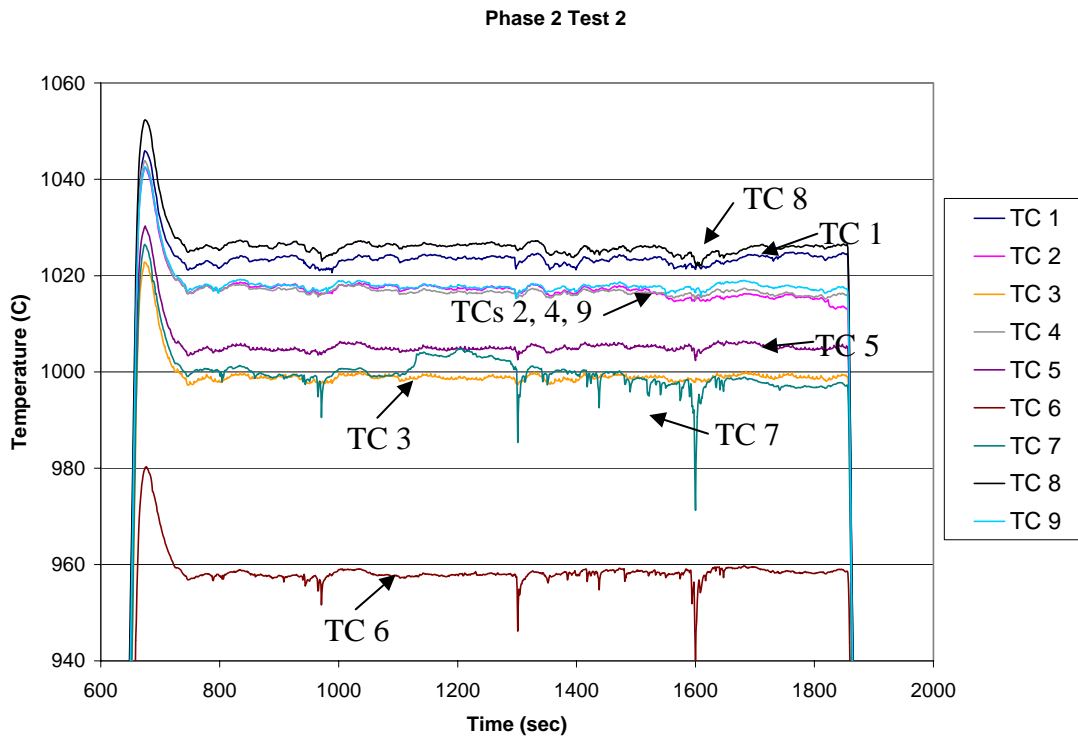


Figure 56 Typical Shroud Temperatures During a Phase 2 Experiment

An average TC temperature was calculated for each TC over a quasi-steady period of approximately 200 seconds. The average temperatures (calculated from Tests 1-3) for each TC type (intrinsic and 40-mil) are shown in Figure 57. Also shown are uncertainty bars for each TC which includes the uncertainty due to the experimental variability of the TC and DAS and temperature variations about the mean for a 95% confidence interval ( $2\sigma$ ). A value of  $\pm 0.6\%$  of the temperature in Kelvin was used as the TC and DAS uncertainty, based on analyses in [4].

TCs 6 and 7 malfunctioned so those data were not used. Data from TC2 has a larger spread than other TCs and it appeared that the junction location may have changed between tests 2 and 3; the first two tests were similar and the last two tests were similar. Behavior such as this is not unexpected based on past experience with intrinsic TCs; therefore, it is assumed faulty.

A single overall shroud temperature average was estimated using the limited number of TCs of each type (two 40-mil, five intrinsic TCs, not TCs 6 or 7) for all three experiments. This approach provided an indication of how accurately an average shroud temperature can be obtained using only a limited number of discrete data points (compared to an IR image which has hundreds of data points). The intrinsic average was  $1020 \pm 19^{\circ}\text{C}$  and the 40-mil average was  $1002 \pm 17^{\circ}\text{C}$ , where the range represents the 95% confidence interval including the uncertainty due to experimental variability, TC reading, and DAS as described above. The variabilities ( $\pm 17^{\circ}\text{C}$  and  $\pm 19^{\circ}\text{C}$ ) estimated in this manner amount to approximately 1.4% of the nominal temperature (in K).

Phase 4 discussions indicate that intrinsic TCs also have a slight error. They do not record the “true” shroud temperature because they also have an effective junction displaced from the surface. Intrinsic TCs are made from 63-mil sheathed TCs with the sheath removed from the end. For 0.063 inch diameter sheathed TCs the wire diameter (chromel and alumel wires) is about 0.012 inch. The effective distance the junction is displaced off the surface 0.005 inches (see Phase 4 discussion). For a 40-mil TC the displacement is assumed to be half of the sheath diameter, or 0.020 inches.

Phase 1 work (Figure 17) shows that the shroud temperature is slightly higher toward the shroud edge. This result is likely due to the edge being mounted on top of insulation. Figure 50 shows that TCs 1, 7, 8, and 9 are located toward the edge of the shroud while the remaining TCs are located toward the center, and Figure 57 shows that TCs 1, 8, and 9 are generally higher than the remaining TCs, consistent with the IR camera image trends in Figure 17. A direct comparison of temperatures should not be made since the camera emissivity was assumed to be 1.0.

### TC Variability and Averages - Phase 2

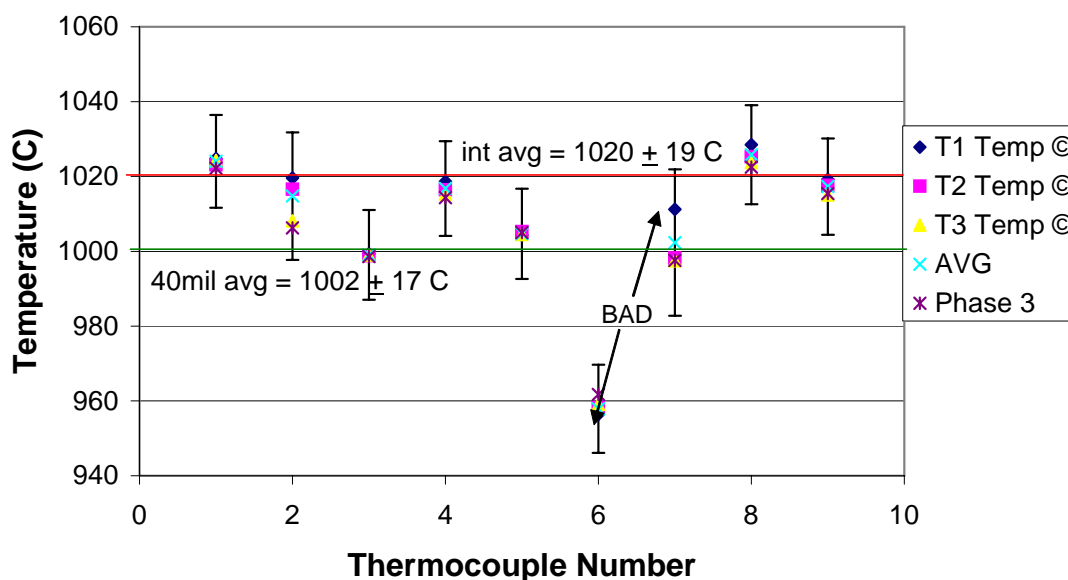


Figure 57 Phase 2 and 3 TC Results

An average shroud temperature was calculated using only a limited number of thermocouple measurements, shown in Figure 57, and the most complete assessment of the shroud temperature distribution is obtained using IR imagery. Because an extensive number of data points compose the image, less discretization error is incurred in the calculation of the average temperature. The temperature output of the IR camera is dependent on the emissivity of the surface, an operator input variable. In this study the emissivity of the shroud painted with Pyromark was measured and compared with previously measured values.

### Pyromark Emissivity

A literature search was performed to gather as much data as possible on the emissivity of Pyromark black paint. The results of that search are provided in Appendix C. Unfortunately, data indicate that Pyromark emissivity depends on the substrate to which it is attached, the curing process, and the number of times the shroud has been cycled to high temperatures (e.g., 1000°C). Measurements of Pyromark were made (summer 2003) by Rod Mahoney of Sandia's Primary Standards Laboratory, with shrouds of inconel that were cycled several times. Measurements (after heating to over 1000°C) revealed that the emissivity of the back (cold) surface was  $0.81 \pm 0.04$  (see Figure 58 or Appendix C) at 1000°C. Additional measurements using the Phase 1 circular shroud indicated that the emissivity at 1000°C was  $0.90 \pm 0.04$  (see Figure 59 or Appendix C). Results of the emissivity measurements for the plate and the disk as a function of temperature are shown in Figure 58 and Figure 59.

Differences in the two emissivity measurements were caused by a number of factors, including the severity of the heating the shroud endured. The material with lower emissivity was exposed to more cycles that likely caused additional changes in the paint matrix, thereby impacting the emissivity of the surface. It should also be noted that front (hot) and back (cold) surfaces of the shrouds have slightly different emissivities. The front is exposed directly to the lamps, resulting in a lower post-test surface emissivity. The back surface of the shroud radiates to the test article and is, therefore, the most important emissivity measurement.

In addition, the trend with temperature is also different. As Figure 58 indicates, the emissivity drops with increasing temperature (0.85 to 0.80) up to about 1000°C, then begins to rise again. In Figure 59 the emissivity rises with temperature (0.85 to 0.90) up to 1000°C. Results from previous studies of Pyromark black were equally diverse (see Appendix C).

The literature review resulted in the finding that, unfortunately, Pyromark emissivity varies from a low of about 0.77 to a high of 0.95, and the actual value is somewhere in between. It is dependent on the substrate, cure temperature, and number of times the paint was cured to high temperatures. With reasonable confidence, the best estimate is that Pyromark emissivity is between 0.77 and 0.95, or  $0.86 \pm 0.09$ .

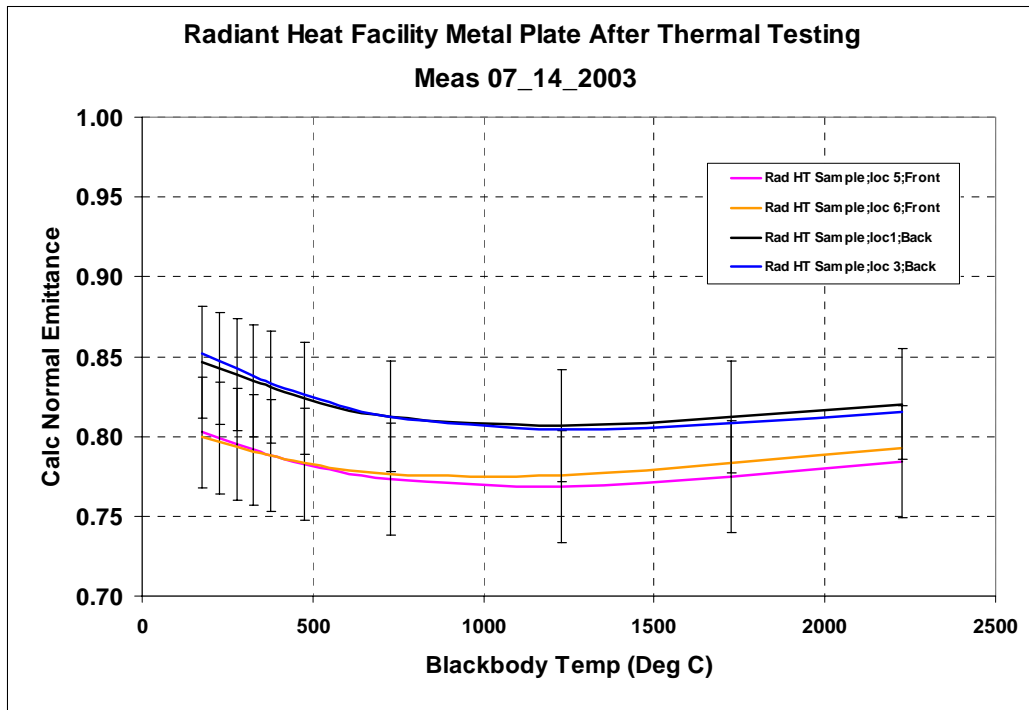


Figure 58 Emissivity Measurements for Inconel Plate

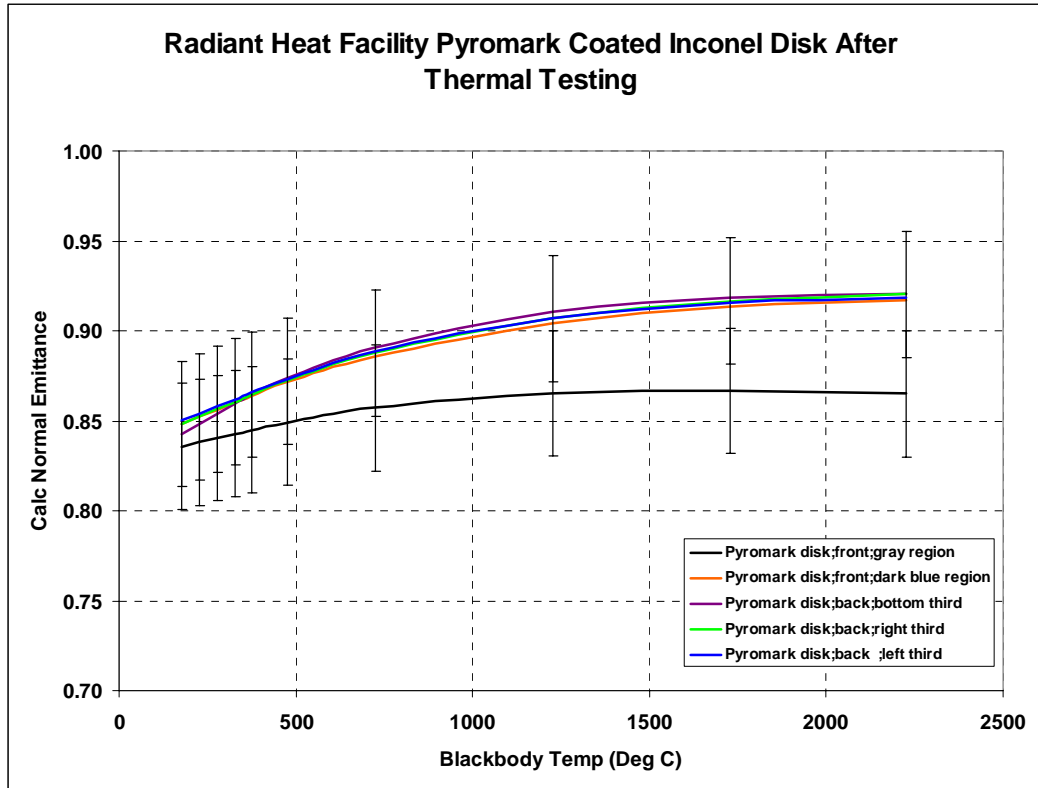


Figure 59 Emmissivity Measurements for Phase 1 Inconel Disk

Additional studies are ongoing to try to more precisely quantify Pyromark emissivity in our applications. Samples of common shroud and test fixture materials have been sent to Surface Optics Corporation (San Diego, CA) for emissivity measurements. The Radiant Heat Facility has the ability to make supplemental emissivity measurements at a wavelength of 1.55 microns using a handheld device. Also, there is interest in finding an alternate method that provides a high emissivity surface, but one that is more consistent with temperature and not as variable with other factors. Development in this area is currently outside the scope of this project but should be considered to refine the fidelity of the boundary condition.

### Analysis of the IR images

Analysis of the IR images was performed using FLIR Researcher software which allows the user to change the emissivity of each point or of the whole domain after the images have been captured. In order to compare IR images of varying emissivities with TC readings to evaluate the agreement and estimate the discretization error, the emissivity of the image was changed to values thought to be reasonable based upon data from Appendix C and the discussion in the previous section.

A correction factor was required to account for a reduction in flux to the IR camera caused by the mirror. An experiment was designed to determine the flux reduction due to the mirror. First, a blackbody source was viewed using a 2-color pyrometer (Micron Model M668). This instrument

does not require an emissivity input because it uses radiation from two closely spaced wavelengths to estimate the source temperature. The pyrometer measured the temperature of the blackbody source to within about  $\pm 7^\circ\text{C}$ . Once the blackbody temperature was determined, the IR camera viewed the source in two different ways, as shown in Figure 60 below.

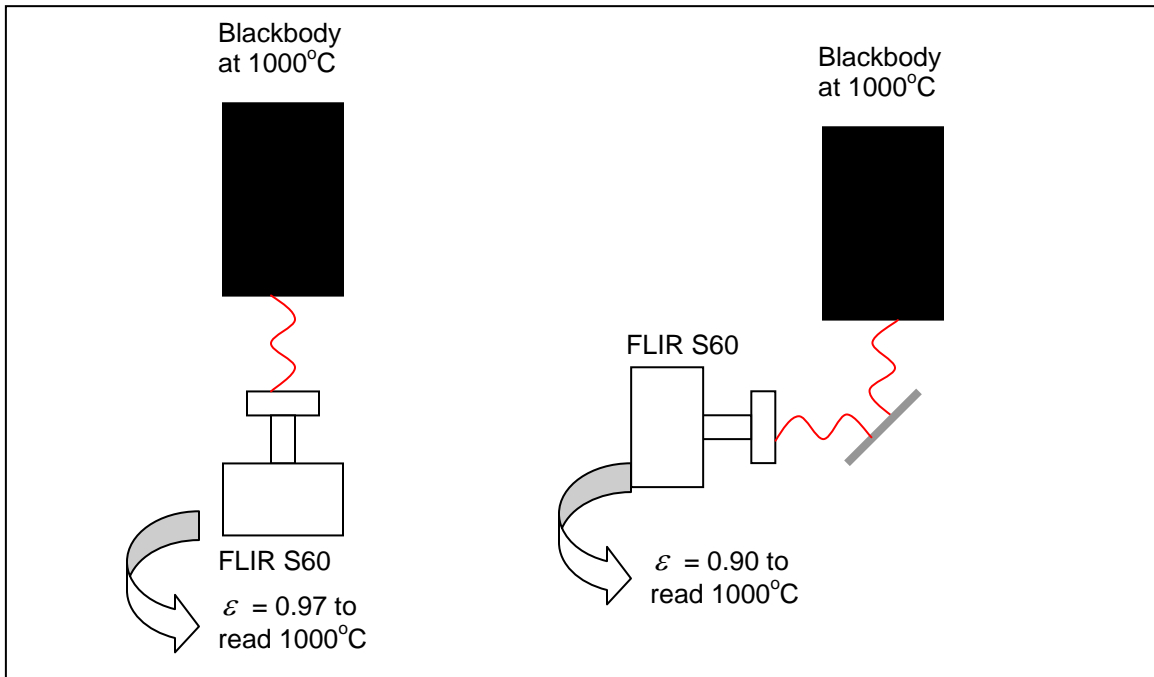


**Figure 60 Setup for Mirror Emissivity Experiment**

The image on the left in Figure 60 shows how the experiment was configured to measure the emissivity of the blackbody cavity. The IR camera was placed directly in line with output of the cavity. Because the cavity temperature of  $1000^\circ\text{C}$  was known from the 2-color pyrometer, the emissivity calculator within the camera was varied until the IR camera also read  $1000^\circ\text{C}$ . The estimated emissivity was 0.97, which is reasonable for this type of source and close to the theoretical value of 1.0 for a blackbody.

The experiment was then repeated with the camera at a  $90^\circ$  angle to the black-body. A mirror with a silvered front surface was placed between the blackbody and the camera. This was required because during ERB and MVTU-2 testing the IR camera cannot be placed to look at the shroud without use of a mirror. The emissivity calculator was then used again to determine the emissivity of the surface required to produce a temperature of  $1000^\circ\text{C}$ . The result was an emissivity of 0.90.

The change in the emissivity is due to a non-perfect reflection from the silvered mirror. The process is depicted in Figure 61 and the mirror reflectivity ( $\rho_{\text{mirror}}$ ) can be estimated using the equation shown in the figure. Once the reflectivity is known

( $0.97 \times 0.93 = 0.90$ ), it can be used to reduce Phase 2 data from the IR camera. A 0.93 correction factor was used to determine the actual emissivity of the target.

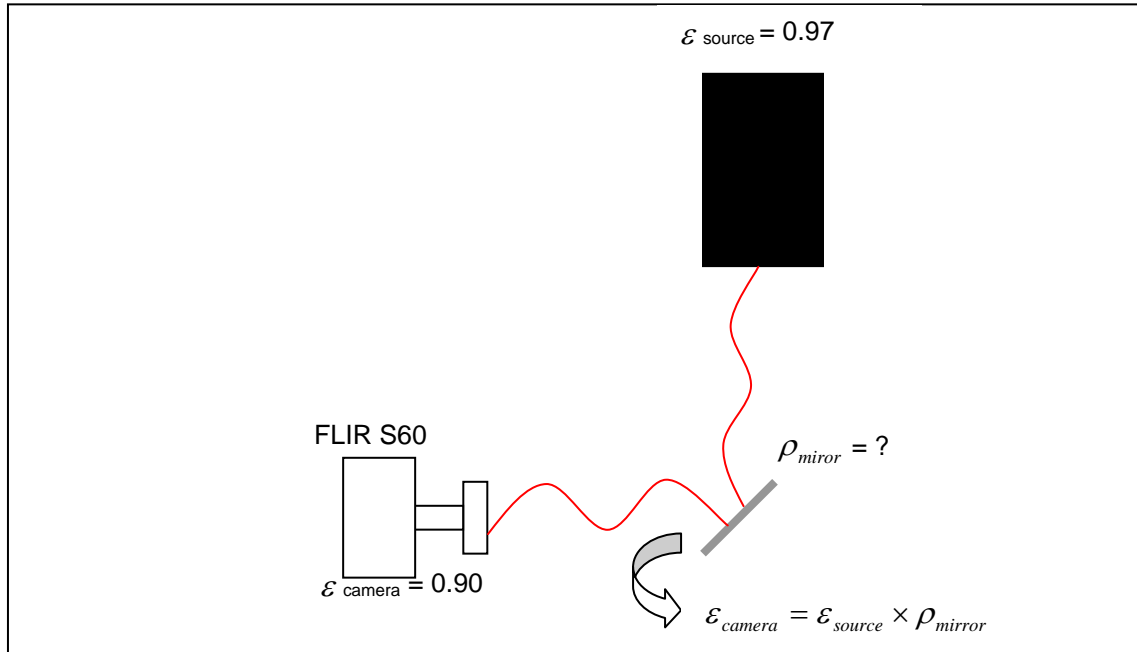


**Figure 61 Calculation of the Mirror Correction Factor**

### Comparison of TC and IR Camera Image Data

Intrinsic and 40-mil TC temperature measurements are shown in Table 8 below. The average temperature of each TC was calculated using data from Tests 1-3. Additionally, the table shows the overall average for the 40-mil and the intrinsic TCs and the standard deviation (due to the experimental variability).

**Table 8 Summary of TC temperatures (average of Tests 1-3)**

	<u>AVG</u>	<u>EXP VAR</u>	<u>0.6% of TEMP in K</u>	<u>2*sigma</u>
TC # 1	1024.0	0.9	7.8	15.7
TC # 2	1014.7	5.9	7.7	19.5
TC # 4	1016.8	1.7	7.7	15.9
TC # 8	1025.8	2.5	7.8	16.3
TC # 9	1017.3	2.1	7.7	16.0
TC # 3	999.0	0.3	7.6	15.3
TC # 5	1004.7	0.5	7.7	15.4

AVG INT = 1020 ± 19 C  
 AVG 40 mil = 1002 ± 17 C

Table 9 summarizes the average shroud temperature calculated from the IR images as the emissivity of the IR camera was varied (note that the emissivity was corrected for the reflectivity of the mirror – column 1 is the uncorrected emissivity and column 2 is the corrected emissivity).

The results from Test 3 are shown, as they are representative of all the tests in this phase. The FLIR Researcher software was used to vary the emissivity and look at the temperature distribution. Example images using an emissivity of 0.78 and 0.82 are shown in Figure 62 and Figure 63, respectively. Shown on the images are averages of the entire shroud and an average of a line of temperatures between the two 40-mil TCs.

Comparing the average IR image temperature to the “true shroud temperature” provides an estimation of the discretization error. The “corrected shroud temperature” was calculated from the 40-mil TC data and the Phase 4 results. The 40-mil average temperature was increased by 3.25% (of the temperature in Kelvin) (lowest value in range 3.25-3.86%) to obtain the “true shroud temperature” of 1043°C.

This “true shroud temperature” was then compared to the average of a line of temperatures in the IR image between the two 40-mil thermocouples. The standard deviation along the line was only 6°C, indicating that the temperature distribution was quite uniform. Analysis of the results in Table 9 reveals reasonable agreement between the true shroud temperature and the line average for an emissivity of 0.76 (highlighted values). This result is slightly below the lower limit ( $-2\sigma$ ) of the emissivity measurements ( $0.86 \pm 0.09$ ) as described earlier. However, if thermocouple uncertainties ( $\pm 17^\circ\text{C}$ ) and IR camera uncertainties ( $\pm 36^\circ\text{C}$ ) are considered, the results are consistent. Figure 64 shows the shroud temperature distribution with an emissivity of 0.76.

**Table 9 Summary of IR Image Temperatures (from Test 3)**

<u>e</u>	<u>camera e</u>	<u>Line Avg</u>	<u>Shroud Avg</u>
0.75	0.7	1048	1036
<b>0.76</b>	<b>0.71</b>	<b>1037</b>	<b>1025</b>
0.77	0.72	1027	1015
0.78	0.73	1016	1005
0.80	0.74	1007	995
0.81	0.75	997	986
0.82	0.76	987	976
0.83	0.77	978	967
0.84	0.78	969	958
0.85	0.79	960	950
0.86	0.8	952	941
0.87	0.81	943	933
0.88	0.82	935	925
0.89	0.83	927	917
0.90	0.84	919	909
0.91	0.85	912	901
0.92	0.86	904	894
0.94	0.87	897	887
0.95	0.88	890	880

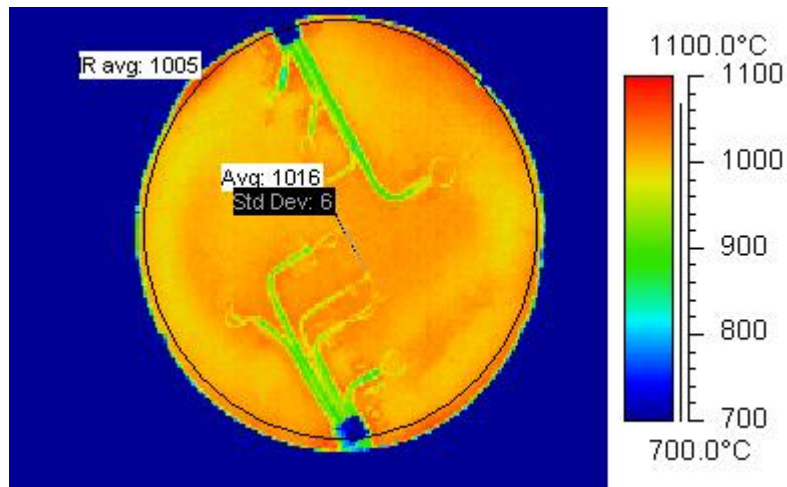


**Figure 62 IR Image of Shroud with e=0.78**

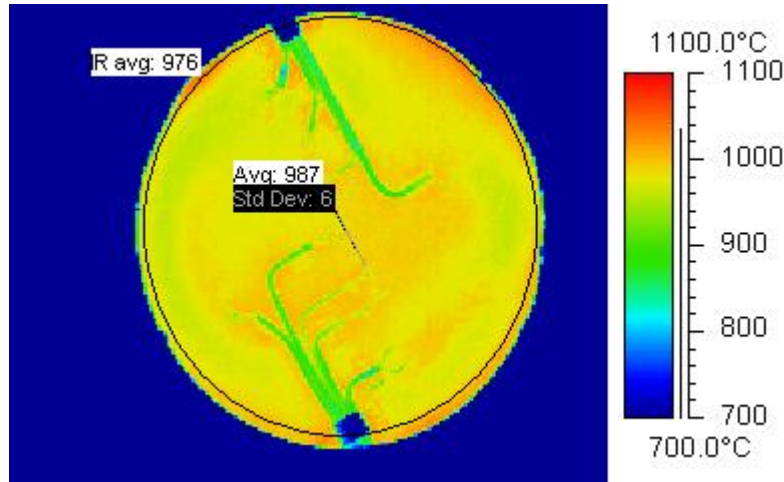


**Figure 63 IR Image of Shroud with  $\epsilon=0.82$**

In summary, two representations of the shroud temperature are available.

- The “true shroud temperature” as determined by averaging two 40-mil TC readings and increasing the value by 3.25% to account for the thermocouple error. The resulting shroud temperature is 1043°C.
- An estimation of the shroud temperature using a camera emissivity of 0.76 as shown above. The average shroud temperature using the IR image is 1025°C.

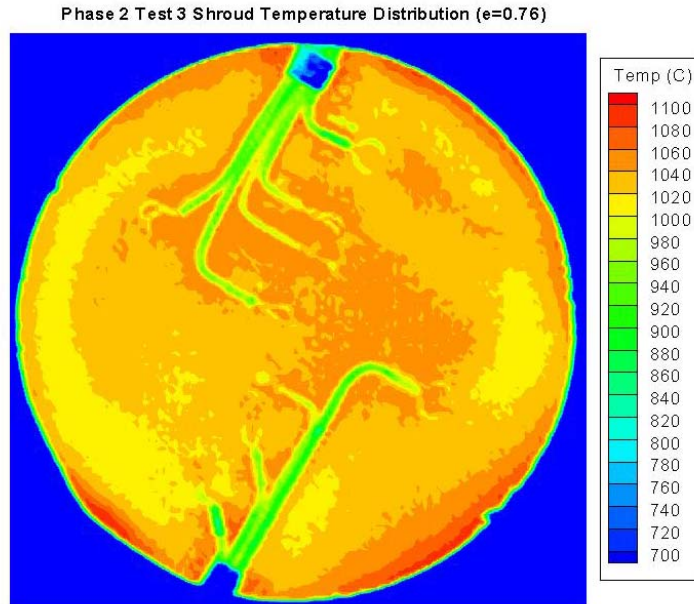
The IR image is a more complete average of the shroud temperature since it contains significantly more data points over a wider area, while the 40-mil average is from two thermocouples near the center of the shroud. Thus, a discretization error occurs by using a limited number of temperatures in the average. The shroud average temperature using corrected 40-mil thermocouples is 1.7% higher than the average computed from the IR image with an assumed emissivity of 0.76. This is comparable to the uncertainty in the IR image alone ( $\pm 2\%$  of temperature in °C). When emissivity uncertainties are included the overall IR image uncertainty is closer to  $\pm 4\%$ .

Since the IR image contains much more detail on the temperature distribution, it is interesting to investigate the impact of using a single temperature, as opposed to a distribution, on the heat flux to an object 4 inches away (relevant to the W76 ERB and MVTU-2 experiments). In the images that follow, the flux from three different shroud temperatures will be compared:

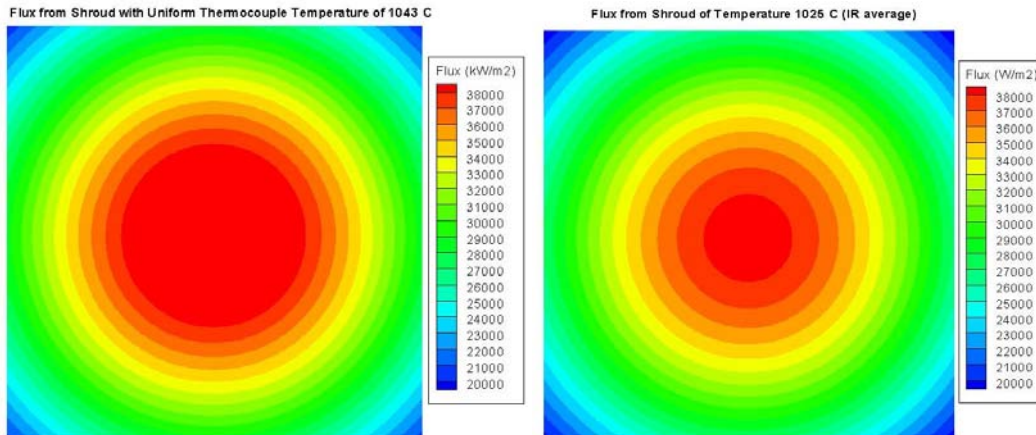
- uniform “true shroud temperature” of 1043°C;
- uniform temperature from IR average of 1025°C; and
- temperature distribution from IR image ( $\epsilon=0.76$ ) shown in Figure 64 (note that Tecplot inverts the data from the IR images shown earlier)

The flux results shown in Figure 65 were compared to determine the percent difference in heat flux that would result when using an average temperature (IR, TC) or a distribution. The flux when using the TC average of 1043°C is consistently 6% higher than when using the IR average

of 1025°C. A comparison of the flux resulting from the IR average temperature to the flux from the IR distribution revealed a difference of 3-5% in the flux to a target 4 inches away, as shown in Figure 66.



**Figure 64 Shroud Temperature Distribution from IR image with e=0.76**



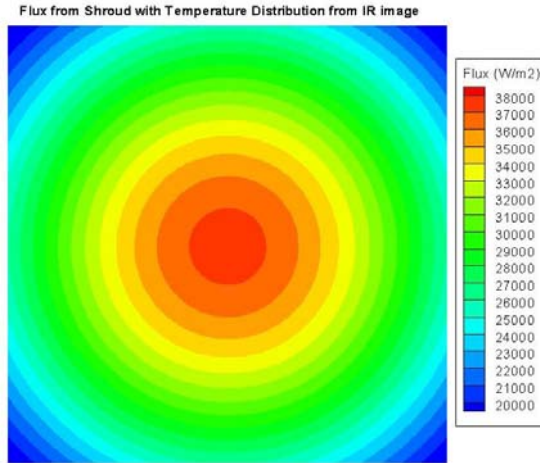


Figure 65 Flux Comparisons (TC average of 1043°C, IR average of 1025°C, IR distribution from Figure 63)

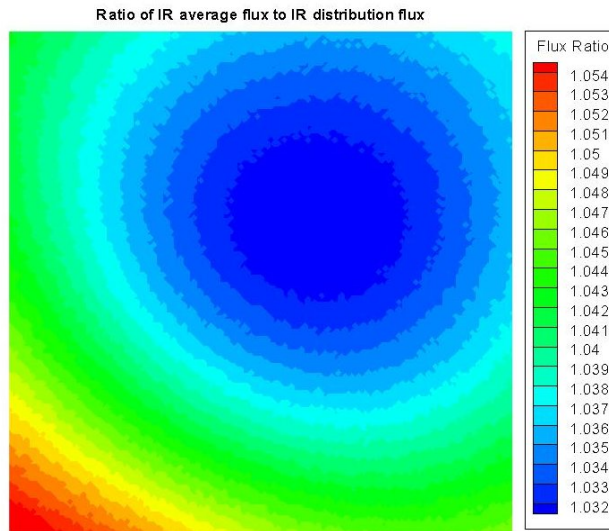


Figure 66 Ratio of Flux from the IR Average Temperature to the IR Distribution

### Typical Overall Uncertainty Estimate

Given the information provided in various sections above, an overall uncertainty estimate can be provided to the computational analysts who have expressed interest in using only a single average temperature to represent the shroud boundary condition. Uncertainty in this representation of the shroud boundary condition can be attributed to the following items.

- Experimental variability – a minimum of three experiments should be performed to determine the variability. Phase 1 showed that this is typically 10°C.
- Instrument and DAS uncertainty – experience has revealed that this is approximately 0.6% of the temperature in Kelvin, or 8°C (using the TC average shroud temperature from tests above of 1043°C).

- Using an average temperature instead of a distribution (based on IR images) – Phase 2 results showed that this results in a 3-5% difference in flux. This flux difference directly relates to a temperature difference of approximately 11°C.

Combining all of the above contributions results in an uncertainty of 34°C (95% confidence interval) or <3.4% of the nominal shroud temperature. The emissivity also plays a role in the shroud temperature and its impact should be assessed by sensitivity studies with the computational model.

An analysis similar to what was described above shall be provided with all experimental data.

## Phase 2 Summary and Conclusions

- Intrinsic TCs read about 18°C higher than 40-mil sheathed TCs when mounted on the cold side of the shroud, which is about a 1.4% difference.
- TC measurements show the same trend of higher shroud temperatures near the shroud edge, as compared with the center, as do IR camera measurements.
- IR camera measurements for the five Phase 2 tests show an average standard deviation of 20°C, similar to Phase 1 tests (indicates test-to-test variability, comparing the same spots in different experiments).
- The shroud temperature difference from center to side is about 75°C, consistent with Phase 1 IR camera measurements.
- The shroud temperature estimated via the IR camera changes by about 30°C for every emissivity change of 0.04 units, which is the uncertainty in the emissivity measurements, as measured by Sandia’s Primary Standards Laboratory.
- The IR camera temperature uncertainty for  $\epsilon = 1.0$  is  $\pm 2\%$  or  $\pm 20^\circ\text{C}$  for a nominal shroud temperature of 1000°C.
- Total IR camera uncertainty (smallest value using root-sum-square estimation) is  $\pm 36^\circ\text{C}$  at 1000°C nominal temperature (includes  $\pm 2\%$  camera accuracy and emissivity uncertainty).
- IR camera emissivity of 0.76 gives best agreement and it is reasonable given recent and historical data on Pyromark emissivity.
- Discretization error is about 18°C (1.7% of absolute) determined by comparing the “true shroud temperature” of 1043°C to the IR image average of 1025°C ( $\epsilon=0.76$ ).
- Using a pair of 40-mil TCs averaged and corrected by 3.25%, rather than a mean based on a typical profile from the IR camera, the impact on the flux is 6%. The difference between the flux from the IR average and an IR camera distribution is 3-5%.
- Total shroud temperature uncertainties are  $\sim 34^\circ\text{C}$  (95% confidence interval) or <3.4% of the nominal shroud temperature. The emissivity also plays a role in the shroud temperature and its impact should be assessed by sensitivity studies with the computational model.

## **Summary and Conclusions**

### **Summary**

A series of experiments was performed in four phases to obtain better information on the boundary condition (temperature) from a “shroud” radiating to a test target. Objectives of the four phases follow.

#### **Phase 1:**

1. Assess the repeatability of the experiments; and
2. determine the shroud temperature profile based on IR measurements.

#### **Phase 2:**

1. Provide information that will allow assessment of the “true” shroud temperature;
2. provide more data on the shroud temperature distribution; and
3. provide information on discretization errors.

#### **Phase 3:**

1. Assess the magnitude of the TC error based on coupling between the shroud and target/test unit; and
2. test the hypothesis that fin theory can partially explain the TC error as a function of sheath diameter and environment temperature.

#### **Phase 4:**

- 1 Obtain experimental data on the response of thermocouples (TCs) of various sheath diameters and intrinsically mounted TCs;
- 2 develop a methodology to estimate the “true” shroud temperature;
- 3 provide correction factors for various sized TCs (20, 40, and 63-mil diameter ungrounded junction, inconel sheathed) to estimate the true shroud temperature; and
- 4 further test the hypothesis that fin theory is an appropriate way to explain the temperature variation with sheath diameter.

### **Phase 1 Results**

- Experiment-to-experiment repeatability of shroud control temperature was about 2°C at a nominal temperature of 1000°C. Repeatability of another TC, not used as a control, was about 7°C.
- For IR images averaged over five tests using two methods, results from two methods were consistent.
- Point to point comparison of data from five experiments indicate that the results were repeatable within a standard deviation of about 10°C.
- Average shroud temperature profiles showed higher temperatures at the shroud edges and lower temperatures near the center. An assessment of the shroud temperature uniformity revealed the maximum spread over the circular shroud surface (not including TC leads) was about 75°C (825-900°C). With TC leads included, the range in temperatures was 800-900°C.

- Standard deviations have an effect on heat flux to a target 4 inches from the shroud of about  $\pm 6\%$ .

## Phase 2 Results

- Intrinsic TCs read about  $18^{\circ}\text{C}$  higher than 40-mil sheathed TCs when mounted on the cold side of the shroud, about a 1.4% difference.
- TC measurements show the same trend of higher shroud temperatures near the shroud edge, as compared with the center, as do IR camera measurements.
- IR camera measurements for the five Phase 2 tests show an average standard deviation of  $20^{\circ}\text{C}$ , similar to Phase 1 tests (indicating test-to-test variability, comparing the same spots in different experiments).
- For the case tested, the shroud temperature difference from center to side is about  $75^{\circ}\text{C}$ , consistent with Phase 1 IR camera measurements.
- The shroud temperature estimated via the IR camera changes by about  $30^{\circ}\text{C}$  for every emissivity change of 0.04 units, which is the uncertainty in the emissivity measurements, as measured by Sandia's Primary Standards Laboratory.
- The IR camera temperature uncertainty for  $\epsilon = 1.0$  is  $\pm 2\%$  or  $\pm 20^{\circ}\text{C}$  for a nominal shroud temperature of  $1000^{\circ}\text{C}$ .
- Total IR camera uncertainty (smallest value using root-sum-square estimation) is  $\pm 36^{\circ}\text{C}$  at  $1000^{\circ}\text{C}$  nominal temperature (including  $\pm 2\%$  camera accuracy, and emissivity uncertainty).
- IR camera emissivity of 0.75-0.76 gives best agreement and is in reasonable agreement with experimental data given variability of recent and historical data on Pyromark emissivity.
- Discretization error in the temperature for the conditions tested is 1.7%, determined by comparing the "true shroud temperature" of  $1043^{\circ}\text{C}$  to the IR image average of  $1025^{\circ}\text{C}$  ( $\epsilon=0.76$ ).
- Using a pair of 40-mil TCs, averaged and corrected by 3.25%, rather than a mean based on a typical profile from the IR camera, the impact on the flux is 6%. The difference between the flux from the IR average and an IR camera distribution is 3-5%.
- Total shroud temperature uncertainties are  $\sim 34^{\circ}\text{C}$  (95% confidence interval) or  $< 3.4\%$  of the nominal shroud temperature. The emissivity also plays a role in the shroud temperature and its impact should be assessed by sensitivity studies with the computational model.

## Phase 3 Results

### Results relevant to MVTU-2 and Exclusion Region Barrier Experiments

- Four experiments obtained information on the coupling effect of test target presence and shroud TC response.
- Two experiments were performed with and without a shutter.
- Two experiments were performed with a calorimeter in place to simulate a test target similar to ones used in the Campaign 6 MVTU-2 and W76-1 Firing Set Exclusion Region Barrier (ERB) projects, with an increasing temperature.
- Fin theory estimated the effect of both TC sheath size and test target presence.
- Fin theory predicted that the difference between different sized TCs would be greater with no target present, and less with a hot target present (1000K) which was consistent with experimental data.
- Fin theory predicted an increasing error with sheath diameter, and an almost linear trend.
- Experimental results showed negligible difference between a cool target (MVTU-2 calorimeter at 300K) and a hotter target (same calorimeter 773K), but did show qualitative results consistent with fin theory when an insulated target (shutter in place) was compared to one at 300K.
- For targets except an insulated, hot surface, coupling considerations on shroud temperatures are negligible. This result applies to the ERB and MVTU-2 tests.

### Results From FCU Experiments

- Results from testing with no FCU in place (shroud radiating to a cold environment) showed the largest differences between intrinsic and 63-mil TCs (45-65°C at nominal 1000°C). This result is about 3.5-5.1% difference. (To obtain a correction factor the intrinsic TC has to be corrected as well – see Phase 4 results.)
- Results from testing with the FCU in place (shroud radiating to and being irradiated by a large steel structure) showed the smallest differences between intrinsic and 63-mil TCs (14-20°C) at a nominal 900°C shroud temperature. This result is about a 1.2-1.7% difference.

### Overall Conclusions for Phase 3

- For MVTU-2 and ERB experiments, the effect of test object/target coupling is negligible on TC bias error.
- For other setups (e.g., a large object whose temperature increases with time) the TC bias error can be much less, but coupling is important.

## Phase 4 Results

- Eight experiments were performed.
- Shroud had two 40-mil TCs on one side and eight TCs on the other. These eight TCs consisted of two groups of four TCs, a 20-mil diameter, a 40-mil diameter, a 63-mil diameter, and an intrinsic TC made from stripping away the sheath of a 63-mil TC.
- On hot side of shroud, larger diameter TCs read higher and had largest errors.
- On hot side, intrinsic TCs read lowest; on cold side intrinsic TCs read highest.
- On cold side, larger diameter TCs read lowest and had largest errors.
- Behavior of TCs with respect to size (sheath diameter) can be qualitatively explained via fin theory.
- Correction factors are estimated for 40 and 63-mil TCs at three relevant nominal shroud temperatures (900, 1000, and 1100°C).
- At 1000°C nominal shroud temperature, the 40-mil TC reads low by about 3.3-3.8% and the 63-mil TC reads low by about 6.1-6.2% (Temperature in K).
- If analysts use a single shroud temperature, they should increase the effective radiation temperature by the correction factors or use the averaging method (average of a hot and cold side shroud temperature).
- An alternate method is to install two outwardly identical TCs, one on each side of the shroud, at the same location. An average of the two readings provides an estimate of the true shroud temperature.
- It is recommended that both the extrapolation and averaging methods be used to provide the most confidence in the shroud temperature estimation.

## **Conclusions and Recommendations**

1. Mineral-insulated, metal-sheathed (MIMS) TCs attached to a shroud exhibit a bias error that depends on the size of the TC and the environment to which it is exposed.
2. The TC error is smaller for smaller diameter TCs.
3. Fin theory predicts the same behavior seen in experimental data – i.e., that the error increases with the fin/TC size.
4. One can estimate the true shroud temperature by extrapolating data to zero displacement.
5. One can also estimate the true shroud temperature by mounting nominally identical TCs one each side of the shroud, and averaging the steady state results.
6. To provide the most confidence possible, it is recommended that both the averaging method and the extrapolation method be used.
7. IR camera measurements showed the shroud temperature was not uniform – as much as a 75°C change was apparent from the edge to the center of a circular shroud. This result has implications if one wants to use a single temperature for the shroud. The flux can vary by 6% to a target 4 inches away from the shroud if an average temperature is used. Use of an IR camera to refine shroud TC locations will better quantify variations.
8. Pyromark emissivity is difficult to confidently specify. It is recommended that for model validation purposes, the shroud emissivity be measured after each test.

## **Lessons Learned**

1. Don't use intrinsic or 20-mil TCs for shroud temperature measurements. They are not reliable enough.
2. Wherever possible, provide a backup measurement for shroud temperature because of inherent difference between nominally identical TCs.
3. Bake the Pyromark at least once to the nominal shroud temperature being used (e.g., 1100°C), after the manufacturer's cure cycle is completed, to completely bake out and stabilize the paint. It is believed that the first bake-out is the most important, because most of the volatiles burn off and the paint stabilizes after the first test.
4. Be careful when locating the TCs as they exit the setup. If exposed to the lamps they can fail.

## **References**

[1] "Experimental Characterization of Shroud Boundary Condition and Uncertainty Quantification for Radiant Heat Experiments," by J. Suo-Anttila and J.T. Nakos, Fire Science & Technology Department 09132, memorandum to distribution, July 14, 2003.

[2] "Fundamentals of Heat and Mass Transfer," by Frank P. Incropera and David P. DeWitt, Fifth Edition, John Wiley & Sons, 2002.

[3] "Final Report – Summary of Thermal Testing of the Furnace Characterization Unit (FCU) for the Coast Guard," by J.T. Nakos, J. Pantuso, and J. Bentz, Sandia National Laboratories report SAND2000-1534, printed June 2000.

- [4] “Uncertainty Analysis of Thermocouple Measurements Used in Normal and Abnormal Thermal Environment Experiments at Sandia’s Radiant Heat Facility and Lurance Canyon Burn Site” draft report SAND2004-1023, by J.T. Nakos (, April 2004.
- [5] “Surface Temperature Measurement Errors,” by N.R. Keltner and J.V. Beck, *Journal of Heat Transfer*, Vol. 105, May 1983, pp. 312-318.
- [6] “Transient Temperature Measurement Errors,” by N. R. Keltner, B.L. Bainbridge, and J.V. Beck, ASME Paper 83-HT-86, ASME National Heat Transfer Conference, 1983.
- [7] “Measurement Errors for Thermocouples Attached to Thin Plates: Application to Heat Flux Devices,” by K.B. Sobolik, N.R. Keltner, and J.V. Beck, ASME HTD – Vol. 112, Heat Transfer Measurements, Analysis, and Flow visualization, Editor: R.K. Shah, Book No. H00504 – 1989.
- [8] “The Transient Response of Beaded Thermocouples Mounted on the Surface of a Solid,” by K. Wally, *Proceedings of the 23rd International Instrumentation Symposium*, Instrument Society of America, 1977, pp 127-132.
- [9] “Thermocouple Errors at the Radiant Heat Facility,” by Ronald Dykhuizen and Walt Gill, memorandum to distribution, December 15, 2003.
- [10] “Thermo-physical Properties of a Foam and a Pyromark Paint 2500,” TPRL 1833, Thermo-physical Properties Research Laboratory, Inc., Purdue University Research Park, April 1997.
- [11] “Measurements of Total Emittance of Several Refractory Oxides, Cermets, and Ceramics for Temperatures from 600°F to 2,000°F,” by W.R. Wade, and W. S. Slemph, NASA Technical Note D-998, Langley Research Center, March 1962.
- [12] “Thermal Response of a Small Scale Cask-Like Test Article to Three Different High Temperature Environments”, R.S. Longenbaugh, L.C. Sanchez, and A.R. Mahoney, Sandia National Laboratories, for the U.S. DOT, DOT/FRA/ORD-90/01, Appendix B, February 1990.
- [13] “Remittance Measurement Results for Pyromark Series 2500 Black Paint Coated Inconel Plate from the Radiant Heat Facility,” by Rod Mahoney, 02542, Primary Standards Laboratory, 15 July 2003.
- [14] “Pyromark Series 2500 Black Paint Coated Inconel Disk after Heat Treatment,” by Rod Mahoney, 02542, Primary Standards Laboratory, 4 Sept 2003.

## Appendix A: Fin Analysis

Fin theory is used to analyze the temperature in a square fin. Basic fin theory is provided in many heat transfer texts, e.g., Incropera & DeWitt [2]. In this case a cylindrical TC is approximated by a square fin of the same diameter as a typical TC (e.g., 1/16" or 1.6mm). The TC is assumed to be long and thin so only 1-dimensional conduction is present. Figure A-1 shows a schematic of the setup.

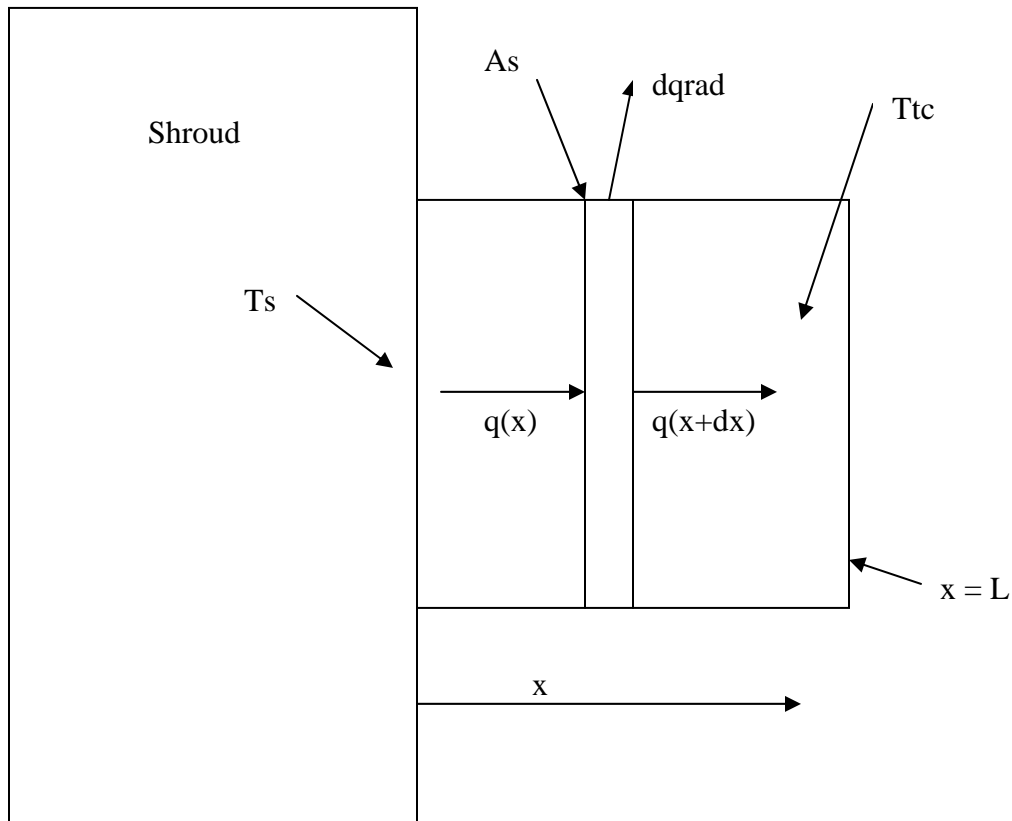


**Figure A- 1 Schematic of TC Setup**

The basic equation assumes 1-dimensional conduction in the fin is

$$q_x = q_{x+dx} + dq_{rad} \quad [A-1]$$

where  $dq_{rad}$  is the radiative heat loss. Convection is neglected, as is the fin surface area, and  $L$  is the fin length which equals the TC diameter. Assuming the radiative heat transfer can be “linearized”, one arrives at the following for  $dq_{rad}$ :

$$dq_{rad} = F_{tc-s} * \sigma \epsilon_{tc} (T_{tc}^4 - T_s^4) * dA_s + F_{tc-target} * \sigma \epsilon_{tc} (T_{tc}^4 - T_{target}^4) * dA_s + F_{tc-amb} * \sigma \epsilon_{tc} (T_{tc}^4 - T_{amb}^4) * dA_s \quad [A-2]$$

where the three view factors are TC to shroud ( $F_{tc-s}$ ), TC to target ( $F_{tc-target}$ ), and TC to ambient ( $F_{tc-amb}$ ). The TC emissivity is assumed to be as if painted with Pyromark paint (0.8 nominally). Note that the first term is negative, i.e., energy is coming into the TC from the shroud. The other two terms are positive. Typical setups have both a target and ambient, and the shroud can see both. For example, in the MVTU-2 setup, the target is the calorimeter or MVTU-2, while the ambient is the water-cooled plate.

For simplicity, values for the view factors were estimated assuming the fin was cylindrical. For this case the following values were used (Typical for MVTU-2 setup):

$$F_{tc-s} = 0.5, F_{tc-target} = 0.3, \text{ and } F_{tc-amb} = 0.2.$$

$F_{tc-s}$  for a square fin, in the limit of a small fin and large shroud is also 0.5. Therefore, the cylindrical view factors are likely accurate enough for a square fin.

Defining  $h_s$  (shroud),  $h_{target}$  (test object), and  $h_{amb}$  (ambient) as “radiative” heat transfer coefficients, and assuming  $T_{tc} = T_s$ , the following was obtained:

$$h_s = F_{tc-s} * \sigma \varepsilon_{tc} (T_{tc}^3 + T_s^3 + T_{tc} T_s^2 + T_{tc}^2 T_s) \cong F_{tc-s} * \sigma \varepsilon_{tc} * 4T_s^3, \quad [A-3]$$

$$h_{target} = F_{tc-target} * \sigma \varepsilon_{tc} (T_s^3 + T_{target}^3 + T_s T_{target}^2 + T_s^2 T_{target}), \text{ and} \quad [A-4]$$

$$h_{amb} = F_{tc-amb} * \sigma \varepsilon_{tc} (T_s^3 + T_{amb}^3 + T_s T_{amb}^2 + T_s^2 T_{amb}). \quad [A-5]$$

Assuming Fourier’s law and a constant cross-sectional area ( $A_c$ ), equation [1] is simplified to

$$\begin{aligned} & d^2 T_{tc} / dx^2 - (h_s / kA_c)(dA_s / dx)(T_{tc} - T_s) - (h_{target} / kA_c)(dA_s / dx)(T_{tc} - T_{target}) - \\ & (h_{amb} / kA_c)(dA_s / dx)(T_{tc} - T_{amb}) = 0 \end{aligned} \quad [A-6]$$

where ‘k’ is the effective thermal conductivity of the TC. K is varied so results agree with experimental data. The surface area  $A_s = Px$  where P is the fin perimeter. So, substituting for  $dA_s/dx$  and grouping terms one arrives at

$$d^2 T_{tc} / dx^2 - m_1^2 T_{tc} + m_2^2 = 0 \quad [A-7]$$

where

$$m_1^2 = (P / kA_c)(h_s + h_{target} + h_{amb}) \quad [A-8]$$

$$m_2^2 = (P / kA_c)(h_s T_s + h_{target} T_{target} + h_{amb} T_{amb})$$

By inspection the solution to [7] is.

$$T_{tc} = C_1 e^{m_1 x} + C_2 e^{-m_1 x} + m_2^2. \quad [A-9]$$

$C_1$  and  $C_2$  are found using boundary conditions

$$@ x = 0, T_{tc} = T_s \quad [A-10]$$

$$@ x = L, h_{end} (T_{tc}(L) - T_{target}) A_c = -k A_c (dT_{tc} / dx)_{x=L}$$

where  $h_{end}$  is defined

$$h_{end} = F_{end-target} * \sigma \epsilon_{tc} (T_{tc}(L))^3 + T_{target}^3 + T_{tc}(L) T_{target}^2 + T_{tc}(L)^2 T_{target}. \quad [A-11]$$

Contact resistance between the TC and shroud is assumed negligible (see analysis in main body in Phase 3 discussions). Therefore, it will be assumed that  $T_{tc}(0)=T_s$ . Also, for simplicity, it will be assumed that  $T_{tc}(L)=T_s$ , and that the end of the fin is radiating only to the target, and not the environment. The target will have different temperatures to simulate a cold surface (300 K) or one that is hot (1000 K). The ambient is assumed to be at 300K.

Solving for  $C_1$  and  $C_2$  one obtains:

$$C_1 = T_s - (m_2 / m_1)^2 - C_2$$

$$C_2 = ((T_s e^{m_1 L} - (m_2 / m_1)^2 e^{m_1 L}) + (h_{end} / km_1)(T_s e^{m_1 L} - (m_2 / m_1)^2 e^{m_1 L} - T_{target} + (m_2 / m_1)^2)) / 2(\cosh m_1 l + (h_{end} / km_1) \sinh m_1 l)$$

The value for the apparent conductivity  $k$  is adjusted until the predicted results agree with experimental data (approximate difference between 20-mil and 63-mil diameter TC data of about 40 K for a cold target). The result is  $k = 5$  W/m-K. This is a reasonable result because the MIMS TC is made of inconel ( $k = 12$  W/m-K) and MgO insulation (0.7 W/m-K at 1300 K), so an effective conductivity would be between the two extremes. Note that results for the 1000 K target (about a 12 K decrease at 63-mils) are consistent with data from Figure 35 in the main body of the text.

A plot of fin temperature is shown below. These data show several trends consistent with experimental data. They are

1. The fin temperature decreases with distance from the shroud, or assuming the TC analogy is correct, the TC temperature decreases with increasing size (larger error);
2. The relationship with distance from shroud (or sheath diameter) is almost linear; and.

3. The error decreases with a hot target or test object.

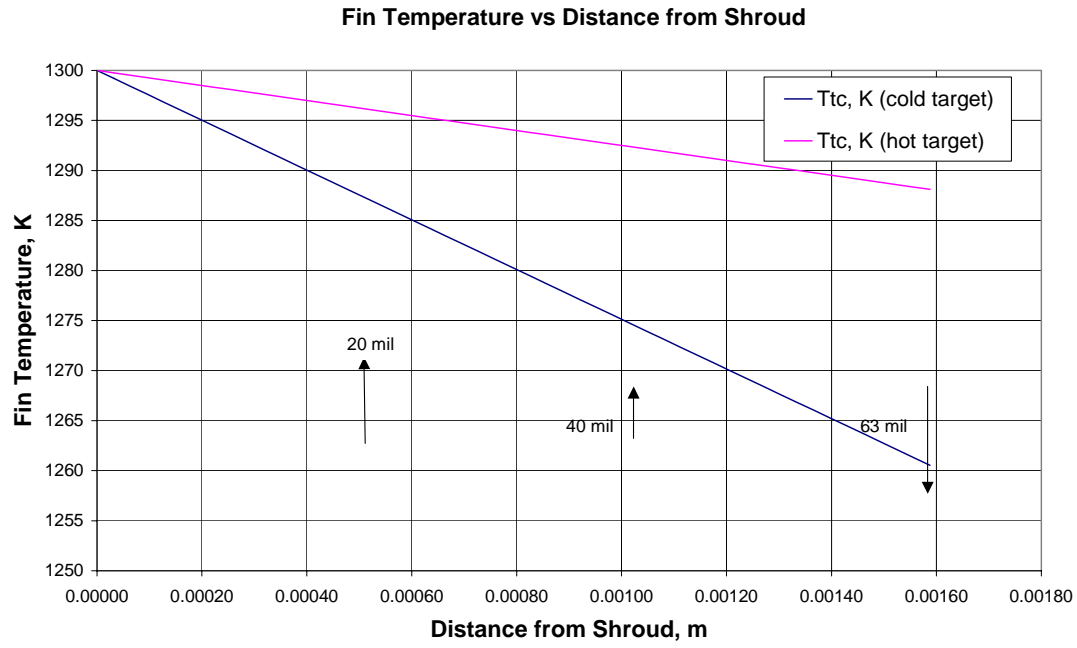


Figure A- 2 Plots of Fin Temperature vs Distance from Shroud for a Hot (1000 K) and Cold (300 K) Target

## Appendix B: Average Shroud Temperature Analysis



Operated for the U.S. Department of Energy by  
**Sandia Corporation**  
Albuquerque, New Mexico 87185-

*date:* December 15, 2003

*to:* James Nakos, Org 9132, MS 1135

*from:* Ronald C. Dykhuizen, Org 9116 and Walt Gill, Org. 9132

*subject:* Thermocouple Errors at the Radiant Heat facility

**Summary.** We were asked to investigate the source of thermocouple reading errors in a specific installation configuration at the Radiant Heat facility. An empirical model is put forth that explains and quantifies the errors, allows for the thermocouple reading corrections, and suggests an alternate installation method.

**Background.** Often sheathed thermocouples are attached to a shroud that is placed between the heat producing lamps and the test item. These thermocouples are parallel to the shroud, and tacked down with a thin metallic strip. Figure B- 1 shows the type of installation under consideration here.

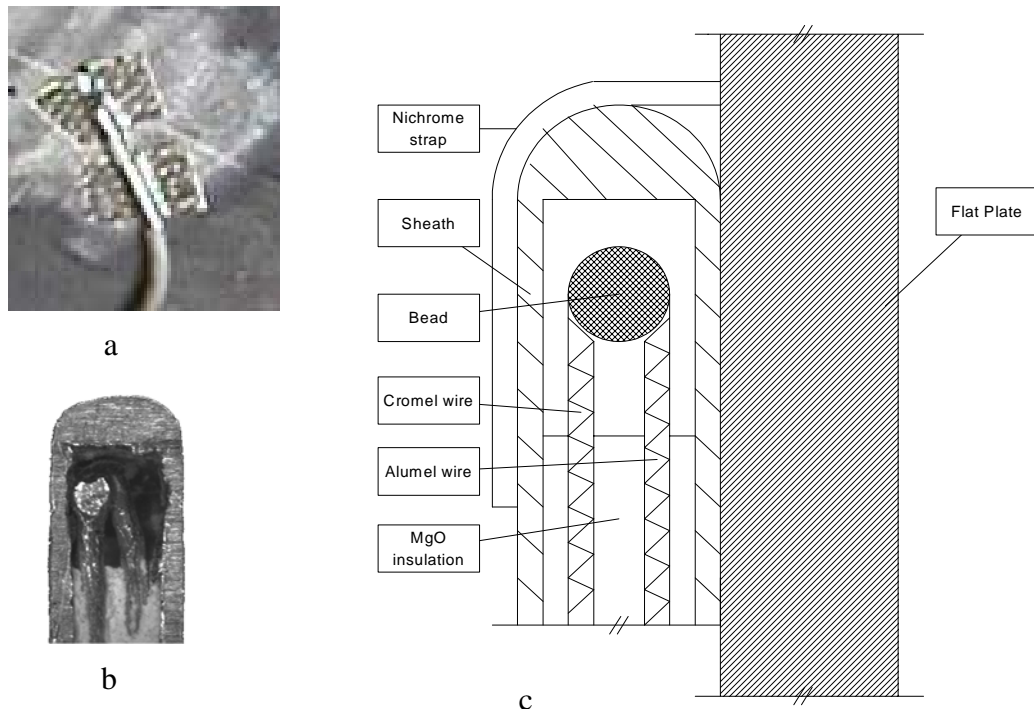


**Figure B- 1 a) Welded thermocouple installation on a heater shroud. b) Cross section of sheathed thermocouple sensor tip. c) Schematic of installation.**

Figure B- 2 is an IR image of the shroud taken from the side away from the lamps. It is easily seen that the thermocouples are cooler than the plate. The metallic strips that hold down the

thermocouple are also visible. Since the shroud surface temperature is the boundary condition of choice for test item response models, it is important to relate the thermocouple reading to the actual surface temperature. It is possible to directly use IR imagery to quantify the difference between the thermocouple temperature indication and the actual shroud temperature. However, this requires extensive characterization of the IR system and surfaces, or assumptions about the various emissivities as a function of temperature. Furthermore, in normal testing a direct view of the shroud is not always obtainable.

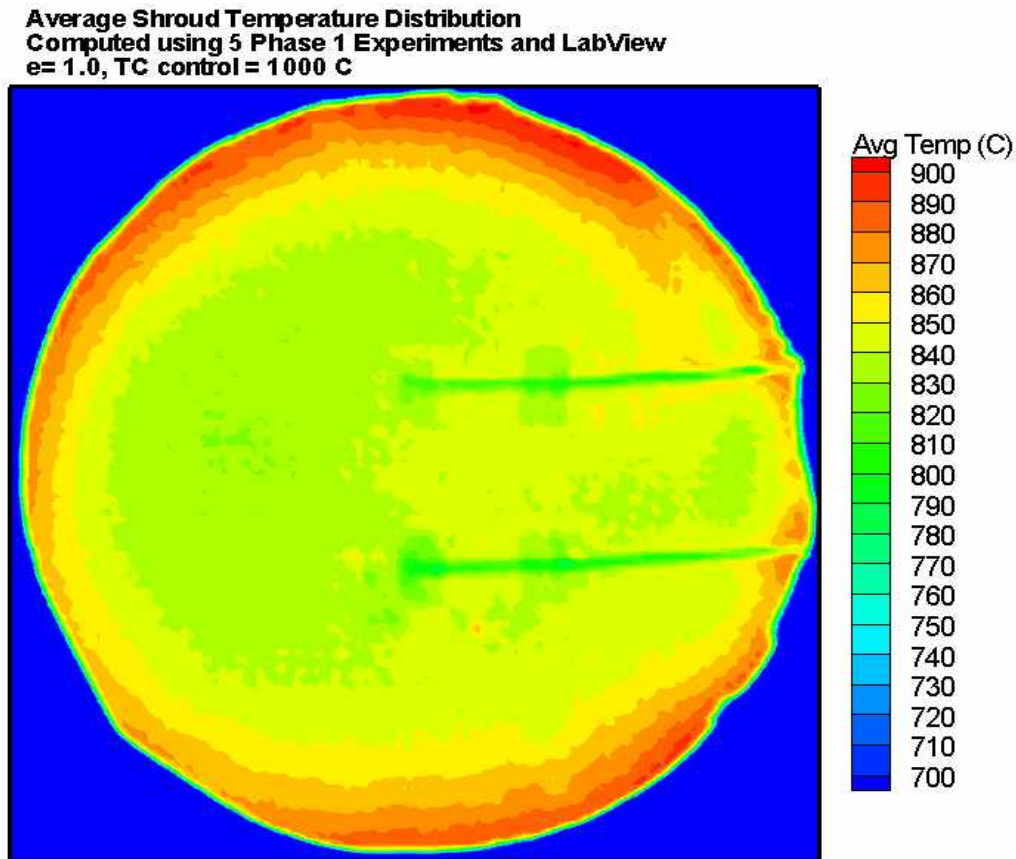
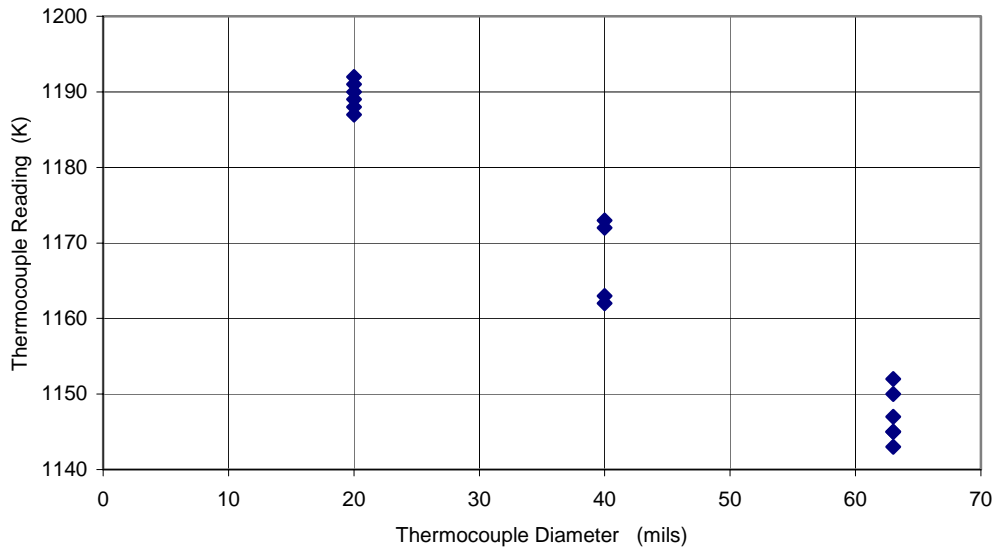


Figure B- 2 IR image of the lower side of the shroud, two thermocouples are visible.

By using various size thermocouples attached to the same shroud, it has been found that a smaller thermocouple outputs a higher temperature (when mounted on the side of the shroud away from the lamps) [1]. Figure B- 3 illustrates this effect where the indicated thermocouple temperature increases with decreasing thermocouple size. It is logical to assume that the smaller thermocouple will provide a more accurate answer.



**Figure B- 3 Recorded temperature as a function of thermocouple size.**

A test was recently performed where a pair of thermocouples was mounted on opposing sides of the shroud. The shroud was driven to and held at three nominally constant temperatures. The purpose was to gather data and create a model that would relate the actual shroud temperature to the thermocouple output. An idealization of the installation is shown in Figure B- 4.

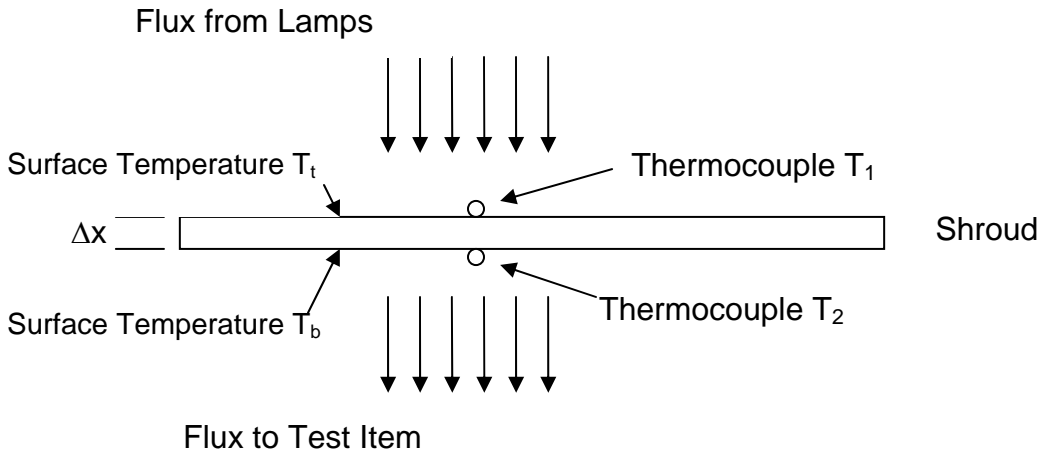


**Figure B- 4 Two thermocouples mounted on opposite sides of the shroud.**

During the test, a control thermocouple on the bottom surface was used to modulate the lamp power to maintain the desired temperature levels. The time-temperature history of the two thermocouples is shown in Figure B- 5.

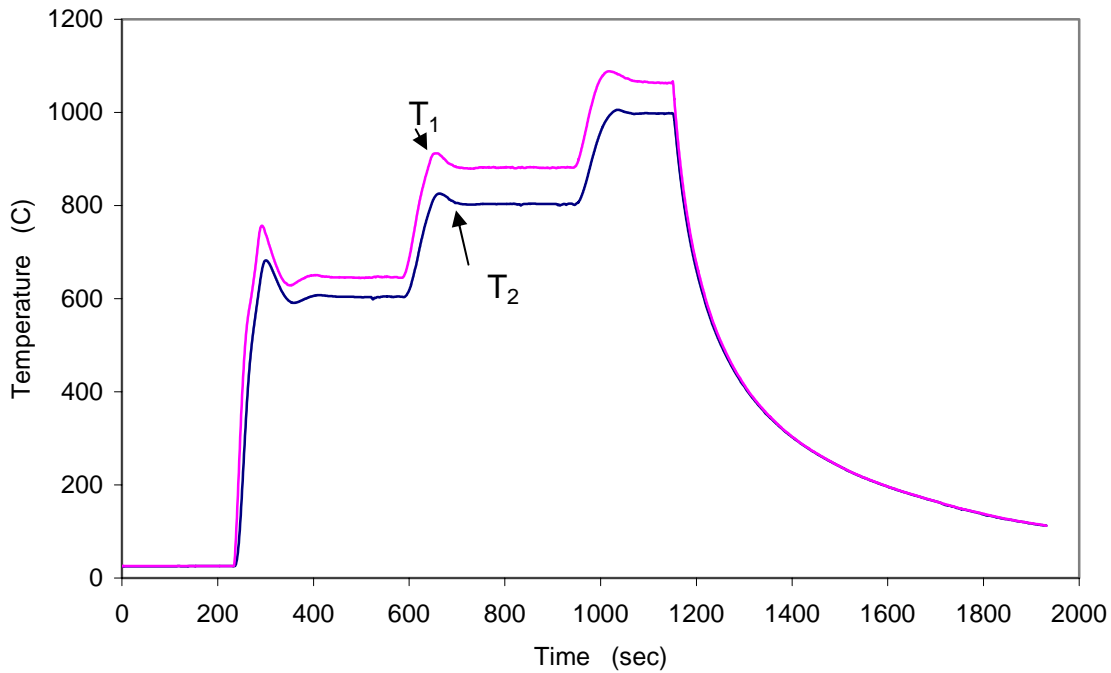


**Figure B- 5 Thermocouple readings from a shroud held at nominal 600C, 800C, and 1000C.**

**Model Development.** The heat flux through the plate can be modeled as one-dimensional conduction:

$$Q = k(T_t - T_b) / \Delta x \quad [1]$$

where  $k$  is the thermal conductivity,  $T_t$  is the plate temperature for the top surface (facing the heat lamps),  $T_b$  is the plate bottom surface temperature, and  $x$  is the plate thickness.

We then assume that the temperatures indicated by the thermocouples are in error. The top thermocouple indicates a temperature hotter than the top surface, and the bottom thermocouple indicates a temperature colder than the bottom surface. This is consistent with the experimental observations. The error is assumed to be proportional to the heat flux ( $Q$ ). For when there is no heat flux, one would expect that the errors would go to zero.

$$T_1 = T_t + \frac{\alpha D Q}{T^n} \quad \text{equations 2 and 3}$$

$$T_2 = T_b - \frac{\alpha D Q}{T^n}$$

where  $T_1$  is the top thermocouple measurement,  $T_2$  is the bottom thermal thermocouple measurement and  $\alpha$  is a free parameter. The error term is assumed to be identical in form for both thermocouples. It is assumed that the error is proportional to the thermocouple size ( $D$ ) as previously determined. We have also made the error to be inversely proportional to the absolute

temperature level raised to the  $n$  power. Initially the power  $n$  was considered to be zero, which makes the error independent of the temperature level.

To complete the equation set, a second expression for the heat flux from the shroud is written:

$$Q = \sigma \varepsilon (T_b^4 - T_{amb}^4). \quad \text{equation 4}$$

The above equation set is then applied to the experimental data set using the Solver function in Excel. A value of  $n$  is chosen so that the difference in heat flux from the two expressions (equation 1 and 4) is minimized for all temperature settings. Figure B- 6 shows the result heat flux calculated from equations 1 and 4 that was obtained with the parameter  $n$  equal to zero. This is the best match obtainable by adjusting the parameter  $n$ .

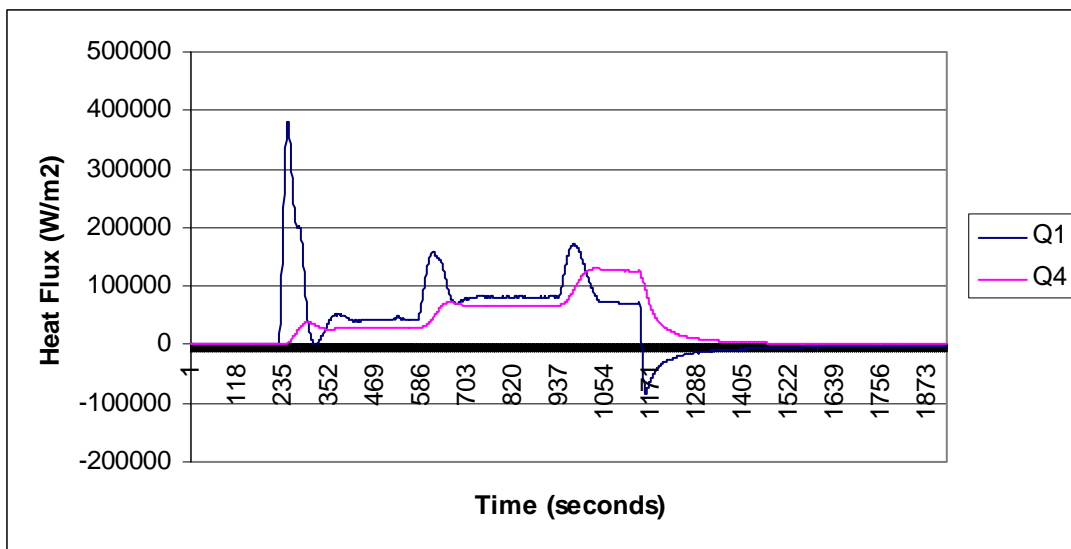


**Figure B- 6 Comparison of calculated heat flux from equations 1 and 4 (parameter  $n$  set to 0).**

Figure B- 7 shows how the calculated shroud top and bottom temperatures compare with the measured top and bottom thermocouple measurements (using the parameter  $n$  equal to zero and the optimum  $n$ ). As can be seen from this plot, the calculated temperatures are much closer together than the measured temperatures. Due to the symmetry assumed in the model, they appear near the average of the two measured temperatures at all times.

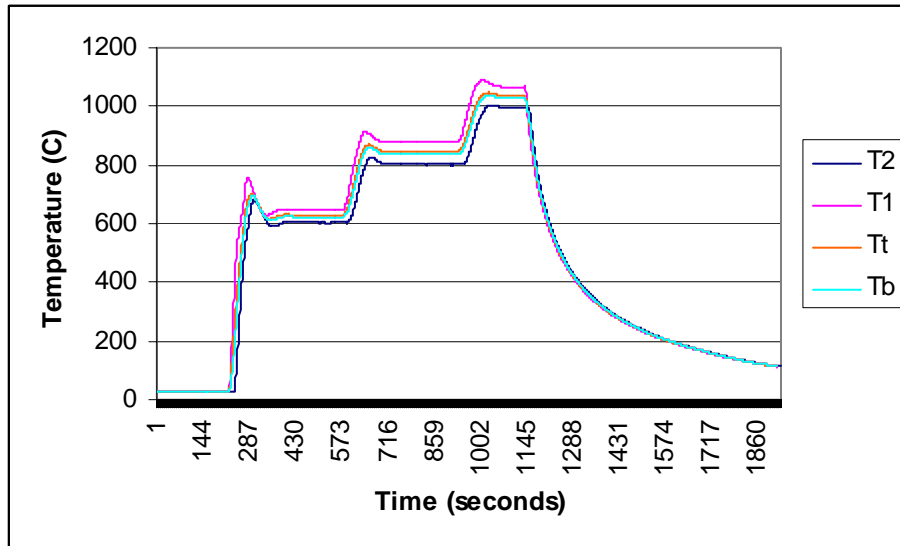


Figure B- 7 Comparison of calculated temperatures to the measured values (n set to 0).

Figure B-8 shows the difference between the top thermocouple measurement and the calculated top surface temperature. The difference between the bottom thermocouple measurement and the calculated bottom surface temperature is identical due to the symmetry assumed in the model. Also, for comparison, the difference between the top thermocouple temperature and the average of the two measured temperatures is also given. This clearly shows that the average of the two thermocouple measurements is a good approximation of the shroud temperature (top or bottom).

Examination of Figure B- 6 shows a disturbing trend. As the temperature in the experiment is ramped up from 600 C to 800 C and 1000 C, the heat flux calculated from equation 4 increases as expected. However, the heat flux calculated from equation 1 decreases slightly between the 800 C setting and the 1000 C setting. This is because our assumed linear dependence of the temperature measurement error with the heat flux. While it is reasonable to assume that the error goes to zero when the heat flux goes to zero, the linear relationship may not be correct. As the temperature level increases, the radiation from the shroud to the thermocouple may become more efficient resulting in a lower error. Thus, the fitting process was repeated with the parameter  $n$  fixed at 3. This resulted in a better comparison between the heat fluxes calculated with equations 1 and 4. This is presented in Figure B-9. As is seen, the comparison between the flux calculated from equations 1 and 4 is greatly improved over that presented in Figure B- 6.

Figure B- 10 presents the calculated surface temperatures, and compares them to the measured temperatures with the parameter  $n$  set to 3. Again, it is seen that the shroud surface temperatures are calculated to be close to the average of the two measured temperatures. This is further illustrated in Figure B- 11. In fact, it is difficult to see any difference in Figure B- 7 and Figure B- 10 or Figure B-8 and Figure B- 11. The calculated surface temperatures of the shroud surface are almost independent upon the choice of the parameter  $n$ .

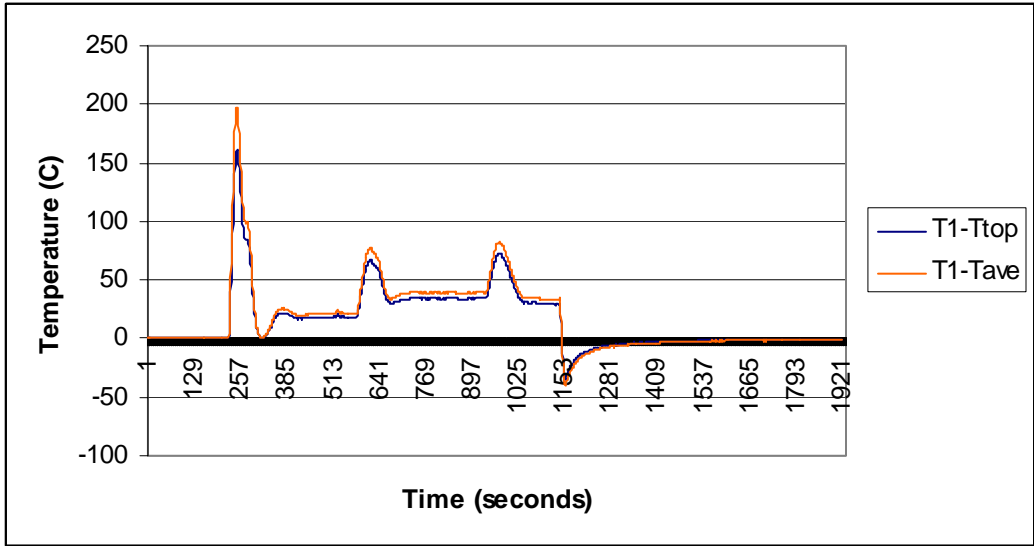


Figure B-8 Calculated difference between the measured temperature and the calculated temperature for the top surface.

This figure also shows the difference between the measured temperature and the average temperature for comparison ( $n$  set to 0).

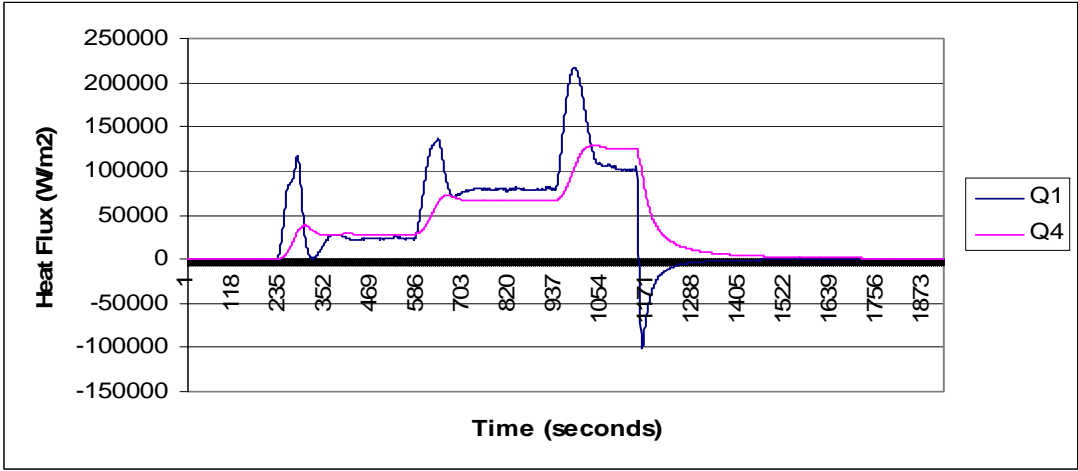


Figure B-9 Comparison of the heat flux calculated with equations 1 and 4 in the model using the parameter  $n$  equal to 3.

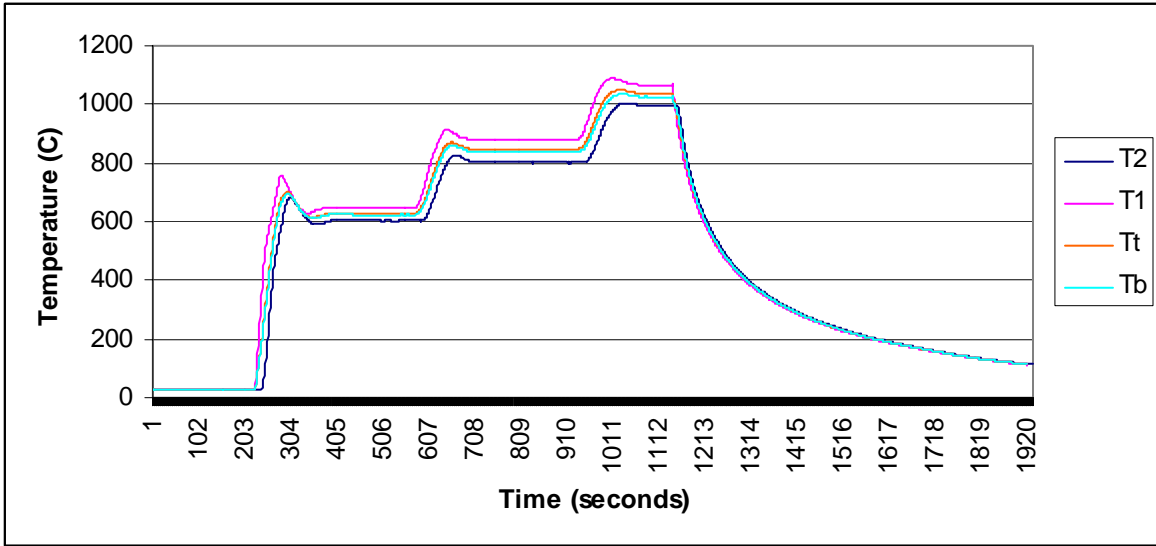


Figure B- 10 Comparison of calculated temperatures to the measured values ( $n$  set to 3).

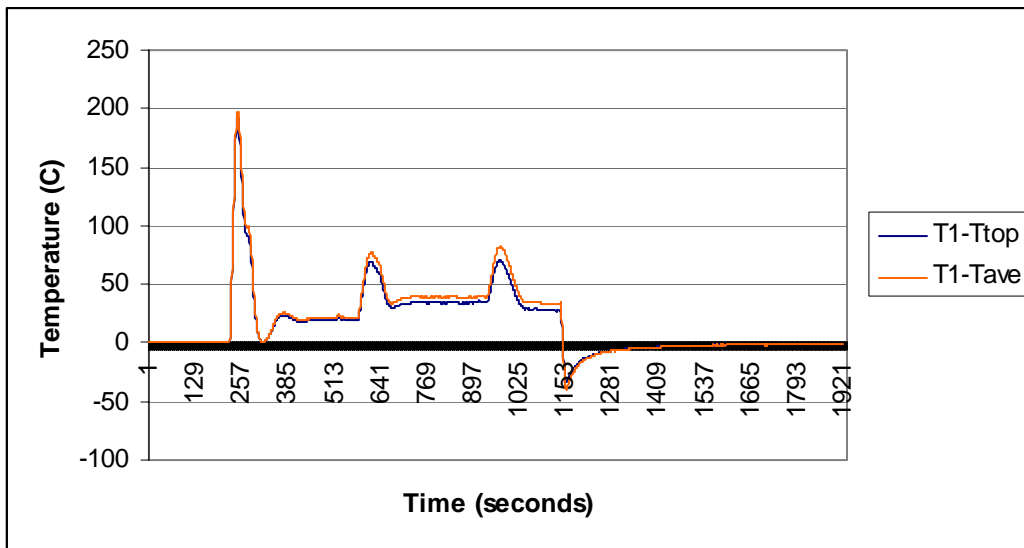


Figure B- 11 Calculated difference between the measured temperature and the calculated temperature for the top surface.

This figure also shows the difference between the measured temperature and the average temperature for comparison ( $n$  set to 3).

**Conclusions.** Examining Figure B- 11 shows that the error in the measurement of the shroud temperature can be on the order of 50 C. Thus, it is wise to develop a correction of this temperature measurement, or find an alternative measurement technique. We propose that the simplest model for estimating the shroud surface temperature is to install identical thermocouples on both sides of the shroud, and use the average of the two readings. This procedure could even be incorporated into the control system so that the shroud average temperature could be

maintained. One should use the smallest thermocouples possible since James Nakos demonstrated that the errors seem to be smaller with smaller thermocouples.

The reason that this simple model can be proposed is that the temperature drop for conduction through the shroud for typical heat fluxes is small. When the shroud is at 1000 C, the temperature drop through the shroud is approximately 10 C. So, accepting the assumption that the measurement errors are equal on both sides of the shroud, use of the average of the two measurements should result in an error on the order of 5 C for the shroud surface.

One could refine this estimate and reduce the error to below 5 C. However, that would require knowledge of the heat flux through the shroud, which will depend upon a lot more information, including the temperature and size of the target. Since it is unlikely that the installation of the two thermocouples is identical, yielding identical errors, any improvement of the proposed model is not justified.

### **References Cited.**

“Summary of Shroud Boundary Condition Characterization Experiments at the Radiant Heat Facility,” James Nakos, Jill Suo-Anttila, and Walt Gill, undated draft SAND report, December 2003.

### **Distribution:**

L. A. Gritzo	Org. 9132, MS 1135
J. T. Nakos	Org. 9132, MS 1135
C. A. Romero	Org. 9132, MS 0836
J. M. Suo-Anttila	Org. 9132, MS 1135
D. D. Dobranich	Org. 9116, MS 0836
B. D. Boughton	Org. 9116, MS 0836
R. E. Hogan	Org. 9116, MS 0836
E. S. Hertel	Org. 9116, MS 0836
W. L. Hermina	Org. 9110, MS 0824

## **Appendix C: Pyromark Emissivity**

Experiments conducted at the radiant heat facility typically use shrouds painted with Pyromark 2500. The goal of the paint is to create a surface with a known emissivity so that the surface properties can be used in modeling efforts. When applied appropriately, Pyromark 2500 should withstand temperatures up to 1300°C without blistering, chipping, cracking, or peeling.

A literature survey was conducted to obtain information on the emissivity of Pyromark black paint (typically the 2500°F version). Results from the following studies will be summarized here (full reference information included in the References section).

1. “Measurements of Total Emittance of Several Refractory Oxides, Cermets, and Ceramics for Temperatures from 600°F to 2000°F”, NASA Technical Note D-998.
2. Thermal Response of a Small Scale Cask-Like Test Article to Three Different High Temperature Environments”, R.S. Longenbaugh, L.C. Sanchez, and A.R. Mahoney, Sandia National Laboratories, for the U.S. DOT, DOT/FRA/ORD-90/01, Appendix B, February 1990.
3. “Thermal Response of a Small-Scale Cask-Like Disk after Heat Treatment,” by Rod Mahoney, 02542, Primary Standards Laboratory, 4 Sept 2003. “Thermo-physical Properties of a Foam and a Pyromark Paint 2500” TPRL, Inc. #1833, Purdue University
4. “Emittance Measurement Results for Pyromark Series 2500 Black Paint Coated Inconel Plate from the Radiant Heat Facility,” by Rod Mahoney, 02542, Primary Standards Laboratory, 15 July 2003.

Figures C1 through C5 below show plots of the emissivities as a function of temperature from all five sources above. Since most of the shroud characterization experiments were conducted at a nominal 1000°C with an inconel shroud, those results are most applicable.

The TPRL measurements (Figure C- 1) resulted in the lowest emissivity of approximately 0.77 at 1000°C. The substrate to which the paint was applied is unknown at this time. NASA measurements (Figure C- 2) indicate that the emissivity increases with temperature from a low of 0.81 at 300°C to 0.95 at 1000°C. The substrate was inconel, but when applied to stainless steel, the resulting emissivity is about 0.05 emissivity units lower. DOT/SNL measurements (Figure C- 3) also indicate that the emissivity of Pyromark on steel is less than the emissivity of Pyromark on inconel. The emissivity at 1000°C for the inconel substrate was 0.91. Lastly, two emissivity measurements were made at SNL as part of this shroud characterization effort (Figure C- 4 and Figure C- 5). The plate sample was severely heated resulting in an emissivity of 0.81 at 1000°C. The disk sample, heated in a manner consistent with the shroud characterization experiments, had an emissivity of 0.90 at 1000°C. The SNL measurements and DOT/SNL measurements have an uncertainty of  $\pm 0.04$  emissivity units. It is evident that the emissivity depends on the substrate and the heating history of the sample.

Emissivity of Pyromark Paint, TPRL Data

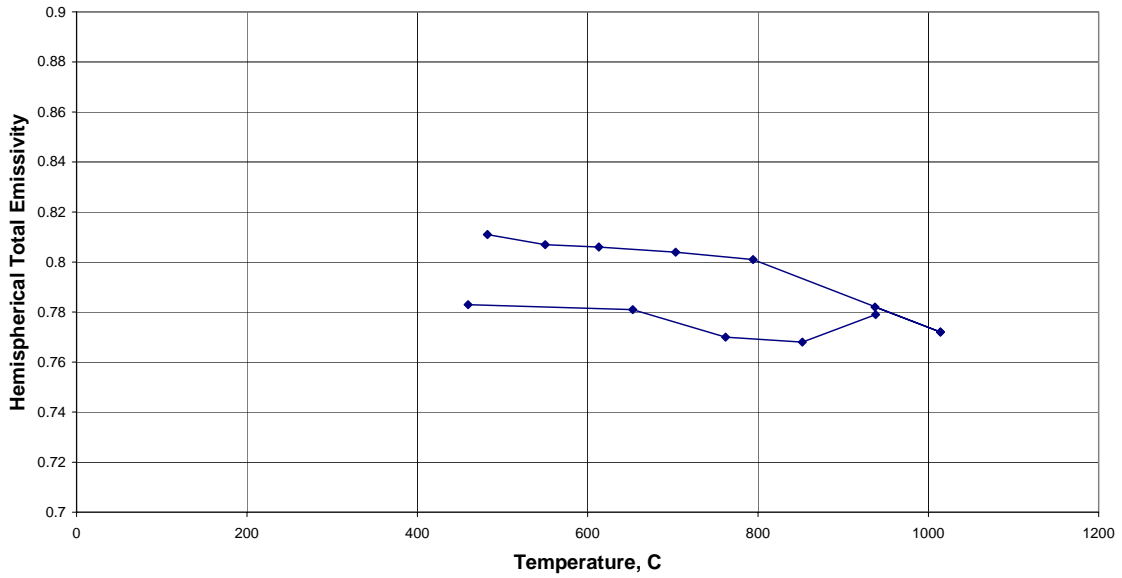


Figure C- 1 TPRL Measurements of Pyromark Emissivity

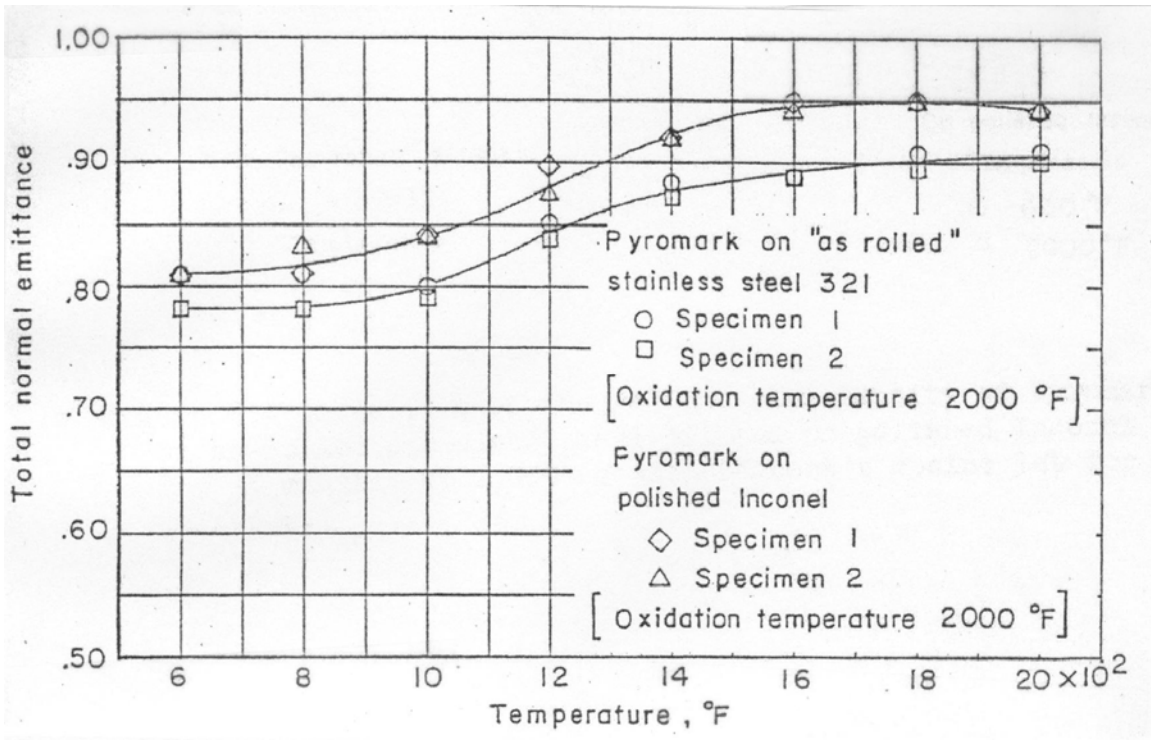


Figure C- 2 NASA Measurements of Pyromark Emissivity

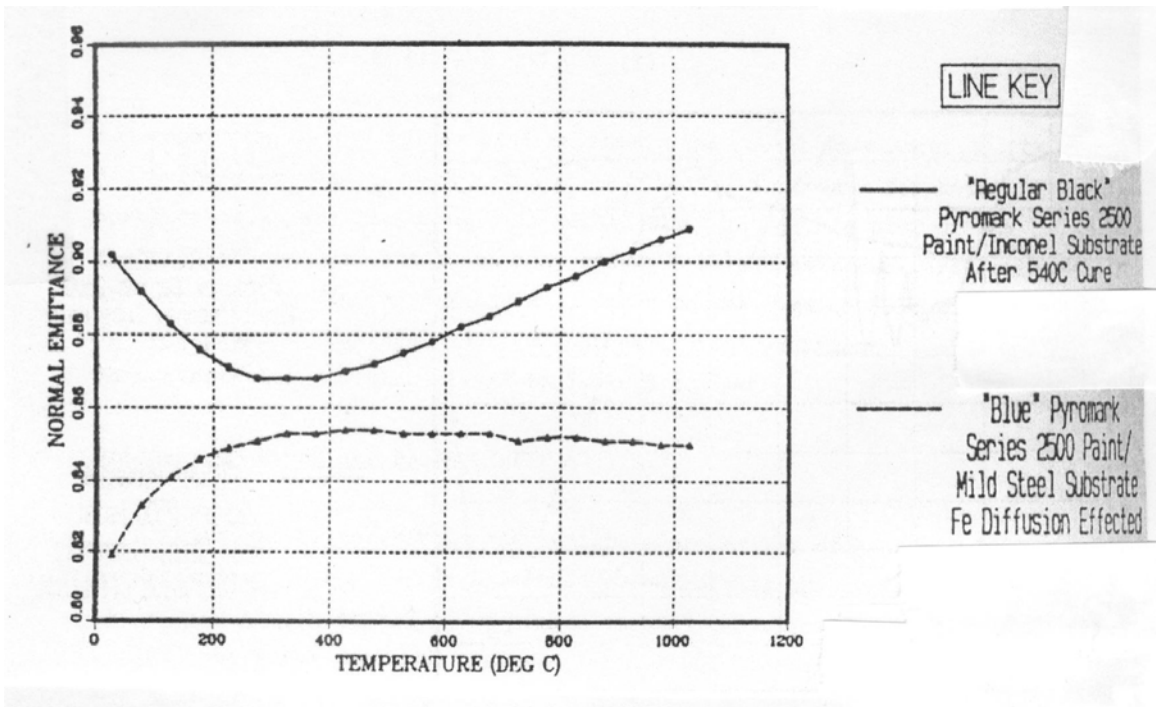


Figure C- 3 DOT/SNL Cask Measurements of Pyromark Emissivity

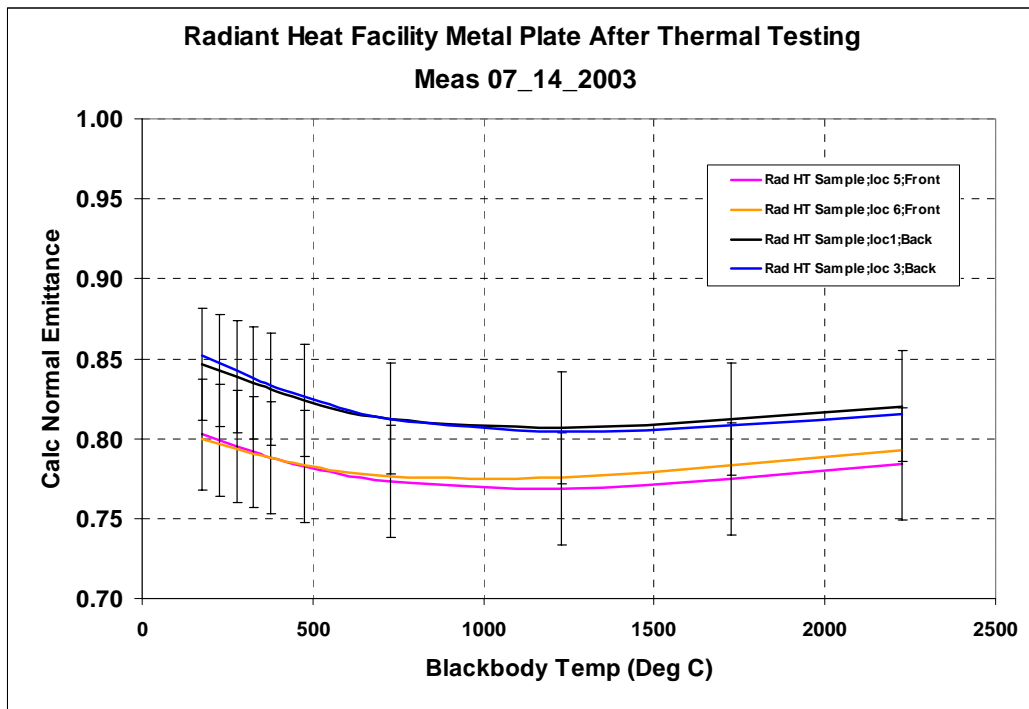


Figure C- 4 Emissivity Measurements for Inconel Plate

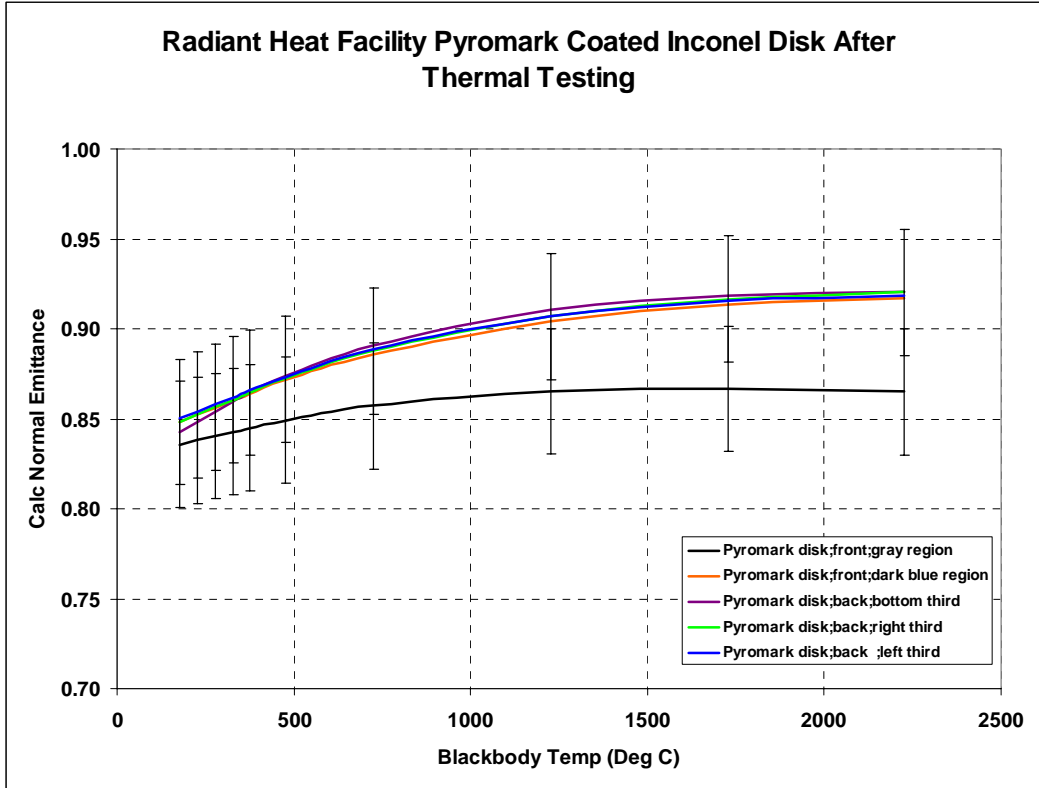


Figure C- 5 Emissivity Measurements for Phase 1 Inconel Disk

**Distribution:**

Mark Rosenthal MS0481, 2132  
Bob Paulsen MS0427, 2134  
J.F. Nagel MS0481, 2137

Tom Hendrickson MS0481, 2137  
Randy Harrison MS0481, 2132  
Scott Slezak MS0481, 2132  
Stephanie Pollice MS0481, 2137

Davina Kwon MS9014, 8242  
Bill Delameter MS9014, 8242  
Alvin Leung MS9014, 8242  
Arthur Ortega MS9014, 8242  
Alfred Ver Berkmoes MS9014, 8242

Carl Peterson MS0384, 9100  
Jaime Moya MS0834, 9110  
Wahid Hermina MS0834, 9120  
Gene Hertel MS0836, 9116  
Justine Johannes MS0834, 9112  
Lou Gritz MS1135, 9132  
Martin Pilch MS0828, 9133  
Steve Heffelfinger MS1135, 9134

Ken Erickson MS0834, 9112  
Sean Kearney MS0834, 9112  
Steve Trujillo MS0834, 9112  
Bruce Bainbridge MS0836, 9116  
Amanda Barra MS0836, 9116  
Barry Boughton MS0836, 9116  
Dean Dobranich MS0836, 9116  
Ron Dykhuizen MS0836, 9116  
Bill Erikson MS0836, 9116  
Nick Francis MS0836, 9116  
Roy Hogan MS0836, 9116  
Walt Gill (2) MS0836, 9132  
Cecily Romero MS0836, 9132  
Tom Blanchat MS1135, 9132  
Jill Suo-Anttila (2) MS1135, 9132  
Sheldon Tieszen MS1135, 9132  
Alex Brown MS1135, 9132  
Rich Streit MS1135, 9132  
Charles Hanks MS1135, 9132  
Bennie Belone MS1135, 9132

D. Mike Ramirez MS1146, 6423  
Dann Jernigan MS1135, 9132  
Sylvia Gomez MS1135, 9132  
Amalia Black MS0828, 9133  
Vicente Romero MS0828, 9133  
Martin Sherman MS0828, 9133  
Bill Oberkampf MS0828, 9133  
James Nakos (5) MS1135, 9132

Central Technical Files, 8945-1,  
MS9018  
Technical Library, 9616 (2),  
MS0899